Republic of Iraq
Ministry of Higher Education
and Scientific Research
Al-Nahrain University
College of Science
Department of Chemistry

Irradiation effect of photostability of poly(vinyl chloride) in presence of inorganic complexes

A Thesis
Submitted to the College of Science Al-Nahrain University as a Partial Fulfillment of the Requirements for the Degree of M.Sc. in Chemistry

By

Rafah Fahem Mohammed

B.Sc. Chemistry/ College of Science/ Baghdad university
(2013)

Supervised by

Dr. Emad A. Yousif
Assist. Professor

Jan. 2016 **Rabi-Al-Thani 1437**

بسم ٱللَّهِ ٱلرحمن ٱلرحيم

إِنَّ فِى خَلْقِ ٱلسَّمَٰوَٰتِ وَٱلْأَرْضِ وَٱخْتِلَٰفِ ٱلَّيْلِ وَٱلنَّهَارِ
لَءَايَٰتٍ لِّأُو۟لِى ٱلْأَلْبَٰبِ ﴿١٩٠﴾ ٱلَّذِينَ يَذْكُرُونَ ٱللَّهَ
قِيَٰمًا وَقُعُودًا وَعَلَىٰ جُنُوبِهِمْ وَيَتَفَكَّرُونَ فِى خَلْقِ ٱلسَّمَٰوَٰتِ
وَٱلْأَرْضِ رَبَّنَا مَا خَلَقْتَ هَٰذَا بَٰطِلًا سُبْحَٰنَكَ فَقِنَا عَذَابَ ٱلنَّارِ ﴿١٩١﴾

صدق ٱللَّه ٱلعظيم

سورة آل عمران

I didicate this work to beloved my mother, my father, grandfather (Mohammed alkhushahly), my uncles martyres (Ghanem, Belal, Khadem, Mohammed and Koutiaba), my brothers and my husband.

Also I didicate to Dr. Emad and all who helped me in this work

Acknowledgements

I would like to express my sincere thanks and gratitude to my supervisor, Assistant Prof. ***Dr. Emad A. Yousif*** *for suggesting the subject of this thesis and supervision in my work. His enthusiasm, encouragement, and faith in me throughout have been extremely helpful. Without him this work would not be completed.*

I would like to express my sincere thanks and gratitude to Assistant Prof. ***Dr. Ahmed A. Ahmed*** *for his supporting me during the course of the study and work.*

I would like to thank miss ***Alaa*** *and mrs.* ***Hadeel*** *for their supporting me during the course of the study and work.*

I would like to thank my ***father****, my* ***mother****, my* ***brothers*** *and all of my* ***friends*** *for their supporting me during the course of the study and work.*

Thanks to the staff of the chemistry department, college of science, Al-Nahrain University.

Finally, I wish to thank all the people who helped me during my work.

Rafah

Supervisor Certification

I certify that this thesis entitled **"Irradiation effect of photostability of poly(vinyl chloride) in presence of inorganic complexes"** was prepared by **"Rafah Fahem Mohammed"** under my supervision at the Department of Chemistry, College of Science, Al-Nahrain University as a partial requirements for the Degree of **Master of Science in Chemistry**.

Signature:

Name: Dr. Emad A. Yousif

Scientific Degree: Assistant Professor

Date:

In view of the available recommendation, I forward this thesis for debate by the Examining Committee.

Signature:

Name: Dr. Nasreen R. Jber

Scientific Degree: Assistant Professor

Title: Head of Chemistry Department

Date:

Examining Committee Certfication

We, the examining committee, certify that we have read this thesis entitled "**Irradiation effect of photostability of poly(vinyl chloride) in presence of inorganic complexes"**and examined the student (**Rafah Fahem Mohammed)** in its contents and that in our opinion; it is adequate as a thesis for the Degree of **Master of Science in Chemistry**.

Signature:
Name: **Dr. Basima M. Sarhan**
Scientific degree: Professor
Date: / / 2016
(Chairman)

Signature:
Name: **Dr. Ahmed A. Ahmed**
Scientific degree: Assistant Professor
Date: / / 2016
(Member)

Signature:
Name: **Dr. Majid S. Khalaf**
Scientific degree: Assistant
Date: / / 2016
(Member)

Signature:
Name: **Dr. Emad A.Yousif**
Scientific degree: Assistant Professor
Date: / / 2016
(Member and Supervisor)

I, hereby certify upon the decision of the examining committee.

Signature:

Name: **Dr. Hadi M. A. Abood**

Scientific degree: Assistant Professor

Title: Dean of the College of Science.

Date: / /2016

Abstract

Five metal ion complexes of Ni(II), Cu(II), Zn(II), Cd(II) and Sn(II) with potassium 2-(4-isobutylphenyl) propanoate, as a ligand (L) has been prepared in alcoholic medium.

These complexes are:

Bis2-(4-isobutylphenyl) propanoato Nickel(II), NiL_2,

Bis2-(4-isobutylphenyl) propanoato Cupper(II), CuL_2,

Bis2-(4-isobutylphenyl) propanoato Zinc(II), ZnL_2,

Bis2-(4-isobutylphenyl) propanoato Cadmium(II), CdL_2,

Bis2-(4-isobutylphenyl) propanoato Tin(II), SnL_2 .

The ligand (L) and its metal ion complexes were characterized quantitatively and qualitatively by using: FTIR, UV-visible spectroscopy, magnetic susceptibility, conductivity measurements and melting point. According to the spectral data of the complexes an octahedral geometry was suggested for these complexes except Cu(II) complex which exhibit a square planer structure.

In this work the prepared complexes of 2-(4-isobutylphenyl) propanoate were used to enhance the photostabilization of polyvinyl chloride (PVC).

PVC has been mixed with these complexes in Tetrahydrofuran solvent which containing 0.5 % concentration of complex by weight, which produced by the casting method from Tetrahydrofuran solvent. The photostabilization of

polyvinyl chloride films were studied at room temperature under irradiation of light(λ= 320)nm wave length with intensity of $7.75*10^{-7}$ Ein Dm^{-3} S^{-1}.

The photostabilization activity of these compounds was determined by monitoring the hydroxyl (I_{OH}) , polyene $I_{(c=c)}$ and carbonyl (I_{CO}) indexes, weight loss method with irradiation time. It was found that carbonyl, polyene and hydroxyl indexes values increased with irradiation time and this increase depend on the type of additives. The surface morphology for these films was studied during irradiation time. The changes in viscosity average molecular weight of PVC with irradiation time were also tracked (using Tetrahydrofuran as a solvent). The quantum yield of the chain scission (Φ_{cs}) of these complexes in PVC films was also evaluated.

The following trend was obtained for the photostabilization effect on PVC films in presence of additives as shown below:

PVC<ZnL_2<CdL_2<CuL_2<SnL_2<NiL_2

Increasing the photostability

According to the experimental results obtained several mechanisms were suggested depending on the structure of the additives. Among these mechanisms, HCl scavenging, UV absorption, peroxide decomposer and radical scavenger for photostabilizer additives.

Table of Contents

List of Tables

List of Figures

Symbols and Abbreviations

AFM	Atomic Force Microscopy
Ch	Chromophore
Cl·	Chloride radical
Cl*	Chloride excited state
CPVC	Chlorinated Poly Vinyl Chloride
DMF	DiMethylFormamide
DP	Degree of Polymerization
FAAS	Flame Atomic Absorption Spectroscopy
FR	Flame Retardant
FTIR	Fourier Transform Infra-Red
H·	Hydrogen radical
HALS	Hindered Amine Light Stabilizer
HCl	Hydrogen chloride
HDPE	High Density Polyethylene
HO·	Hydroxide radical
HOO^-	Hydroperoxy group
h*v*	Energy, ultraviolet or solar radiation
LDPE	Low Density Polyethylene
MBS	Methyl methacrylate-Butadiene-Styrene
mm	Millimetre
µm	Micrometer
nm	nanometre
$^1O_2$	Singlate oxygen
P·	Polymer radical
PA	Poly Amide
PP	Polypropylene
PC	Poly Carbonate
PE	PolyEthylene

PMMA	Poly Methyl MethAcrylate
PO·	Polymer Oxy Radical
POOH	Polymer Hydroperoxy groups
PS	PolyStyrene
PVA	Poly Vinyl Alcohol
PVC	Poly Vinyl Chloride
Q	Quencher
R·	Alkyl radical
RO·	Alkoxy radical
ROO·	Peroxy radical
ROOH	Hydrogen peroxide
THF	Tetrahydrofuran
TPO	Thermoplastic polyolefin
UV-VIS	Ultra Violet-Visible
UV-B	Ultra Violet-B
VCM	Vinyl Chloride Monomer
WPCs	Wood Plastic Composites

Chapter One

1

INTRODUCTION AND LITERATURES REVIEW

Introduction

1.1 Carboxylate:

are a salts of a carboxylic acid. Carboxylate salts have the general formula $M(RCOO)_n$, where M is a metal and n is 1,2,.... Carboxylate esters have the general formula RCOOR'. R and R' are organic groups; R'≠H [1].

Because of their enhanced acidity, carboxylic acids react with bases to form ionic salts, as shown in the following equations. In the case of alkali metal hydroxides and simple amines (or ammonia) the resulting salts have pronounced ionic character and are usually soluble in water. Heavy metals such as silver, mercury and lead form salts having more covalent character (3rd example), and the water solubility is reduced, especially for acids composed of four or more carbon atoms.

$$RCO_2H + NaHCO_3 \longrightarrow RCO_2^{(-)}\,Na^{(+)} + CO_2 + H_2O$$

$$RCO_2H + (CH_3)_3N: \longrightarrow RCO_2^{(-)}\,(CH_3)_3NH^{(+)}$$

$$RCO_2H + AgOH \longrightarrow RCO_2^{\delta(-)}\,Ag^{\delta(+)} + H_2O$$

Carboxylic acids and their salts having alkyl chains longer than six carbons exhibit unusual behavior in water due to the presence of both hydrophilic (CO_2) and hydrophobic (alkyl) regions in the same molecule. Such molecules are termed amphiphilic (Gk. amphi = both) or amphipathic. Depending on the nature of the hydrophilic portion these compounds may form monolayers on the water surface or sphere-like clusters, called micelles, in solution.

1.2 plastics :

Most plastics contain organic polymers. The vast majority of these polymers are based on chains of carbon atoms alone or with oxygen, sulfur, or nitrogen as well. The backbone is that part of the chain on the main "path" linking a large number of repeat units together. To customize the properties of a plastic, different molecular groups "hang" from the backbone (usually they are "hung" as part of the monomers before the monomers are linked together to form the polymer chain). The structure of these "side chains" influence the properties of the polymer. This fine tuning of the repeating unit's molecular structure influences the properties of the polymer [2].

1.3 Uses of plastics

The main uses of plastics in building construction include plastic pipes, siding, windows, soffit, fascia, rainwater goods and decorative panels and a majority of these are made of rigid Poly(vinyl chloride) (rPVC). In fact, 76% of the PVC produced globally is used in the construction of buildings. The most popular cladding in residential housing in North America is rPVC siding produced by a profile extrusion process. In this application, the useful lifetime of the product is generally determined by uneven discoloration and loss of impact strength from photodamage by solar UV radiation. One important advantage of these is their lower thermal conductivity, relative to glass. Polycarbonate [PC] glazing used in architectural window panels as well as continuous windows and domes is similar to or better in performance than the conventional glazing in several characteristics [3].The value of k for PC glazing panels are as low as 1.2–1.9 Wm^{-2} (25 mm thickness), but new

technology such as PC/aerogel composites [4] can bring this value down to 0.5 Wm^{-2} (25 mm section). In these products as well, discoloration induced by solar radiation, determines their useful lifetime. The present push towards sustainable materials in construction has led to some reassessment of the use of PVC materials in buildings [5]. Despite its dominance in the building sector and excellent performance in construction [6]. Not only does the production of PVC result in potential emission of toxic monomers and precursors to air but it is also compounded into soft products with phthalate plasticizers that are potent endocrine disruptors. Nevertheless, no imminent move away from its use in buildings is apparent. Alternative plastics that can replace PVC in construction such as polyolefins are available, but at a greater lifetime cost. The susceptibility of these alternatives to solar UV radiation will also influence their lifetime costs. WPCs are essentially thermoplastic composites of (PE, PP, PVC and PS) highly filled with powdered wood. Often, post-consumer plastics are used in their manufacture. Embedding wood fibers in a polymer matrix restricts absorption of moisture and hence avoids fungal growth and biodegradation of the wood fraction. A higher-grade product results when a single type of plastic such as virgin PP is used [7, 8].

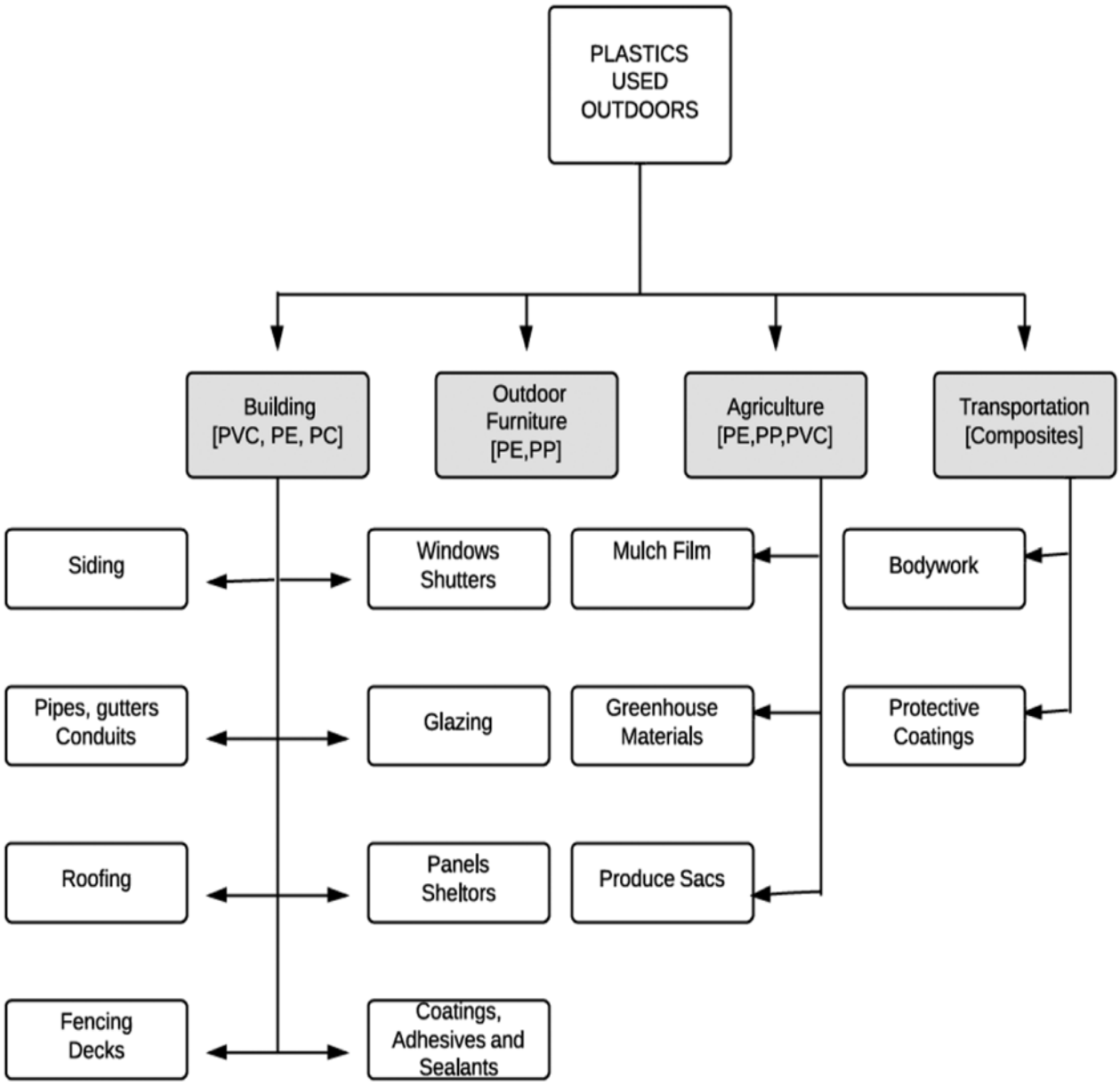

Fig. (1.1) Uses of plastic materials in outdoor applications. PE = polyethylene; PP = polypropylene; PVC = poly vinyl chloride; PC =polycarbonate [3].

1.4 Types of plastic degradation:

Changes in polymer properties due to chemical, physical or biological reactions resulting in bond scissions and subsequent chemical transformations are categorized as polymer degradation. Degradation reflects changes in material properties such as mechanical, optical or electrical characteristics

in crazing, cracking, erosion, discoloration and phaseseparation. Depending upon the nature of the causing agents, polmer degradations have been classified as photo-oxidative degradation, mechanochemical degradation, catalytic degradation and biodegradation [9].

1.5 Weathering and Environmental Degradation of Polymers:

Weathering of polymers involves physical, mechanical and chemical changes in their surface and near the surface regions. May also include the whole polymer sample. These changes are due to the solar energy; moisture (dew, rain, humidity, snow); heat and atmosphere oxidants (ozone, atomic oxygen and siglate oxygen); and air pollutants (sulphur, dioxide, nitrogen oxides, polycyclic hydcarbones, etc.) [10].

The primary cause of weathering damage to wood and plastics is from solar UV-B radiation that is efficiently absorbed by chromophores generally present in these materials, high humidity, temperature, pollutants in air often accelerate light-induced degradation. With plastics, the damage ranges from uneven discoloration or surface changes to cracking, loss of material strength [11]. With wood products, weathering degradation also renders the surface hydrophilic facilitating subsequent moisture absorption and surface biodegradation [12].

Depletion of the stratospheric ozone layer to any extent increases the fraction of UV-B (290–315 nm) in the solar radiation reaching the earth's surface. Potential latitude-dependent increases in UV-B radiation can significantly shorten the service life of wood and plastics used outdoors, especially at locations where the ambient temperatures are relatively high.

Levels of UV radiation are expected to decrease globally in the decades ahead [13], but there is still concern about its impact on materials due to the interactive effects with climate change. Climate change is widely expected to result in an increase in the average global temperature by 1.1–6.4 °C by the end of the century and there is an international effort to keep the increase under 2 °C [14]. Any increase in ambient temperatures exacerbates the damage as weathering reactions in both wood and plastics proceed at faster rates at the higher temperatures [15]. Intrinsic factors such as additives or impurities of trace metals (including pro-oxidant additives to make the plastic photodegradable) [16] also tend to accelerate the rate of light-induced photo-damage to both classes of materials.

Sulphur oxide may react with polymer oxy radical (PO˙) formed during the thermal decomposition and / or photo decomposition of polymer hydroperoxy
groups (POOH) by reactions which lead to the formation of sulphate groups [17].

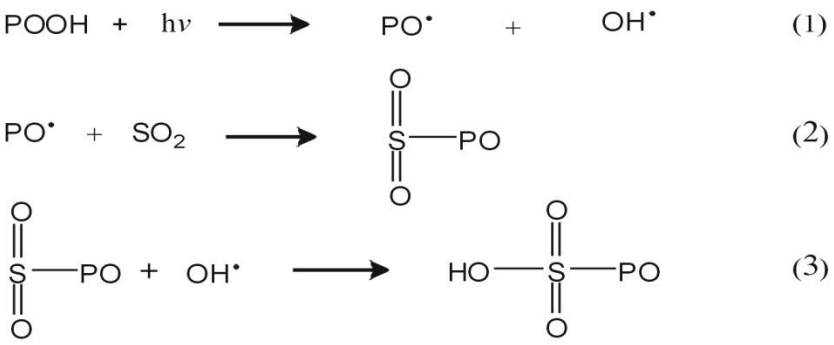

Polycyclic hydrocarbons may photoinitiate free radicals oxidative degradation of polymers or participate in the generation of singlate oxygen by an energy transferred mechanism.

Singlate oxygen $(O_2^*)^1$, which produced in complicated photochemical reactions in smog, may react with unsaturated polymers and produce hydroperoxide groups [18].

1.6 *Poly (vinyl chloride)*

PVC is a synthetic solid resin material (a plastic) also commonly referred to as 'vinyl'. PVC is formed from vinyl chloride monomer (VCM) (in pressurised liquid form) in a manufacturing process that polymerises VCM into solid powder or granule [19]. Structurally, PVC is a vinyl polymer. It's similar to polyethylene, but on every other carbonin the backbone chain, one of the hydrogen atoms is replaced with a chlorine atom. It's produced by the free radical polymerization of vinyl chloride. PVC can also be prepared by treating acetylene with hydrochloric acid (HCl) [20].

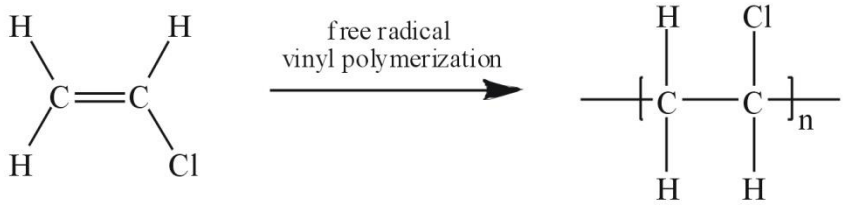

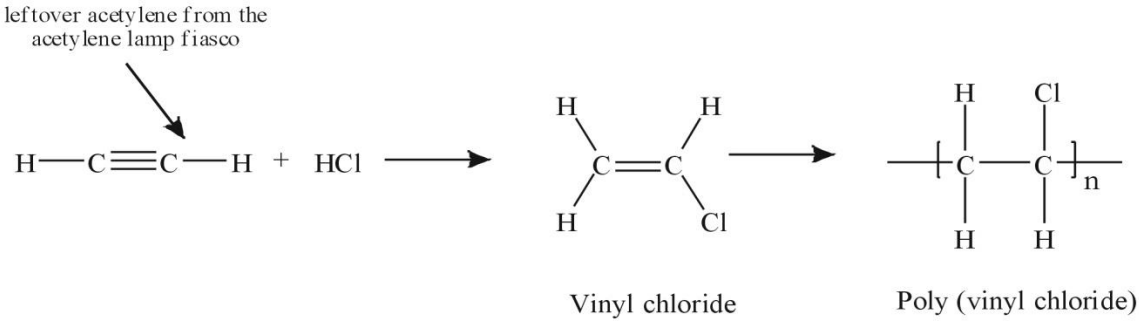

Poly vinyl chloride, better known by its abbreviation PVC, It is the second largest manufactured resin by volume worldwide [21].; currently, its production per annum exceeds 31 million tones. Braun [22] described the

most remarkable milestones in PVC history, their importance to the development of macromolecular chemistry, and some PVC research and industrial applications, with respect to polymerization, stabilization, bulk property modification, and chemical and material recycling of PVC waste [23]., The low cost and the good performance of poly vinyl chloride products have increased the utilization of this polymer in building, mainly in exterior application, such as window profiles, cladding structure and siding [24]., However, ultimate user acceptance of the PVC products for out door building applications will depend on their ability to resist photodegradation over long periods of sunlight exposure. To ensure weather ability, the PVC resin needs to be compounded and processed properly, using suitable additives, leading to a complex material whose behavior and properties are quite different from the PVC resin by itself. On the other hand, it is important to perform reliable accelerated weathering test methods. In this regard, factors that influence the degradation of PVC based materials in the service condition, like light and temperature are accelerated [25].

Its wide range of physical, chemical and mechanical properties, its durability, and its cost effectiveness make PVC useful in applications ranging from packaging to health-care devices, toys, building materials, electrical wire insulation, cloths or furnishing, Figure 1.2.

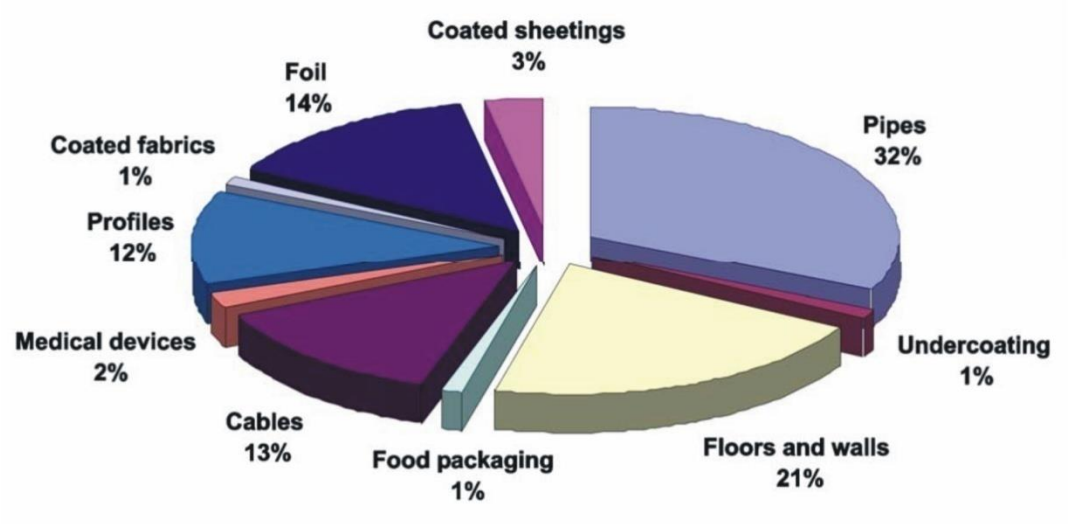

Fig. (1.2) : Application areas of PVC [24].

Poly (vinyl chloride), PVC, is a linear - chain polymer with bulky chloride side - groups which prevent crystalline regions occurring normally. PVC is hard and rigid material at room temperature [26,27]. linear poly (vinyl chloride) is colorless material. It has relatively high density and low softening point [27].The presence of the chlorine atom causes an increase in the inter chain attraction, hence an increase in the hardness and stiffness of the polymer is recognized. PVC is also a polar polymer because of C-Cl dipole. These properties make PVC polymers as good candidate in the application involving high frequencies because high dielectric constant and high power factor values higher than polyethylene owing to the polar carbon - chlorine bond [28].

Poly (vinyl chloride) has very limited solubility. The most effective solvents are those which appear to be capable of some form of interaction with polymer. It has been suggested that poly vinyl chloride is a weak proton donor and effective solvents are proton accepter [27]. Thus the PVC polymer is soluble at room temperature in oxygen-

containing solvents such as ethers e.g. dioxane , tetrahydrofuran; ketones e. g. cyclohexanone, and nitro compounds, e. g. nitrobenzene [23].

1.6.1 Photo-oxidation of polymer PVC :

Sunlight interacts with virtually all organic polymers to cause irreversible chemical changes. The useful lifetimes of polymeric materials are normally measured in terms of their retention of mechanical properties and, for practical purposes, the photo-oxidative degradation of polymers usually manifests itself in the form of embrittlement, followed by loss of tensile properties on greater exposure [29].

The photo-oxidation and thermal degradation of polyolefins has been the subject of extensive studies ever since their commercial introduction. Resistance to oxidation increases with increasing density of the polyolefins because a less branched polymer has a diminished permeability to gases and smaller number of tertiary carbon atoms in themacromolecule (which constitute sensitive points of attack) [30].

When exposed to natural weathering, PVC deteriorates and becomes increasingly colored and brittle, with a steady decrease in mechanical properties such as tensile strength, elasticity and impact resistance., Owing to its large outdoor application, PVC has to be protected against photodegradation [30]. The main factors influencing degradation of PVC products include oxygen, humidity, light, mechanical stress, aggressive media and ionizing radiation, all are accelerated by increasing temperature [31].

In the presence of the UV radiation , oxygen seems to attack the PVC chains randomly or on sites that are not involved in the mechanism of thermal degradation. Flexible (plasticized) PVC weathering resistance is determined

substantially by the plasticizer, its oxidative stability is generally the deciding property. Each component (stabilizer, UV absorber, pigment, colorant, processing additives and plasticizer) of the PVC compound possesses its own weathering stability, but it is the interaction of all the components that determines the utility of the material [32].The mechanism of photooxidation is explained by reaction detailed in scheme 1.1.

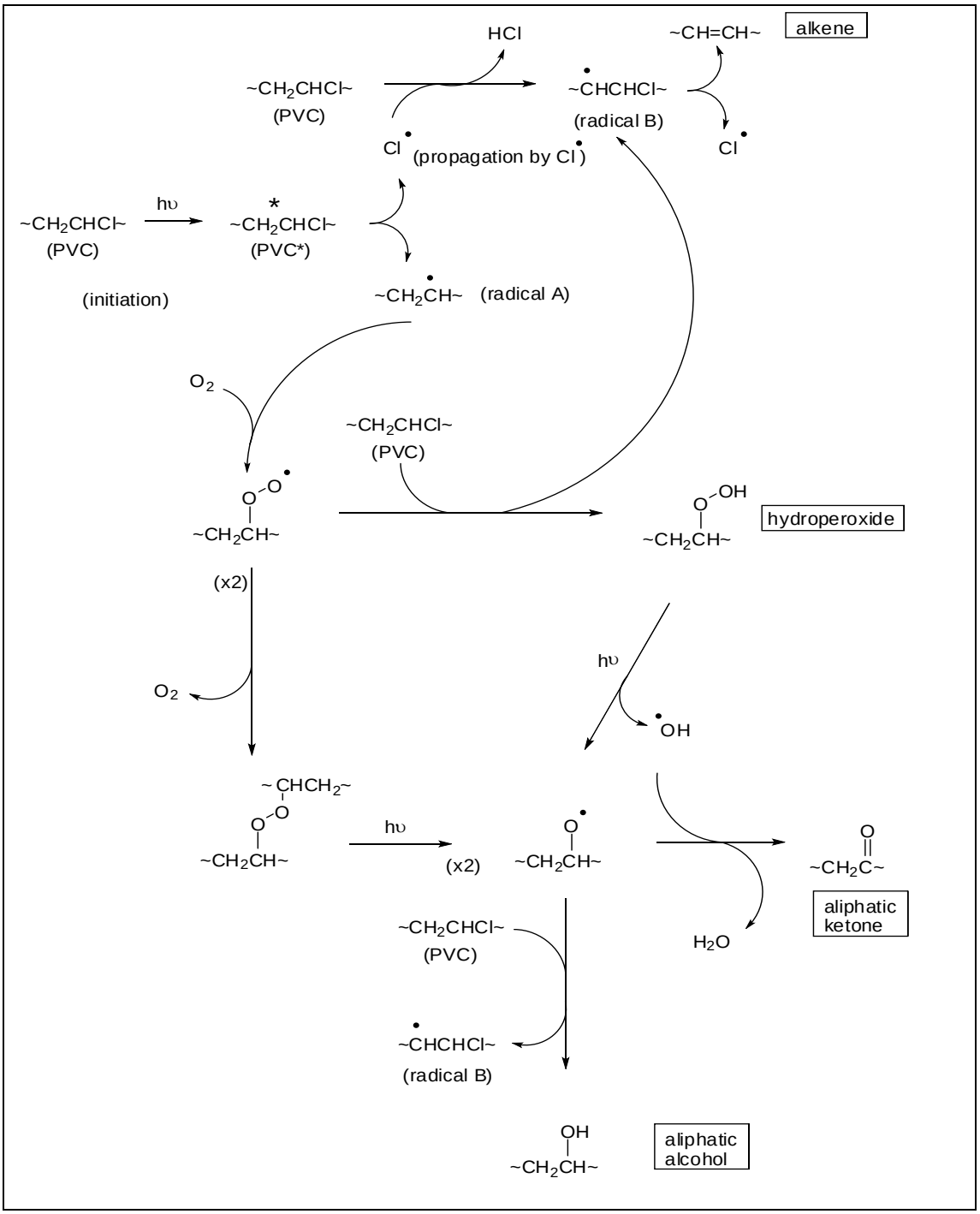

Scheme (1.1): Some of the photooxidation processes of PVC: reactions of radical B with molecular oxygen, akin to those of radical A, would give rise to chloroketone, chloroalcohol and chlorohydroperoxide moieties; further reactions of such reactive functionalities may lead to chain cleavage and reduction in molecular weight [32]..

1.7 Oxidative degradation of polyolfins

When organic materials such as polyolefins are exposed to conditions such as heat, ultraviolet light, or mechanical stress in the presence of atmospheric oxygen, free radicals are formed which initiate the oxidation process. The basic chemistry of oxidation has been known for over sixty years [33].

This process is characterized by initiation (equation 4), propagation (equations 5 & 6), chain branching (equation 7), and termination (equation 8) steps [34]:

Initiation : $P{-}H \longrightarrow P^{\bullet} + H^{\bullet}$ (4)

Propagation : $P^{\bullet} + O_2 \longrightarrow P{-}O{-}O^{\bullet}$ (5)

$P{-}O{-}O^{\bullet} + P{-}H \longrightarrow P{-}O{-}OH + P^{\bullet}$ (6)

Chain branching : $P{-}O{-}O^{\bullet} \xrightarrow{h\nu\,/\,\triangle} P{-}O{-}OH + P^{\bullet}$ (7)

Termination : $2P{-}O{-}O^{\bullet} \longrightarrow P{-}O{-}OP + O_2$ (8)

The alkoxy radical derived from the polypropylene hydroperoxide (in equation 4) readily undergoes fragmentation to give chain scission (equation 9). This is consistent with studies showing chain scission dominates over cross linking in the oxidation of polypropylene.

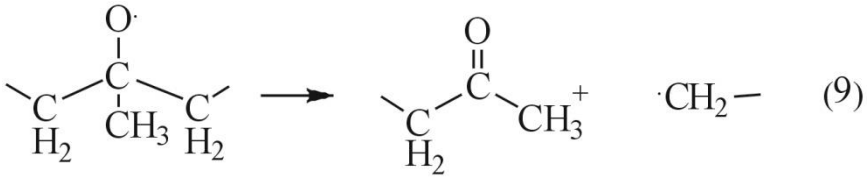

(9)

The damaging effects of oxidation manifest themselves somewhat differently depending on the conditions, but in all cases the changes that take place can compromise the useful properties of the material and limit the lifetime of the part.

1.8 Photostabilization mechanisms in polymers

The photostabilization of polymers involves the retardation or elimination of photochemical process in polymers and plastics. Polymer photostabilization continues to be rapidly advancing area of scientific and technological interest. photodegradation shows that in the absence of strong UV absorption by a polymer, even small amounts of impurities or chromophores are sufficient to induce photo-oxidative degradation. Inhibition or at least retardation of the reaction responsible for degradation is a necessity for a successful UV stabilization [35]. Practice shows that when the polymer contains a photostabilizer, the oxidation rate is much reduced. Stabilizers reduce but do not completely prevent oxidation, so it can be expected that some reactions will take place in the interior of a stabilized polymer. Any consideration of polymer stabilization has to take in account some basic parameters of the additives such as diffusion, solubility, and volatility. It is generally accepted that an efficient additive should be well soluble in the polymer, whereas views on the importance of the mobility or diffusiveness of additives are not as firmly established [36]. The protection mechanism of UV absorbers is based essentially on absorption of the harmful UV radiation and its dissipation in a way that does not lead to photosensitization, e.g. dissipation as heat. In addition to having a very high absorption themselves, these chemicals must be very light stable, because otherwise they would be

consumed too fast in nonstabilizing reaction. An important disadvantage of UV absorbers is the fact that they need a certain absorption depth to provide good protection of a polymer [37]. From the view point of photostability, polymers can be grouped as follows:

i. Highly photostable polymers are commonly used without any photostabilizer added, e.g., poly(tetrafluoroethylene) and poly(methylmethacrylate) and have an outdoor life of many years.
ii. Moderately photostable polymers can be used out doors without any photostabilizer, e.g., poly(ethylenetrephthalate), polycarbonate, poly vinyl fluoride, and poly(vinylidenefluoride) and have life of a few years.
iii. Poorly photostable polymers need extensive photostabilization for outdoor use, e.g., polyolefins, poly (vinyl chloride) (PVC), polystyrene (PS), aliphatic and aromatic polyamides, polyurethanes, diene rubbers, and polymeric coatings and have an outdoor lifetime of less than a year when compounded without any photostabilizer added [38].

An acceptable classification of UV stabilizers groups these additives as follows: UV screeners (absorbers or pigments), excited state deactivators (quencher), hydroperoxide decomposer and radical scavengers **[**37**]**.

1.9 Types of stabilizers :

1.9.1 UV absorbers

UV radiation of wavelength (310) nm is often considered the most damaging to PVC. This wavelength range excites the PVC macromolecules in

the sense of imparting excess energy sufficient to break bonds in the molecular chains. The free radicals formed as a result initiate and participate in the degradation process which is accelerated by the presence of oxygen. The UV protective additives which are frequently included in PVC for outdoor use afford additional and complementary protection. They absorb the incident UV radiation essentially before it can initiate degradation. Carbon black and Titaniumdioxide widely used as pigments for plastics have a light stabilizing effect on many polymers including PVC. They are often referred to as "light screens"; each functions as a physical barrier to radiation both UV and visible. Carbon black absorbs the radiation over both these wavelength ranges and emits the energy in IR region. It is also believed to act as antioxidant by capturing free radicals. TiO_2 has some UV absorption but its screening action is principally due to reflection and scattering of radiation (IR, visible and UV) [39].

Ultraviolet stabilizers that are available commercially can be classified by chemical structure into [40]:

(i) Pigments.

(ii) Metal xanthates.

(iii) Chelates.

(iv) Salicylates.

(v) Salicylanilides.

(vi) Hydroxy phenyl benzotriazoles.

(vii) Hydroxy benzophenones.

Ultraviolet stabilizers can be classified according to their mechanisms of action in the photostabilization process into:

(i) UV absorber and light screeners.

(ii) Quenchers.

(iii) Hydroperoxide decomposers.

(iv) Radical scavengers.

(v) Singlet oxygen, ($^1O_2$), quenchers.

There is some of UV. absorber as shown in Figure (1.3) [41,42].

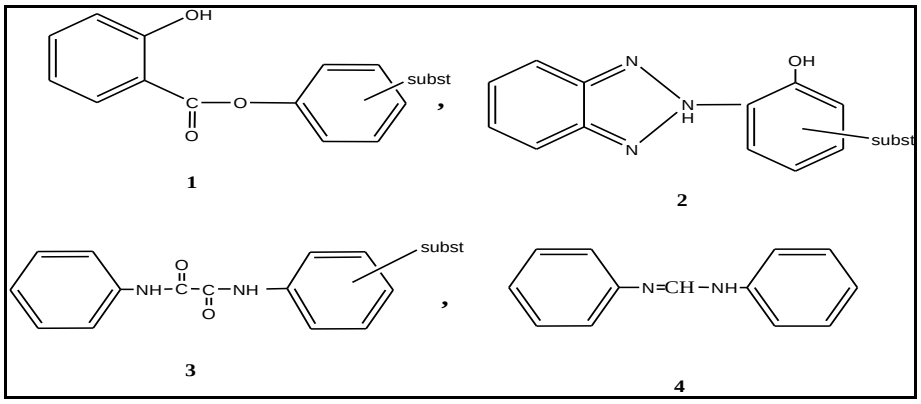

Fig. (1.3): Examples of UV. absorbers

1.9.2 Carbon black

Carbon black is one of the most efficient light absorbers. It consists of very fine particles used together to form primary aggregates. Carbon black absorbs UV radiation more efficiently than conventional pigments, carbon black are efficient light stabilizers for polymers such as polyethylene. Their high efficiency as light stabilizers is probably due to their ability to act as inner filters for UV radiation, and as radical scavengers, because many of the carbon blacks contain stable radicals[47]and quenchers of singlet and triplet

states of polymers. The effectiveness of carbon blacks is dependent upon[44]the type of carbon black, the particle size and the degree of dispersion in the polymer phase.

1.9.3 Antioxidants

Many stabilizers have antioxidant action. Primary antioxidants (without heat- stabilizing action) are also used as additives in PVC either incorporated individually or as constituents of composite commercial stabilizer system. These additives are in general phenol derivatives. Primarily antioxidant action are able to remove peroxide radicals and to decompose hydroperoxide groups(which can act as free radical initiators in the oxidative degradation process) converting them to inactive derivative through chemical reaction. Incorporation of antioxidants can improve the stability of PVC compositions and stability to light [45].

1.9.4Hydroperoxide decomposer

These compounds operate by reacting directly with polymeric hydroperoxide (ROOH). The decomposition of hydroperoxide in polymer to non radical derivatives was first demonstrated [46]. Compounds that belong to this type are organic phosphites and some Nickel chelates. They function by reducing hydroperoxide stochiometrically as presented in the Figure (1.4).

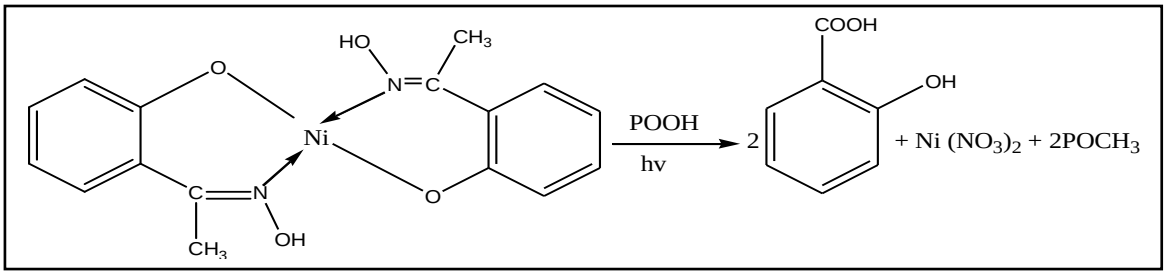

Figure (1.4) Example of Hydroperoxide Decomposer

1.9.5 Hindered amine peroxide decomposer

Hindered amine light stabilizers (HALS) have been found to be remarkably effective in performing both radical trapping and hydroperoxide decomposition. These are one of the most effective photostabilizers for polymers and have been used in a large number of commercial polymers[47].

The mechanism of (HALS) activity includes scavenging of $R^{\cdot}$, ROO and deactivation of hydroperoxides (ROOH), which are based on a complex of chemical transformations. Nitroxide the key intermediate formed from (HALS). Therefore HALS of different structure are able to interconvert in cyclic pathways, destroying species which could lead to polymer degradation and coating species which protect the polymer against degradation.

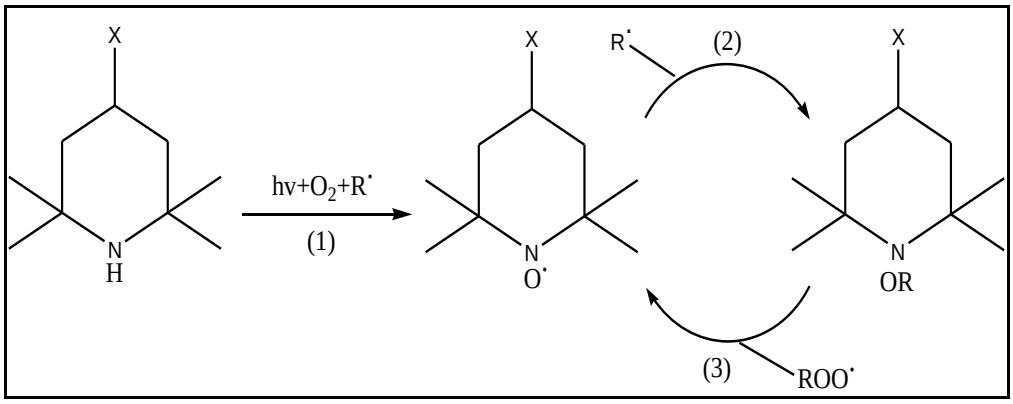

Figure (1.5) The Denisov cycle for mechanism proposed of HALS [47].

Important stabilizing reactions that have been proposed for hindered amines include:

1. Scavenging of alkyl radicals by the nitroxyl radicals derived from HALS[48].

2. Decomposition of alkylhydroperoxides and peracids to nonradical products [49].
3. Scavenging of alkylperoxy radicals and acylperoxy radicals by hindered amines and their NOR derivatives [49]. and
4. Deactivation of polymer-oxygen charge transfer complexes.

Some Commercially Available Hindered Amine Light Stabilizers:

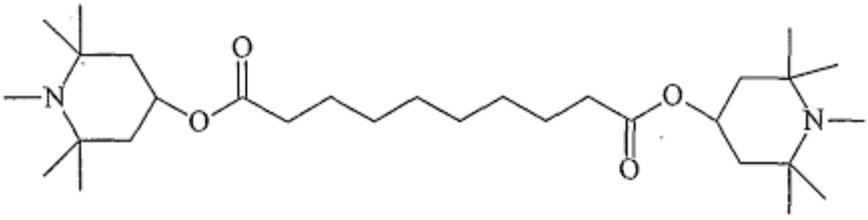

HALS-1

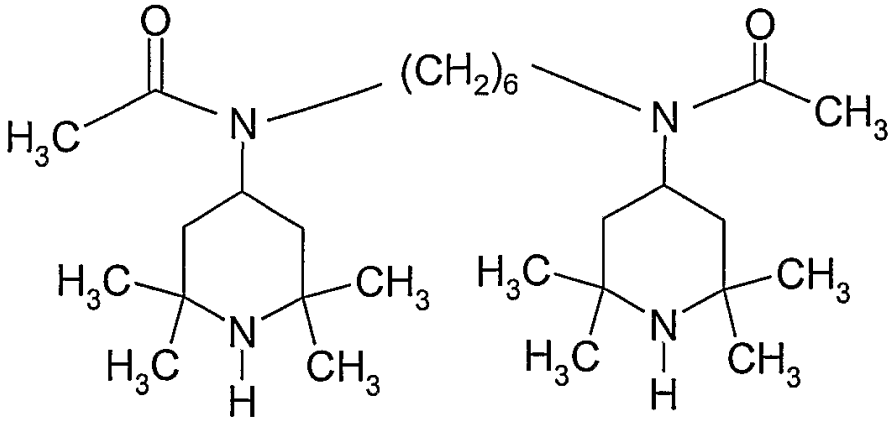

HALS-3

1.9.6 Organotin Carboxylates

Only carboxylates with the following structures are of practical interest. Organotin derivatives of maleic acid may have an additional stabilizer

function, i.e., the Diels-Alder reaction. Their performance is good in all types of suspension, emulsion, and bulk PVC. Optimum results are obtained when they are combined with small amounts of phenolic antioxidants, particularly in plasticized PVC, impact modified PVC, and PVC copolymers. Be a cause stabilizers containing maleic acid occasionally lead to eye and mucous membrane irritations, there have been many attempts to replace them with other systems [50].

1.9.7 Radical scavengers

The scavenging of radical intermediates is another possibility for polymer stabilization, analogous to that used in thermal degradation. Quinones react with alkyl radicals to form radicals that do not initiate polymer oxidation [51].

The radicals scavengers operate by interfering with the propagating step in the oxidative chain and this can be achieved by two routes:

1. Reaction of propagating radicals ($P^{\cdot}$, $PO^{\cdot}$ $POO^{\cdot}$).
2. Reaction with resulting hydroperoxide which are the source of chain branching through the propagating process [52].

1.10 Morphology of polymer

Under ”Morphology” would be concerned with the physical organization of macromolecules. This is important scientifically for the understanding of macromolecular behaviour and for technological and practical applications, as for a polymer of a given chemical constitution it is the determining factor of physical properties. This subject is more than merely describing, shapes

and sizes. It includes in the more generalized sense what is normally termed crystal structure [53].

The bulk polymer morphology compared to suspension which make former there are two areas of interest in PVC processing. The degree of primary particle breakdown is closely related to the mechanical properties and appearance of the final products. A summary of current understanding of the morphology of crystalline polymers the module considers [54] :

(a) Recognition and measurement of crystallinity in polymers

(b) Polymer single crystals

(1) growth and thickness

(2) concept of chain folding

(3) thermal properties

(4) theory of lamellar crystallization

(5) nucleation effects

(6) physical properties

(c) spherulitic(melt) crystalization

(1) single crystals and axialites

(2) spherulite morphology

(3) impurity segregation model of growth

(4) temperature and pressure effects

(5) crystallization from oriented melts

(6) property-morphology relationships

It is worth acquainting the reader at this stage with aspects of bulk polymer morphology compared to suspension which make the former instantly recognisable .If sample of polymer is immersed in plasticizer, allowed to come to equilibrium and then viewed by transmitted light the optical morphology is seen fig.1.7 whereas suspension polymers appear

rounded and slightly different from different manufactures, mass polymer is always typified by square-sided grians and a background of fines, whatever the source [55].

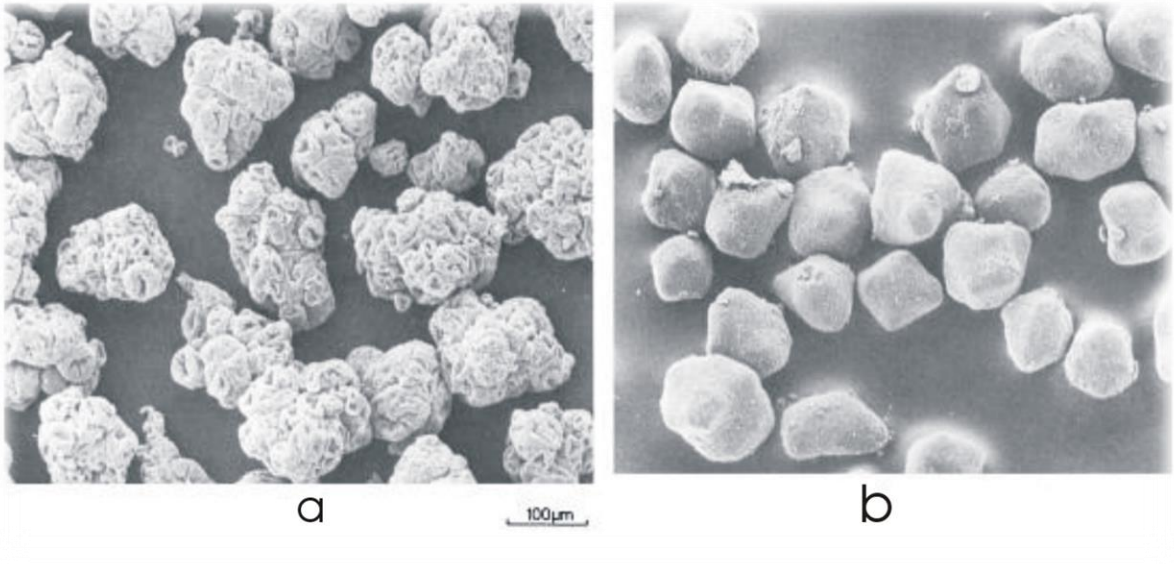

Fig. 1.6: Scanning electron micrographs of typical suspension and bulk PV grians : a) suspension b) bulk [54]**.**

It is clear that PVC morphology covers a wide variety of size scales and for the purposes of discussion three levels are identified. Macro-scopic will refer to all size entities above 10 µm, micro-scopic covers the range 10–0.1 µm and sub-microscopic below 0.1 µ m. significantly different in their macro-morphology, are much more similar in micro-structure and as far as evidence is available at present, virtually identical in the sub-micron range. Because of its commercial importance and the fact that the macro-morphology of suspension PVC is more varied than that from the other processes. The overall size and shape of the final grain together with related properties such as powder flow depend largely on the macro-morphology produced in the droplet coalescence step [56]. Clearly, these parameters depend on the extent to which the polymerization follows routes 1 or 2 (Scheme. 1.2 and Fig.1.8).

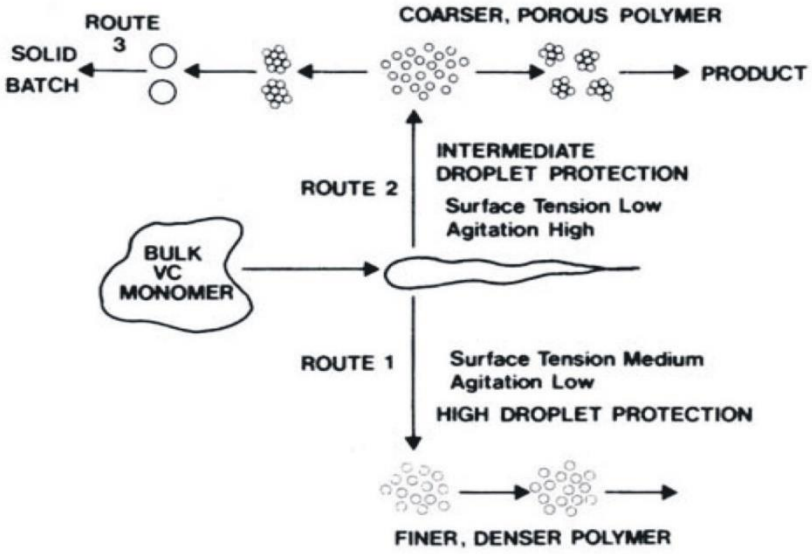

Scheme 1.2: Schematic diagram of the effect of VCM droplet on the macromechanism of polymerization [54].

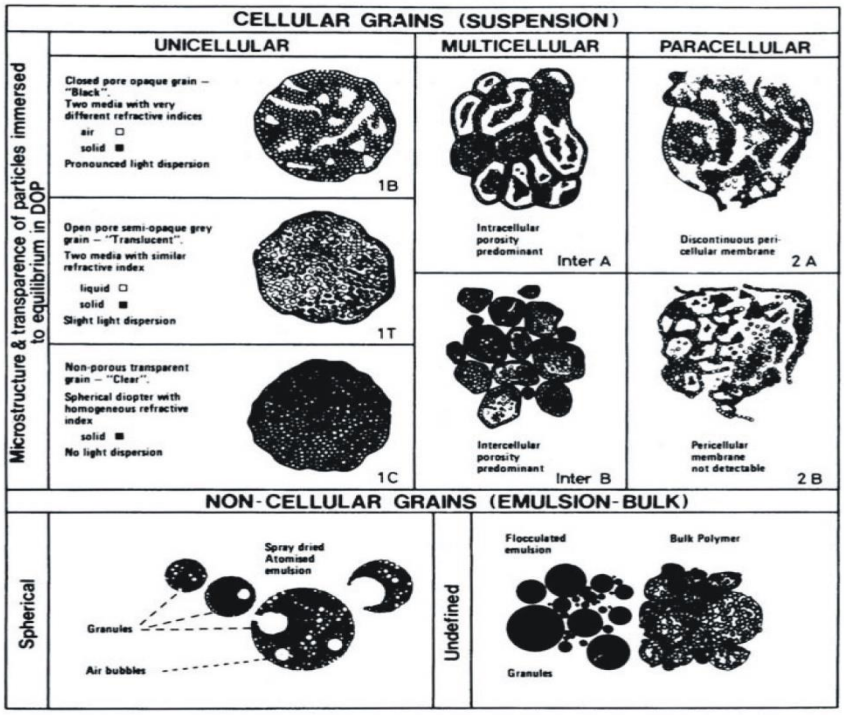

Fig. 1.7: Classification of PVC grians [57]

Depending on the micro-morphology created at about the same time, a variety of internal structures can form. The measurement of porosity by

mercury intrusion is a very powerful tool for characterization of micro-structure. It can give a measure of mean pore diameter and pore size spread as well as the overall porosity of the grain. Since the porosity is a measure of the spaces between primary particle aggregates some ideas of how the aggregates packed when first formed can be gained. If the mean pore diameter is small, for example, it suggests that the degree of stability in the monomer phase was low at the time of flocculation, that a fairly dense floc of aggregates was formed and that a long period of growth, since flocculation occurred at low conversion, has produced considerable densification. Surface area measurements provide useful additional data since the technique measures the area of the aggregates which is accessible, e.g. to plasticiser. This test can also be used to show that the primary particles are solid PVC containing no micro-pores [57].

1.11 Aim of the present work

The aims of the present research are:

a) Synthesis and characterization of metal chelate complexes with potassium 2-(4-isobutylphenyl) propanoate.
b) Estimate the photostabilization activity of these complexes against UV light in presence the poly vinyl chloride polymer.

Chapter Two

2

EXPEREMENTAL

2. *Experimental Part*

2.1 *Materials and reagents*

All of the reagents and starting materials used in the present work are of reagent grade and were used without further purifications unless otherwise noted.

Table (2.1) The reagents and starting materials

No.	Compound	Formula	Mwt	Purity	Supplied from
1	4-(2-isobutylphenyl) propanoic acid	$C_{13}H_{18}O_2$	206.3	95.5%	Scharlau
2	Potassium hydroxide	KOH	56	98%	Scharlau
3	Ethanol	CH_3CH_2OH	46.1	99%	Scharlau
4	Cupper acetate	$Cu(CH_3CO_2)_2$	181.5	98%	BDH
5	Nickel acetate tetrahydrate	$Ni(CH_3CO_2)_2.4H_2O$	189.7	99%	BDH
6	Tinchloride	$SnCl_2$	190	99%	Fluka
7	Zinc acetate dihydrate	$Zn(CH_3CO_2)_2.2H_2O$	219.5	98%	Fluka
8	Cadmium acetate dihydrate	$Cd(CH_3CO_2)_2.2H_2O$	266.5	98%	Fluka
9	Polyvinylchloride	$PVC = (C_2H_3Cl)_n$	n(62.5)	97%	BDH
10	Tetrahydrufuran	C_4H_8O	72.1	99%	LABSCAN
11	Ferrous sulfate	$FeSO_4$	152	98%	Fluka
12	1-10-Phenanthroline	$C_{12}H_8N_2$	180.2	98%	Aldrich
13	Sodium acetate	CH3COONa	82	96%	BDH

2.2 Techniques

2.2.1 Melting point

Melting point apparatus of Electro thermal capillary, Coslab melting point was used to measure the melting points of all prepared compounds. The measurements were carried out in the laboratories of chemistry department/ college of science /Al-Nahrain university.

2.2.2 Fourier Transform Infrared Spectroscopy (FT-IR)

FTIR spectra were recorded by using FTIR 8300 Shimadzu spectrophotometer as CsI disc in the frequency range of (4000-200) cm^{-1}. The spectra were recorded in the laboratories of chemistry department/ college of science /Al-Nahrain university.

2.2.3 Ultraviolet-Visible Spectroscopy (UV-Vis)

The UV-visible spectra were measured using Shimadzu UV-vis. 160 A-Ultra-violet Spectrophotometer in the range (200-800) nm in chemistry department/ college of science /Al-Nahrain university.

2.2.4 Magnetic susceptibility measurements

The magnetic susceptibility values of the prepared complexes were obtained at room temperature using Magnetic Susceptibility Balance of Bruke Magnet B.M.6 (England) in chemistry department/ college of science /Al-Nahrain university

2.2.5 Conductivity measurements

The molar conductivity measurements were obtained using WTW 740 (Germany) in chemistry department/ college of science /Al-Nahrain university.

2.2.6 *Metal analysis*

The metals percentage of the complexes were measured using atomic absorption technique by Shimadzu Atomic Absorption 680 Flame Spectrophotometer. These were carried out in chemistry department/ college of science /Al-Nahrain university.

2.2.7 *Elemental analysis (CHNS)*

The percentage compositions of the elements (CHNS) for the prepared compounds were determined using EuroEA Elemental instrument.These were carried out in chemistry department/ college of science /Al-Nahrain university.

2.2.8 *Microscope and atomic force microscopy (AFM)*

Surface topography of samples were analyzed by atomic force microscopy (AFM) (Veeco, USA), and using microscope (MEIJI TECHNO microscope, Japan), in chemistry department / college of science / Al-Nahrain University.

2.3 *Synthesis of Material*

2.3.1 *Synthesis of potassium 2-(4-isobutylphenyl) propanoate* [58]

A mixture of 2-(4-isobutylphenyl) propanoic acid (0.018) mole (3.68 g) and (0.018 mole) (1.0 g) of KOH (to make the medium alkaline) dissolved in (10 ml) ethanol and then refluxed for three hours and then add excess of KOH to give potassium 2-(4-isobutylphenyl) propanoate. The white precipitate which formed was filtered and recrystallized from ethanol to give the final

product. The steps of the synthesis of potassium 2-(4-isobutylphenyl) propanoate can be shown in reaction (2.1).

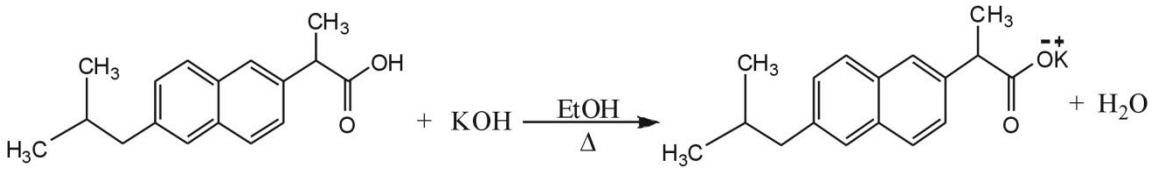

Reaction 2.1: preparation of ligand salt.

2.3.2 *Preparation of complexes* [58]

Addition of ethanol solution (5 ml) of the suitable metal salt (Nickel (II) acetate tetrahydrate [$Ni(CH_3CO_2)_2.4H_2O$] (0.11 g), Tin (II) chloride [$SnCl_2$] (0.07 g), Copper (II) acetate [$Cu(CH_3CO_2)_2$] (0.08 g), Cadmium (II) acetate dihydrate [$Cd(CH_3CO_2)_2.2H_2O$] (0.08 g) and Zinc (II) acetate dihydrate [$Zn(CH_3CO_2)_2.2H_2O$] (0.09 g) to an ethanol solution (5 ml) of potassium2 -(4-isobutylphenyl)propanoate (0.2 g) in 2:1 (ligand : metal) molar ratio were carried out. After reflux for half an hour, crystalline colored precipitates formed at room temperature. The resulting precipitates were filtered off, washed with ethanol, dried and recrystallized from ethanol and dried at 50 ^oC. The steps of the synthesis of complexes can be shown in reaction (3.1).

2.4 *Photodegradation measuring methods*

2.4.1 *Films preparation* [22]

A solution of fixed concentrations of poly vinyl chloride or modified poly vinyl chloride (5g/100ml) in tetrahydrofuran (THF) were used to prepare (40 µm) thickness of polymer films, and finally dried under vacuum at room temperature for 24 hours. The prepared complexes (0.5% concentrations by wieght) were added to the films. The films were prepared by evaporation

technique at room temperature for 24 hours for removing the possible residual tetrahydrofuran solvent, film samples were further dried at room temperature.

2.4.2 *Incident Light Intensity Measurement*

The intensity of the incident light (I_o) was measured by the use of potassium ferrioxalate actenometer methods as described by Hatchard and Parker [59].The actenometer solution (6 x 10^{-3} M) was prepared by dissolving (3.00 g) of $K_3[Fe(C_2O_4)_3].3H_2O$ in (800 ml) of distilled water, (100 ml) of (1 N) H_2SO_4 was added and the whole solution was dilute to one liter with distilled water. The actenometer solution absorbed 100% of incident light at λ= 510 nm.

The light intensity measurement involves irradiation of the actenometer solution for known period of time (3 mins); ferrous ion concentration was estimated spectrophotometrically using 1-10-phenathroline (0.1 %) as complexing agent.According to the Hatchard and Parker [59], Ferric ions are reduced to Ferrous ions:

$$Fe^{3+} \longrightarrow Fe^{2+} \quad \ldots\ldots\ldots\ldots\ldots\ldots (2.1)$$

Thus the phenathroline complex is formed with Fe^{2+}, which strongly absorbed at 510 nm. For Fe^{2+} ion formation (Equation 2.1), the quantum yield (Q) is equal 1.24 [60], so the intensity of light can be calculated after a calibration curve for Fe^{2+} was obtained using the following solution:

i. 4*10^{-4} M of $FeSO_4$ in 0.1 N H_2SO_4
ii. 0.1% w/v phenanthroline monohydrate in water
iii. Buffer solution was prepared from mixing (600 ml) 1N CH_3COONa and (360 ml) of 1N H_2SO_4 dilute to 1L

Solutions of different concentrations of Fe^{2+} ion were prepared from solution (i) by taking different amount in 25 ml. volumetric flask, to each

a- (2 ml) phenanthroline solution was added,

b- (5ml) of buffer solution,

c- (10 ml) of 0.1 N H_2SO_4 and diluting the whole solution to (25 ml) with distilled water.

The volumetric flasks were covered with aluminum foil, kept in the dark for (30 min). Then the optical densities at λ=510 nm were measured. The plot of optical density versus ferrous ion concentration was a straight line, the slope obtained gave the extinction coefficient of ($FeSO_4$) solution, which is equal ($\varepsilon = 1.112\times 10^4 mol^{-1}. dm^3. cm^{-1}$).

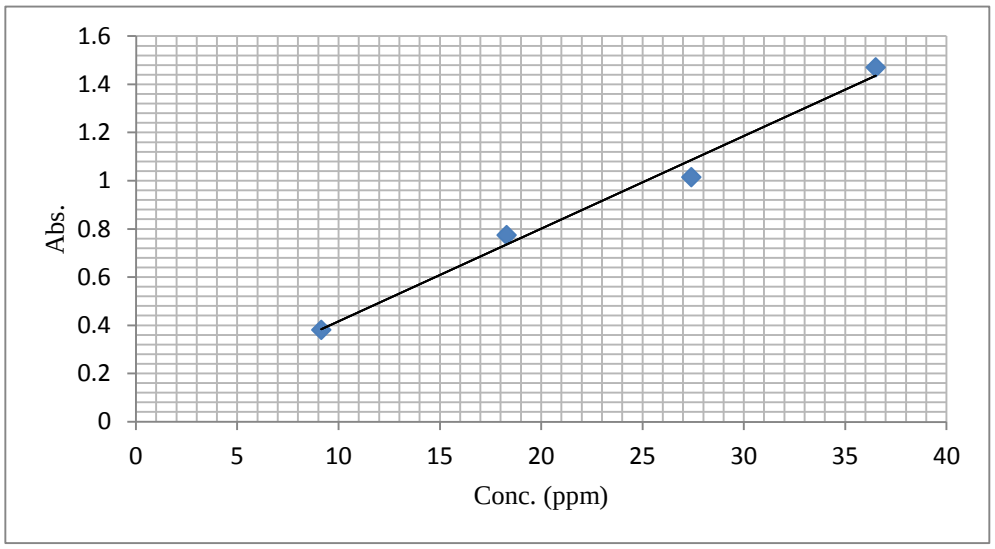

Figure 2.1 Calibration curve

In order to determine the light intensity, (3 ml) of actenometer solution was irradiated. A stream of nitrogen bubble stirred the solution and excluded the dissolved oxygen gas. The cell was irradiated in the same position used for irradiation samples. After illumination, (1ml) of irradiation solution was transferred to (25 ml), volumetric flask, (2 ml) of solution (ii) and (0.5 ml) of solution (iii) then the flask was diluted to (25 ml) with distilled water.

Blank solution was made by mixing (1ml) of unirradiated mixture ferrioxalate solution with other components. The potassium was left in the dark for (30 min), and then the optical density at (λ=510 nm.) was measured.

The intensity of incident light was calculated using the following relation [61] :

$$I_o = \frac{A \times V_1 \times 10^{-3} \times V_3}{Qy \times \varepsilon \times V_2 \times t} \text{ einstein dm}^{-3} \text{ sec}^{-1} \quad \text{..... (2.2)}$$

I_o= Intensity of incident light

A= Absorbance at λ= 510

V_1= Initial volume

V_2= Volume used of irradiation solution

V_3= Final volume (25 ml)

Q_y= Quantum yield (1.24)

ε= Molar extinction coefficient (slope of calibration curve)

t= Irradiation time in seconds

2.5 *Accelerated testing technique*

Accelerated weatherometer Q.U.V. tester (Philips, Germany), was used for irradiation of PVC films. These lamps are of the type (UV-B 313) giving wavelength range between (290 to 360 nm) and the maximum wavelength light intensity is at (313 nm). The polymer film samples were fixed parallel to each other and the lamp of the UV incident radiation is vertically incident on the samples. The distance between the polymer films and the source was 25 cm. The irradiation samples were changed place from time to time to insure homogeneous intensity of incident radiation on all the samples.

2.5.1 *Measuring the photodegradation rate of PVC films using infrared spectrophotometery*

The photodegradation of PVC film samples were followed by monitoring by FT-IR spectra in the range (4000-400) cm^{-1}. The position of

carbonyl absorption is specified at 1722 cm^{-1}, polyene group at 1602 cm^{-1} and the hydroxyl group at 3500 cm^{-1} [5]. The progress of photodegradation during different irradiation times was followed by observing the changes in carbonyl and polyene peaks. Then carbonyl (Ico), polyene (Ipo) and hydroxyl (I_{OH}) indices were calculated by comparison of the FTIR absorption peak at 1722, 1602 and 3500 cm^{-1} with reference peak at 1328 cm^{-1} attributed to oscissoring and bending of CH_2 group, respectively. This method is called band index method which includes [62]:

$$I_s = \frac{A_s}{A_r}$$

A_s = Absorbance of peak under study.

A_r = Absorbance of reference peak.

I_s = Index of the group under study.

The percentage transmittance (%T) is change into absorbance (A) using Beer-Lambert law as in the following equation. (2.3):

$$\left.\begin{aligned} A &= 2 \log \%T \\ A &= \log 100 \log \%T \\ A &= \log(100/\%T) \end{aligned}\right\} \quad \ldots\ldots\ldots\ldots (2.3)$$

Actual absorbance, the difference between the absorbance of base line and top peak (A Top Peak – A Base Line), is calculated using the Base Line method [63].

2.5.2 *Measuring the photodegradation rate of polymer films using Ultraviolet-Visible spectrophotometer* [64]

The Ultraviolet-Visible spectrophotometer type (Shimadzu Uv-Vis. 160) was used to measure the changes in the Uv-Visible spectrum during the irradiation time for each compound at the maximum absorption band (λ_{max}).

The absorption spectrum was measured in the range of (200-400 nm) and the (λ_{max}) at each absorption was also recorded at different irradiation times. The infinite irradiation time was considered and the infinite absorption (A_∞) was assumed to be after the infinite irradiation time.

The first order equation was used to determine the photodegradation rate constant for modified polymer (K_d):

$$\ln(a-x) = \ln a - K_d\, t \quad \text{.....(2.4)}$$

Where a, represent the stabilizer concentration before irradiation and x, represent the change in stabilizer concentration after irradiation time (t).

If A_o represent the absorption intensity of the polymer film containing stabilizer before irradiation, and A_t represent the absorption intensity after (t) time of irradiation, then:

$$a = A_o - A_\infty \quad \text{.....(2.5)}$$

$$x = A_o - A_t \quad \text{.....(2.6)}$$

$$a - x = A_o - A_\infty - A_o + A_t = A_t - A_\infty \quad \text{..... (2.7)}$$

Then equation (2-1) becomes

$$\ln (A_t - A_\infty) = \ln(A_o - A_\infty) - K_d t \quad \text{..... (2.8)}$$

Thus a plot of ln (A_t-A_∞) versus irradiation time (t) gives straight line with a slope equal to (K_d) which indicates that photodecomposition of the modified polymers is first order.

2.5.3 *Measuring the photodegradation by weight loss* [65]

The stabilizing potency of the stabilizer was determined by measuring the weight-loss percentage of photodegraded PVC films in absence and in presence of additives.The weight loss measurements were carried out according to the following equation;

Weight loss % = $(W_1 - W_2 / W_1)\ 100$ …… (2.9)

Where W_1 is the weight of the original sample (before irradiation) and W_2 is the weight of sample after irradiation.

2.5.4 *Determination of viscosity average molecular weight* $(\bar{M}_v)$ *using viscometry method*

The viscosity property was used to determine the molecular weight of polymer, using the Mark-Houwink relation [66].

$[\eta]=K\bar{M}_v^{\alpha}$……..(2.10)

$[\eta]$ = is the intrinsic viscosity.

$\bar{M}_v$ = is the molecular weight of polymer.

K, α = are constants dependent upon the polymer-solvent system at a particular temperature.

The intrinsic viscosity of a polymer solution was measured with an Ostwald U-tube viscometer. Solutions were made by dissolving the polymer in a solvent (gm/100ml) and the flow times of polymer solution and pure solvent are t and t_o respectively. Specific viscosity (η_{sp}) was calculated as follows:

$$\eta_{re} = \frac{t}{t_o} \text{……..(2.11)}$$

η_{re} = Relative viscosity.

t = the flow times of polymer solution.

t_o = the flow times of pure solution.

$$\eta_{sp} = \eta_{re} - 1 \quad \text{.....(2.12)}$$

η_{sp} = Specific viscosity.

The single–point measurements were converted to intrinsic viscosities by the relation (2.11).

$$[\eta] = \left(\sqrt{2}/c\right)\left(\eta_{sp} - \ln\eta_{re}\right)^{1/2} \quad \text{..... (2.13)}$$

C = Concentration of polymer solution (gm/100ml).

By applying equation 5, the molecular weight of degraded and un-degraded polymer can be calculated. Molecular weights of PVC with and without additives were calculated from intrinsic viscosities measured in THF solution using the following equation;

$$[\eta] = 1.38 \times 10^{-4}\, Mw^{0.77} \quad \text{..... (2.14)}$$

Mw = are the molecular weights of PVC.

Equation (2-12) was used to calculate $(\overline{M}_v)$ for PVC without additives before irradiation, and equation (2-7) used to measure $(\overline{M}_v)$ of polymers with additives after irradiation.

The quantum yield of main chain scission (Φ_{cs}) was calculated from viscosity measurement using the following relation [67].

$$\Phi_{cs} = (CN_A/\overline{M}_{v,o})\left[([\eta_o]/[\eta])^{1/\alpha} - 1\right]/I_o\, t \quad \text{.....(2.13)}$$

Where:

C = concentration.

N_A = Avogadro's number.

$(\overline{M}_{v,o})$ = the initial viscosity – average molecular weight.

$[\eta_o]$ = Intrinsic viscosity of polymer before irradiation.

$[\eta]$ = Intrinsic viscosity of polymer after irradiation.

α = Exponent in the relation: $[\eta] = KM^{\alpha}$.

I_o = Incident intensity

t = Irradiation time in second.

2.5.5 *Measuring the Photodegradation by Morphology Study* [68]

Microscope and atomic force microscopy (AFM) were used to determine the morphology of the sample surfaces before and after 300 hours irradiation time. This devices were used to provide information concerning polymer morphology and permit the changes on the studied surface.

Chapter Three

3

RESULTS & DISCUSSION

3.1 Identification of prepared complexes

3.1.1 Physical properties of prepared complexes

Melting points and physical properties of all the compounds studied are tabulated. The percentage of Ni(II), Cu(II), Zn(II), Cd(II) and Sn(II), in metal chelates were estimated by flame atomic absorption spectroscopy (F.A.A.S) using Shimadzu Atomic Absorption 680 Flame Spectrophotometer. The calculated values were in a good agreement with the experimental values, indicating the purity of the prepared compounds. The physical analytical data, melting point and its complexes are tabulated in Table (3.1).

Table (3.1) Physical data of the ligand and prepared complexes

Comp.	Color	M.P. C°	M.wt g.mol^{-1}	Yield (%)	Molar ratio M:L	Elemental analysis theoretical (Experimental) %			Found (Calc.)
						C %	H %	O %	
L	white	222 - 224	244	83.5	----	63.89(63.19)	7.01(7.02)	13.09(13.56)	----
[$NiL_2(H_2O)_2$]	Pale Green	81 -83	504.7	67.5	1:2	61.81(61.97)	7. 60(7.11)	19.00(18.73)	10.69 (10.74)
$Cu(L)_2$	Dark Green	83 - 87	473.6	66.5	1:2	65.87(66.01)	7.23(6.96)	13.50(12.63)	13.42 (3.36)
[$Zn(L)_2(H_2O)_2$]	Pale yellow	100 - 102	511.4	78.5	1:2	60.99(60.9)	7.48(7.59)	18.75(19.07)	14.57 (14.55)
[$Cd(L)_2(H_2O)_2$]	white	138 - 140	558.4	71.5	1:2	55.87(55.08)	6.85(5.86)	17.70(16.89)	21.61 (21.52)
[$Sn(L)_2(H_2O)_2$]	white	131 - 133	564.7	76.0	1:2	55.24(55.22)	6.78(7.07)	16.98(16.41)	22.50 (22.45)

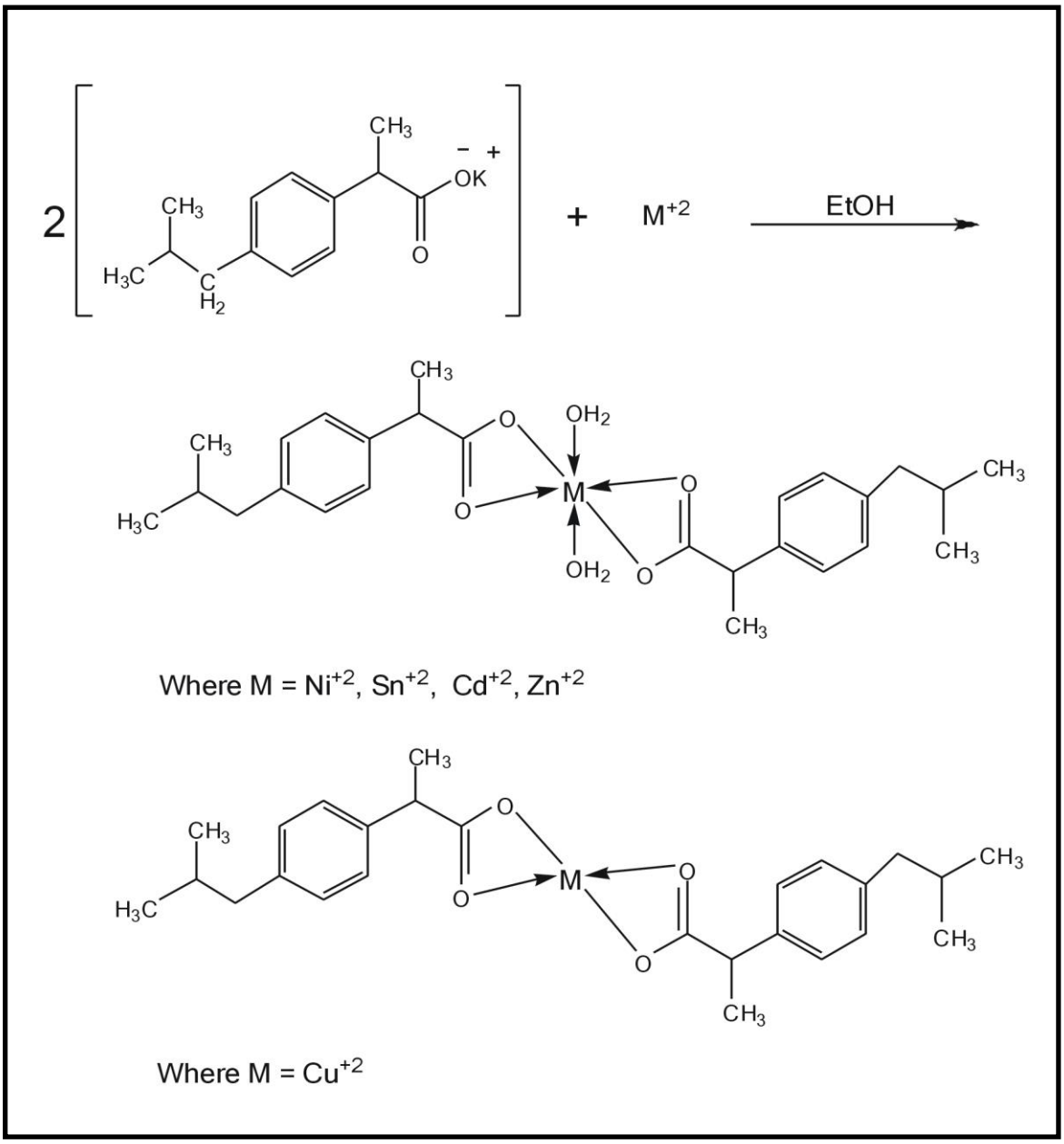

Scheme (3.1): preparation of complexes

The reaction between this ligand with Ni(II), Cu(II), Zn(II), Cd(II) and Sn(II) salts gave different types of complexes.

3.1.2. Characterization of prepared complexes by Infra-Red spectroscopy

The infra-red spectrophotometer technique was used to characterize the prepared compounds through the assignment of stretching vibration bands. Table(3-2) shows tentative assignments of IR peaks for the ligand. The IR spectrum of 2-[4-(2-Methyl Propyl) Phenyl] Propanoate complexes were exhibit the characteristic pattern of the ligand vibrational modes, which were very similar to those of the K salts, but some notable differences can observed in the 3500–3200 cm^{-1}, 1650–1300 cm^{-1} spectral regions attributable to ν(OH) and stretching vibrations of the carboxylate ion (ν_{as} and ν_{s}) respectively.

The IR spectrum of ligand, Figure (3.1) shows abroad band in range (3000-3500cm^{-1})with its maximum at (3340.62cm^{-1}) that refers to streching frequency for ν(OH) vibration confirm the presence of water molecule, strong and sharp absorption band at propanoate acid salt. This band slight shift in prepared complexes which support coordination of these groups with metal ion. The major characteristic bands of the IR spectra was the frequency of the $\nu_{asym}(COO^{-})$ and $\nu_{sym}(COO^{-})$ stretching vibrations. The bands attributed to the carboxylate group for 2-[4-(2-Methyl Propyl) Phenyl] Propanoate Acid potassium salt are centered at 1542.42 cm^{-1}(asymmetric stretching) and 1391.96 cm^{-1}(symmetric stretching). The difference of values between asymmetric and symmetric stretching vibration of COO^{-} in complexes was compared according to equation [$\Delta\upsilon = \upsilon_{asym.(COO^{-})} - \upsilon_{sym.(COO^{-})}$] can give indications about the coordination modalities [69]. When $\Delta\upsilon$ (COO^{-}) displayed a less than 200 cm^{-1}, the carboxylate groups of coordination mode of this ligand with metal ions shows clearly that the ligand behave as bidentate [70]. The $\Delta\upsilon$ for the carboxyl group have been observed between 150-180cm^{-1}. according to these result, the ligand

coordinates through the carboxylate group as a bidentate chelating ligand [71]. The IR spectra of the complexes showed some additional bands in the region of 3357.88-2939.68 cm^{-1} assigned to *v*–OH of coordinated water [72]. another new bands appeared which were supported by the appearance frequency *v*(M–O) bond [73], Stretching of metal-oxygen bands of the complexes appeared in low frequency region (480-432) cm^{-1} [74]. The IR data of the ligand and complexes are shown in Table (3-2), Figures (3-2) to (3-7).

Table (3.2) Characteristic absorption bands of potassium2 -(4-isobutylphenyl) propanoate and its complexes

Compound	υ (COO) asymetrical cm^{-1}	υ (COO) symetrical cm^{-1}	Δυ = [υ asym.(COO) – υ sym.(COO)]	υ M-O
L	1542.42	1391.96	150.46	----
$NiL_2(H_2O)_2$	1560	1398.88	161.12	450
CuL_2	1555.91	1397.99	157.92	473
$ZnL_2(H_2O)_2$	1574.91	1394.44	180.47	433
$CdL_2(H_2O)_2$	1545	1398.32	146.68	430.1
$SnL_2(H_2O)_2$	1550	1392	158	470

The FTIR spectrum of ligand and its complexes was shown in Figures (3.1) - (3.6).

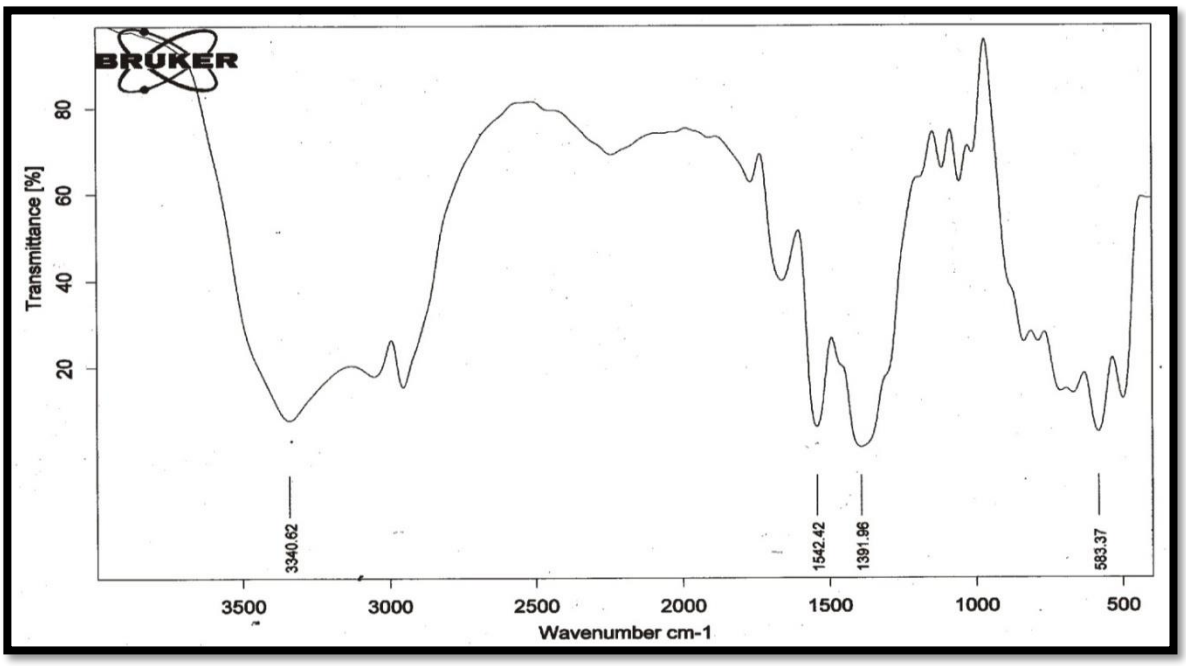

Figure (3.1) FTIR spectrum of ligand

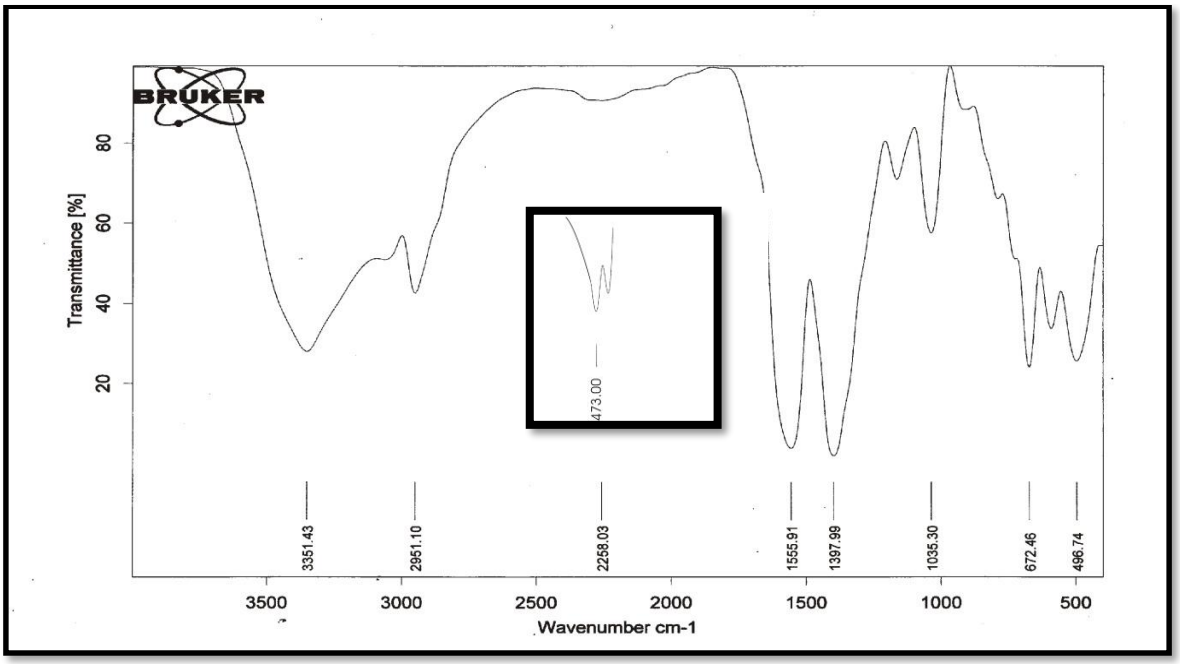

Figure (3.2) FTIR spectrum of CuL_2

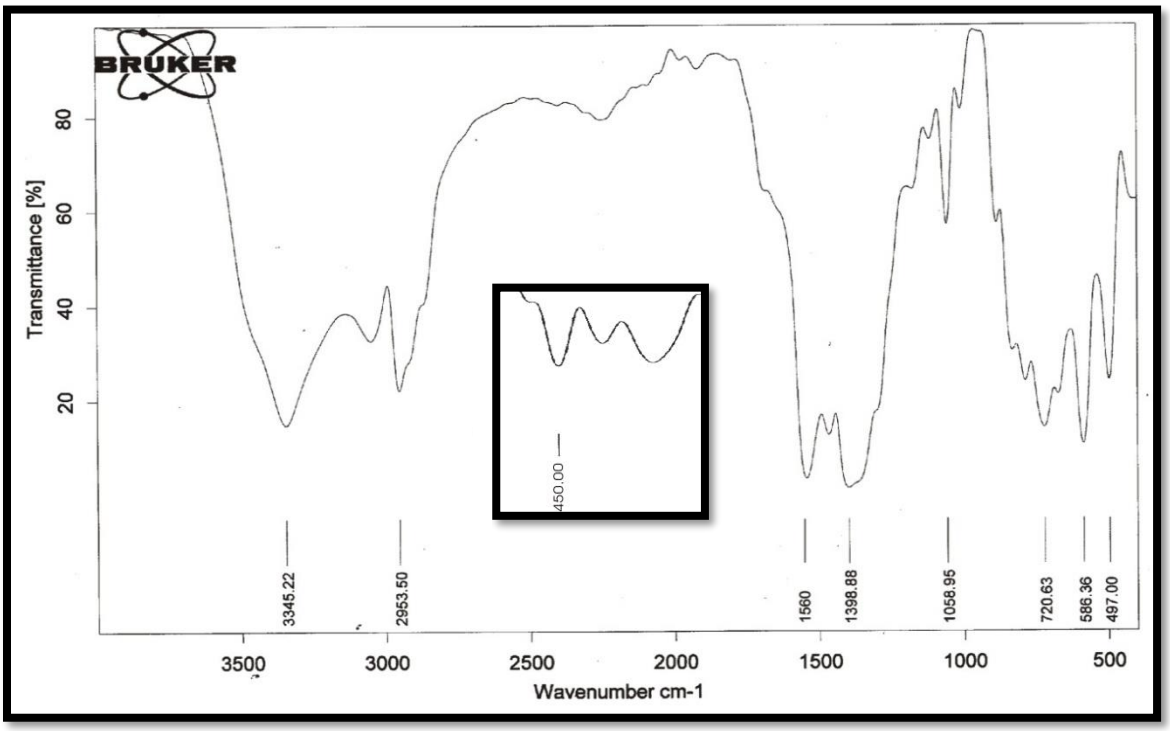

Figure (3.3) FTIR spectrum of $[NiL_2(H_2O)_2]$

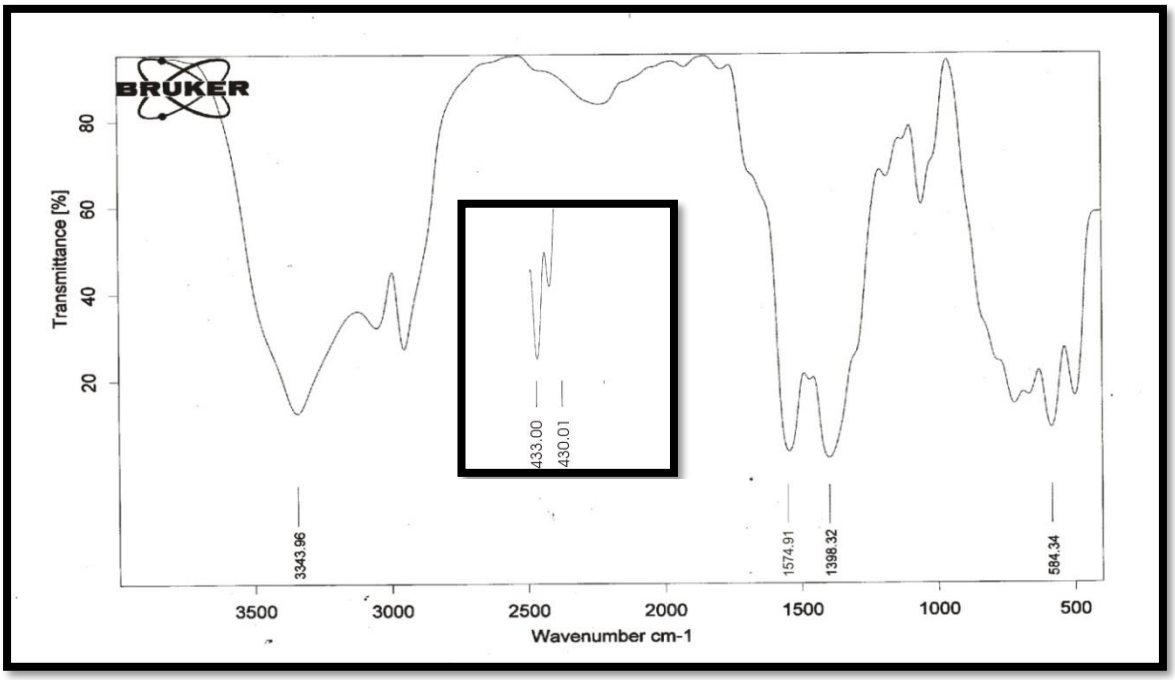

Figure (3.4) FTIR spectrum of $[ZnL_2(H_2O)_2]$

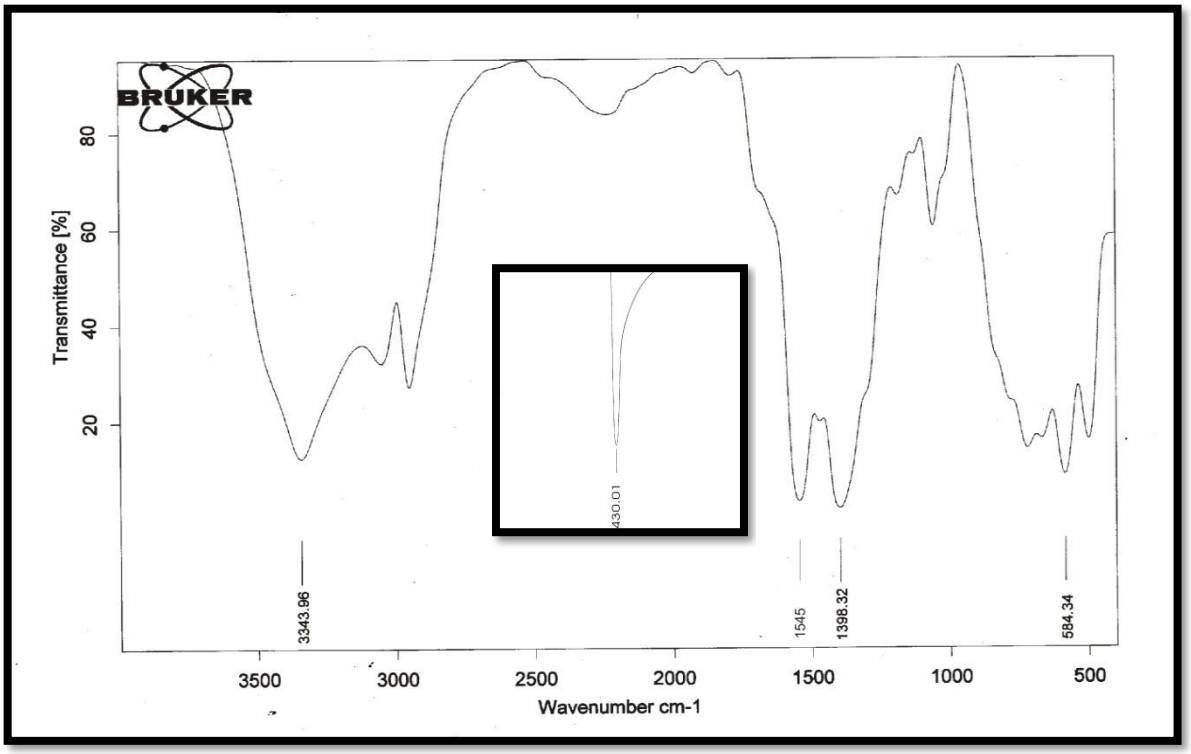

Figure (3.5) FTIR spectrum of $[CdL_2(H_2O)_2]$

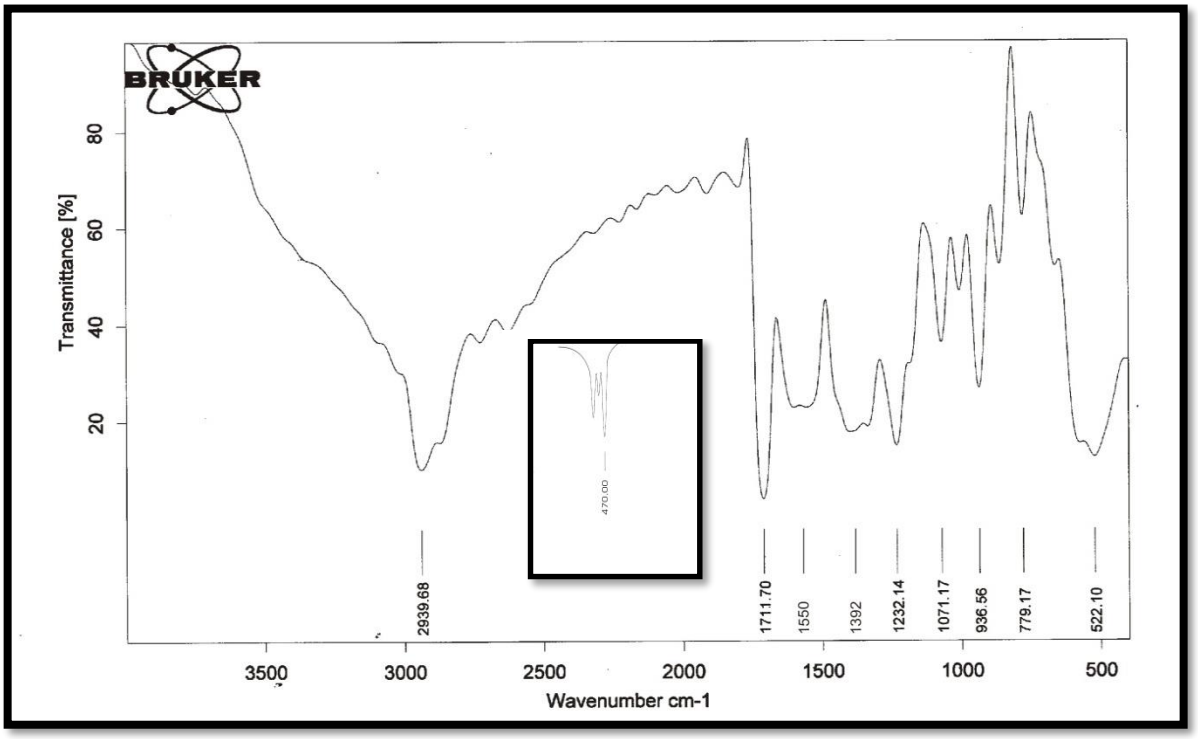

Figure (3.6) FTIR spectrum of $[SnL_2(H_2O)_2]$

3.1.3. *Characterization of prepared complexes by Ultraviolet-Visible spectroscopy, Magnetic susceptibility and Conductivity measurements*

The absorption spectra of the ligand (L) and it's complexes were recorded in DMF solvent in range of 200-800 nm. The electronic spectra of (L) and its complexes were illustrated in Table (3.3). The electronic spectrum of this ligand shows band at (232) nm due to intraligand transition (π-π*) electronic transition. From Table (3.3), complexes also showed the similar electronic transition but with shifting comparing with the ligand. The complexes show one strong absorption band at 225 – 234 nm which may be assigned to benzene ring π→π* transition [75]. In the electronic spectra of copper and nickel complexes, one new band appears, may be assigned to d-d transition. The Cu(II) complex exhibits d-d transition band cantered at 669 nm, attributable to the $^{2}T_{2} \rightarrow {}^{2}E$ transition propose square geometry [76]. The Ni(II) complex shows a band at 450 nm, which may be assigned to the $^{3}T_{1} \rightarrow {}^{3}T_{1(P)}$ transition in a octahedral environment [77].

But Ni(II), Zn(II), Sn(II) complexes were diamagnetic as expected for d^{10} ions, so that no (d-d) transition can be expected in the visible region [78].

Magnetic measurements are widely used in studying transition metal complexes. The magnetic property is due to the presence of unpaired of electrons in the partially filled d- orbital in the outer shell of these elements.

The resultant magnetic moment of an ion is due to both orbital and spin motions [79]. The magnetic moment is given by the following equation:

$Xg = (C * L / 10^9 M) (R-R_o)$ ……. (3.1)

Where:

Xg: magnetic susceptibility

C: constant =1.5

L: length of the tube = 1 cm

M= weight of the sample

R= susceptibility of the tube with the sample

R_o= susceptibility of the empty tube

The value of magnetic susceptibility of the prepared complexes at (25 ºC) temperature is calculated using the following equation:

$$\mu_{eff} = 2.83 \sqrt{X_A.T} \qquad \text{B.M ……. (3.2)}$$

Where: $X_A = X_m + D$

$X_m = X_g$. Mwt.

M.wt. = Molecular weight of complex.

X_g = Mass susceptibility.

D = Pascal`s constant.

X_m = Molar susceptibility which was corrected from diamagnetic.

μ_{eff} = Effective magnetic moment.

T = Temperature in Kelvin (ºC +273).

Magnetic susceptibility measurements provide sufficient data to characterize the structure of the complexes. The magnetic moment for Ni(II) complex is approximately 2.42 B.M., this value refers to a high spin octahedral structure [80]. While the value of Cu(II) complex is approximately 1.64 B.M. indicative of one unpaired electron per Cu (II) ion suggesting this complex within the range consistent to spin free distorted octahedral geometry [81]. the value Cd(II), Sn(II) and Zn(II) Complexes are diamagnetic and there were no magnetic moment recorded [82]. The Magnetic moment values of prepared complexes were illustrated in table (3.3).

Conductivity measurement of these complexes was recorded as a solution in ethanol solvent by dissolving 10^{-3} mole /L in ethanol. This measurement gives an idea if a solution is electrolyte or not. Conductivity measurements have frequently used in elucidation of structure of metal chelates (mode of coordination) within the limits of their solubility. They provide a method of testing the degree of ionization of the complexes, the molecular ions that a complex liberates in solution in case of presence of anions outside the coordination sphere, the higher will be its molar conductivity and *vice versa* [85]. Table (3.3) shows the molar conductivity measurements of complexes, it was shown that all the prepared complexes were found to be non-electrolyte[83].

Table (3.3) electronic spectra of prepared compounds and Conductivity measurement and Magnetic moment of L and its complexes

Compounds	Absorption nm	Transition	Conductivity (µS/cm)	Megnetic moment (BM)
L	232	π-π*	---	---
$[NiL_2(H_2O)_2]$	234 450	π-π* $^3T_1g \rightarrow {}^3T_1g_{(p)}$	12	2.42
CuL_2	225 669	π-π* $^2Eg \rightarrow {}^2T_2g$	10	1.64
$[ZnL_2(H_2O)_2]$	231	π-π*	11	diamagnetic
$[CdL_2(H_2O)_2]$	225	π-π*	11	diamagnetic
$[SnL_2(H_2O)_2]$	225	π-π*	12	diamagnetic

Based on the spectral study, the complexes exhibited octahedral geometry except Cu(II) complex (square planar).

The UV. visible spectrum of ligand and its complexes was shown in Figures (3.7) - (3.12).

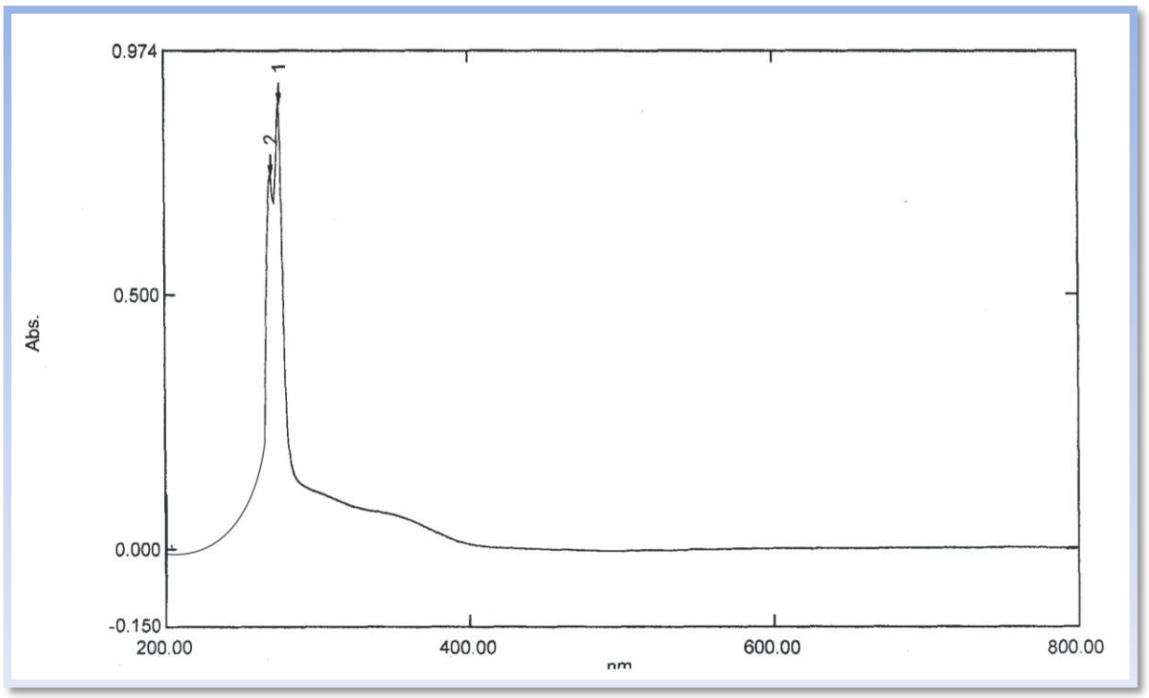

Figure (3.7) The ultraviolet visible spectrum for the ligand in DMF solvent

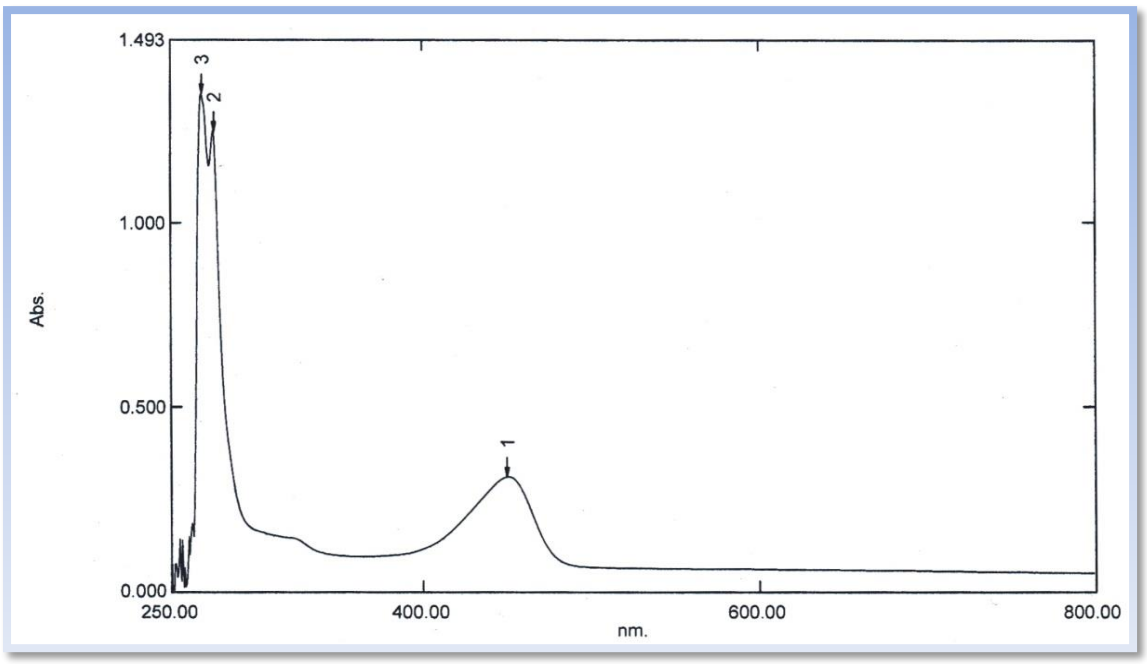

Figure (3.8) The ultraviolet visible spectrum for the [$NiL_2(H_2O)_2$] in DMF solvent

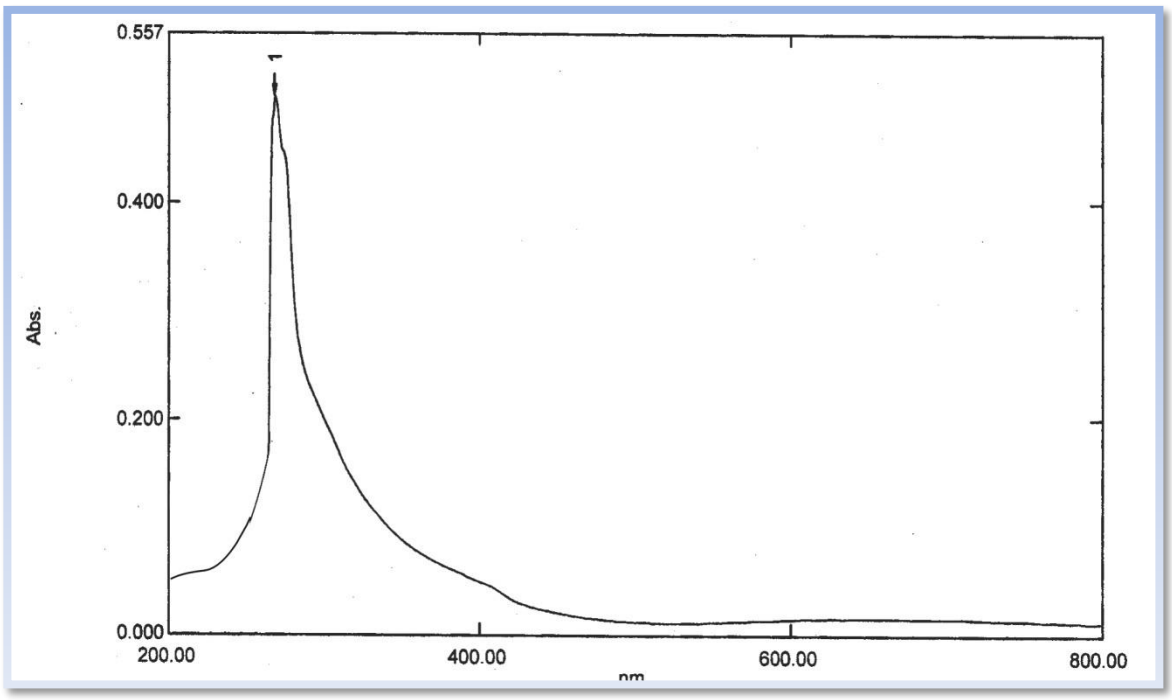

Figure (3.9) The ultraviolet visible spectrum for the CuL_2 in DMF solvent

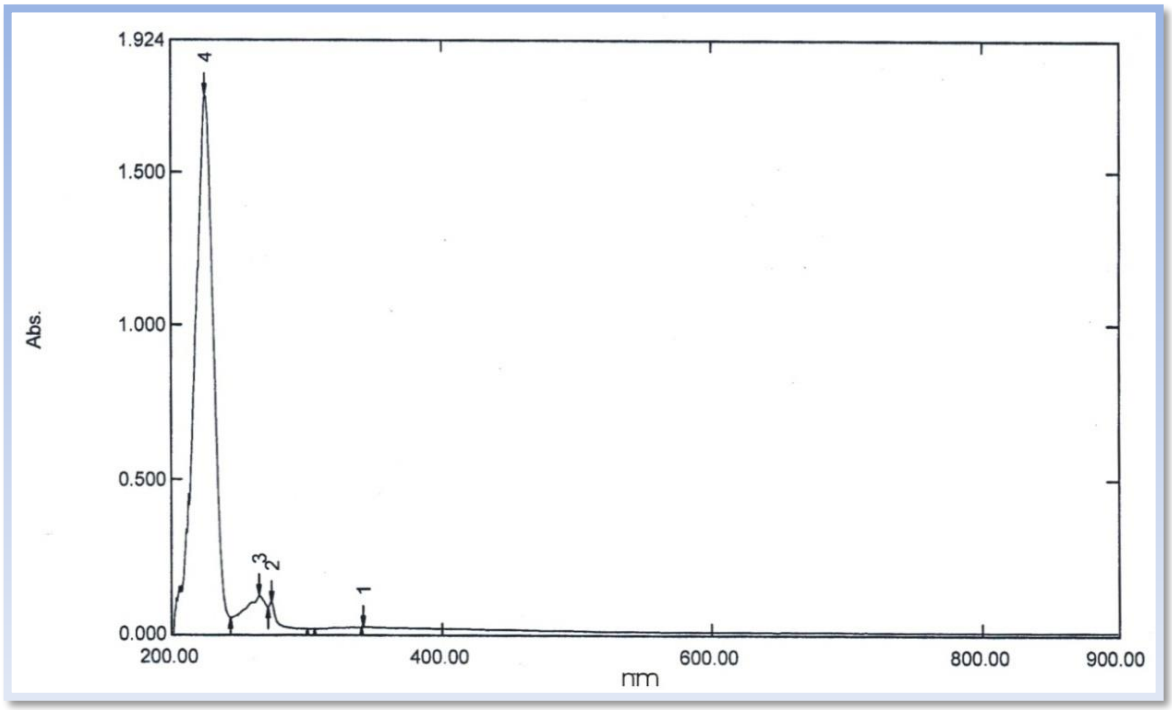

Figure (3.10) The ultraviolet visible spectrum for the $[ZnL_2(H_2O)_2]$ in DMF solvent

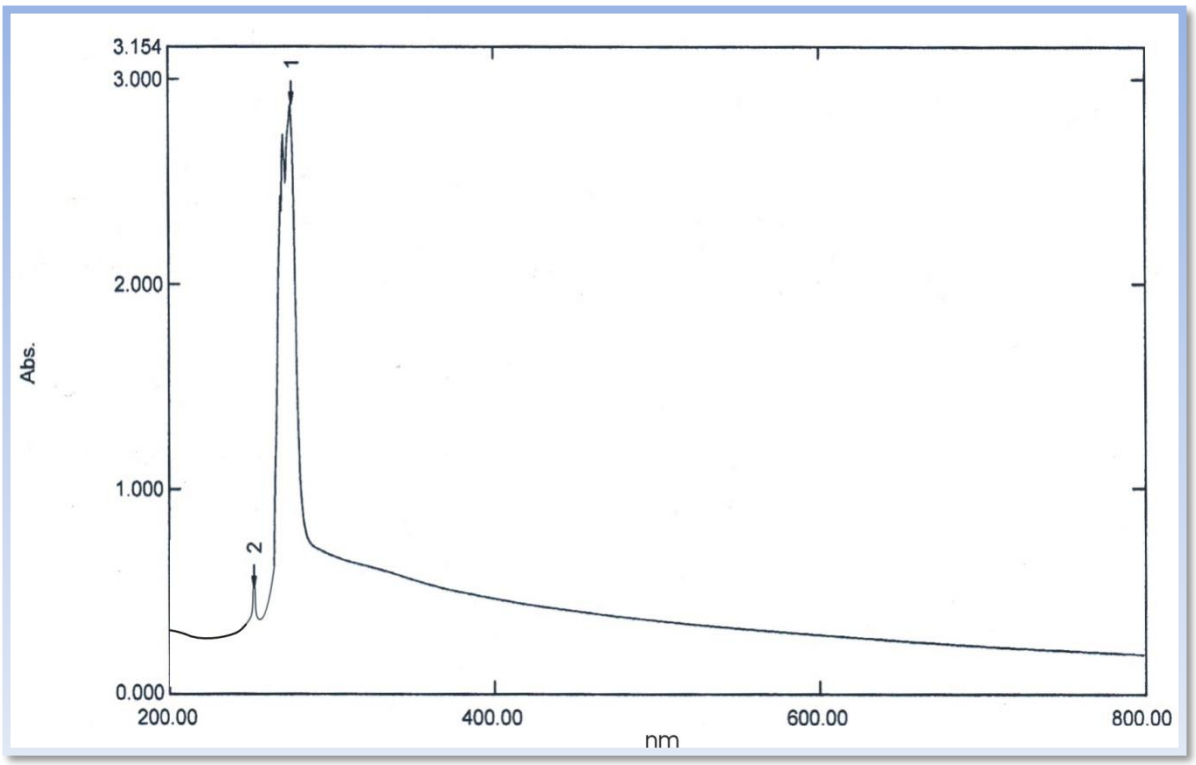

Figure (3.11) The ultraviolet visible spectrum for the $[CdL_2(H_2O)_2]$ in DMF solvent

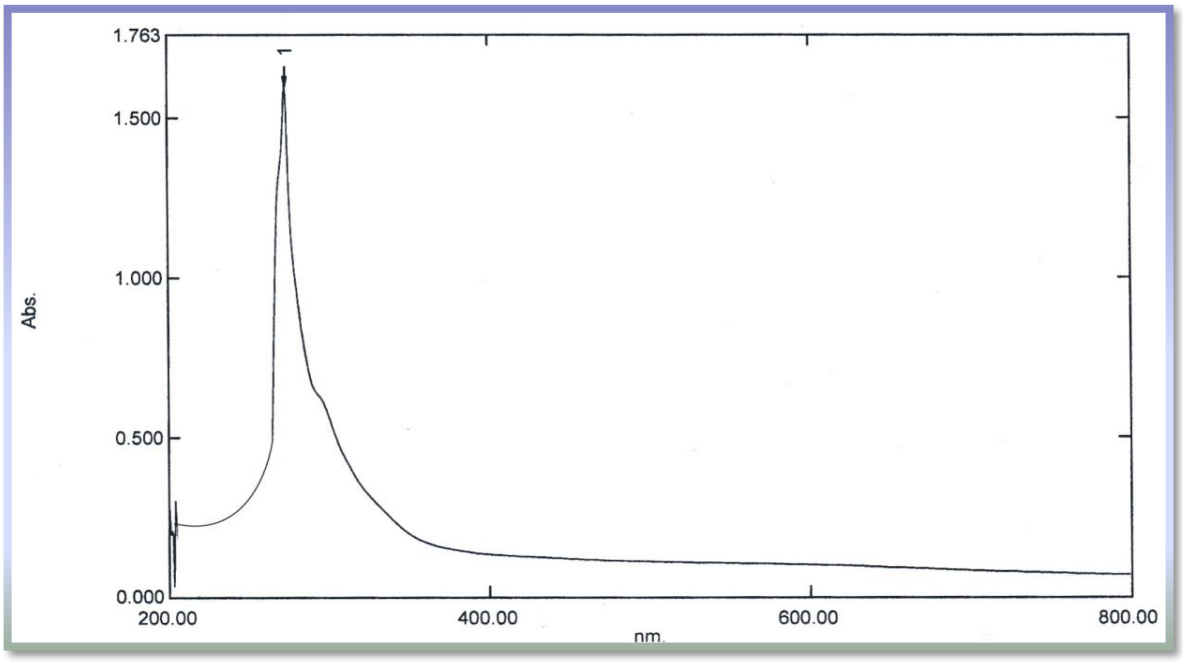

Figure (3.12) The ultraviolet visible spectrum for the $[SnL_2(H_2O)_2]$ in DMF solvent

3.2.1. *Photochemical Study of the PVC films by infra-red spectroscopy*

The irradiation of PVC films with light of wavelength λ=320 nm led to a clear changes in their infrared spectrum.

The photo activity of ligand additives in PVC films has been tested and their efficiency in preventing the photooxidation reaction has been examined by spectroscopic methods.

The prepared complexes were used as additives for the photostabilization of PVC films. The irradiation of PVC films with UV light of wavelength, λ=313nm led to a clear change in the FTIR spectrum [84].

The IR spectra recorded throughout irradiation show an increase in absorbance due to formation of oxidized products so the appearance of intense bands in the 1772 and 1724 cm^{-1}, is attributed to the formation of carbonyl groups related to chloroketone and to aliphatic ketone, respectively. A third band was observed at 1604 cm^{-1} is due to polyene group. The hydroxyl band appeared at 3500 cm^{-1} because of the hydroxyl group [85]. These absorption are calculated as carbonyl index (I_{CO}), hydroxyl index (I_{OH}) and polyene index [86]. **(See chapter 2).**

Therefore, one should expect that growth of hydroxyl index is the measure of the degradation. As seen from Table (3.4) and Figure (3.24) that the presence of Cu**L**$_2$, [Zn**L**$_2$(H_2O)$_2$], [Ni**L**$_2$(H_2O)$_2$], [Cd**L**$_2$(H_2O)$_2$], and [Sn**L**$_2$(H_2O)$_2$], show lower growth rate of hydroxyl index with irradiation time with respect to the PVC without additives (control).

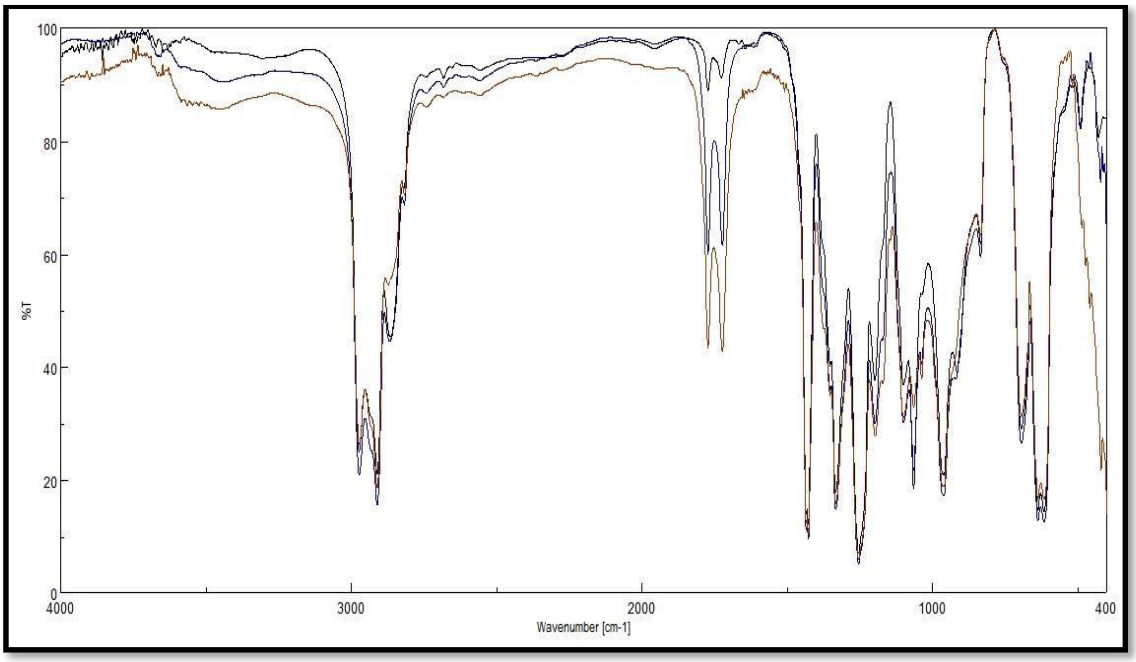

Figure (3.13)Change in IR spectrum of PVC film (40 µm) in the presence of CuL_2 complex. (Numbers n spectra are irradiation time in 150 hours)

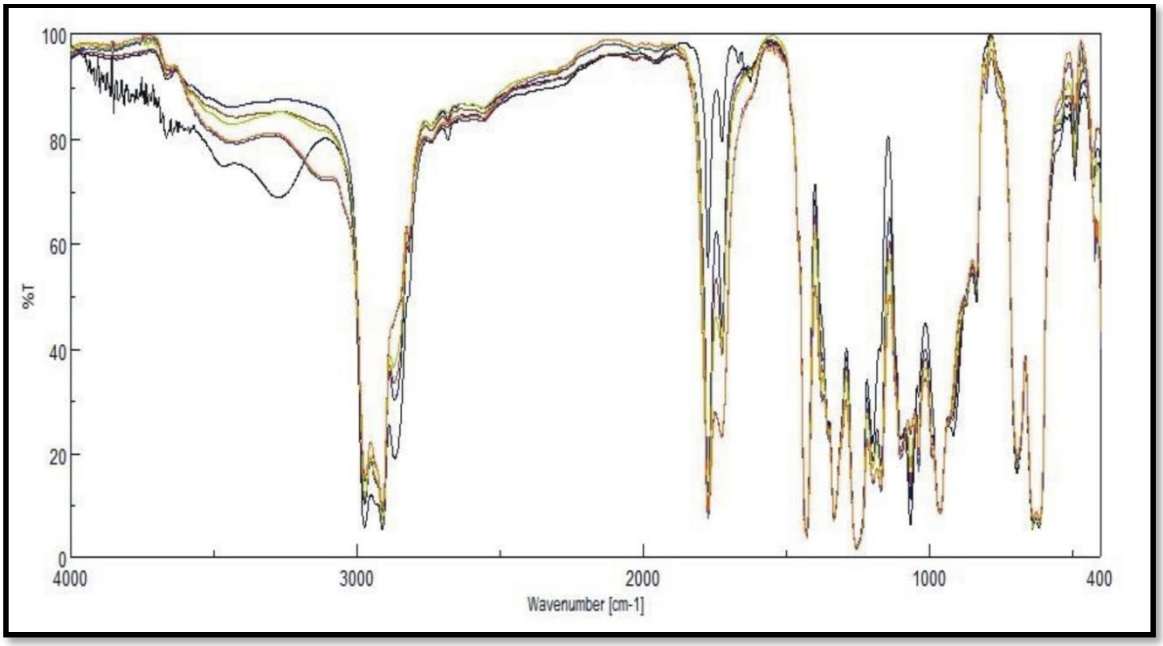

Figure (3.14) Change in IR spectrum of PVC film (40 µm) in the presence of CuL_2 complex. (Numbers n spectra are irradiation time in 300 hours)

Table (3.4) Hydroxyl index (I_{OH}) with irradiation time for PVC films in (40µm) thickness containing 0.5% w\w from the additives

Additives	Irradiation time (hours)					
	0	50	100	150	220	300
PVC (blank)	0.552	0.634	0.731	0.851	1.068	1.269
PVC+[$ZnL_2(H_2O)_2$]	0.549	0.567	0.645	0.767	0.956	1.116
PVC+[$CdL_2(H_2O)_2$]	0.534	0.527	0.586	0.668	0.876	1.006
PVC+CuL_2	0.497	0.468	0.533	0.569	0.791	0.972
PVC+[$SnL_2(H_2O)_2$]	0.484	0.442	0.489	0.531	0.691	0.864
PVC+[$NiL_2(H_2O)_2$]	0.421	0.411	0.456	0.462	0.583	0.764

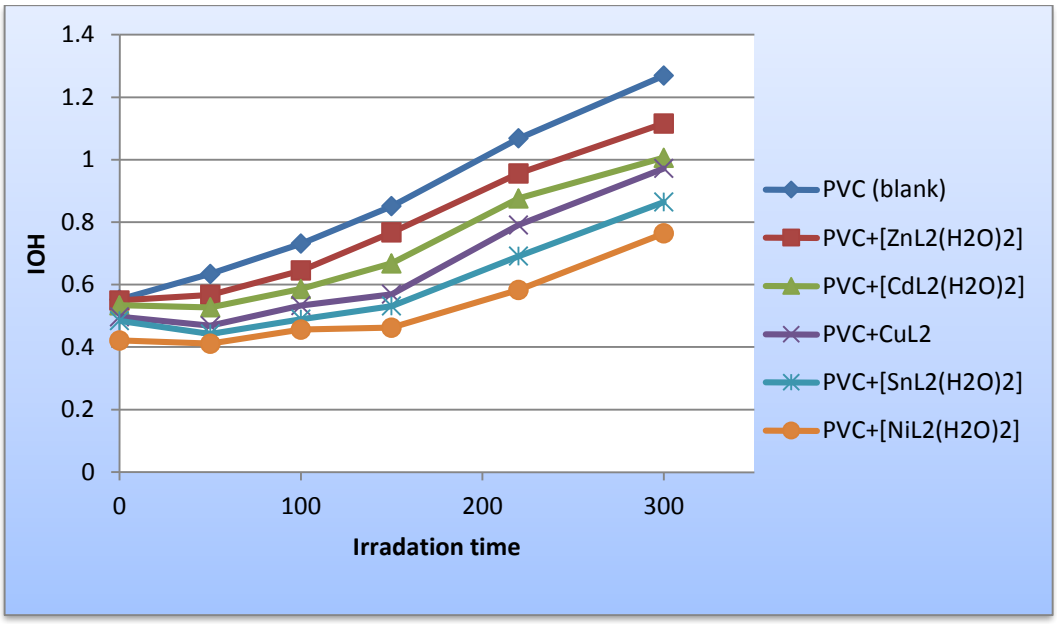

Figure (3.15) The relationship between the (I_{OH}) and irradiation time for PVC films (40µm) thickness containing 0.5%w\w from the additives

So these additives might be considered as photostabilization of PVC films. The induction period shown by these additives is clear.

The good photostabilizer show a longer induction period. Therefore, from Figure (3.15), the $[NiL_2(H_2O)_2]$ is the most active photostabilizer, followed by $[SnL_2(H_2O)_2]$, CuL_2, $[CdL_2(H_2O)_2]$and $[ZnL_2(H_2O)_2]$, are less active.

It was mentioned before that several types of polyene compounds are produced during photodegradation of PVC. Therefore, polyene index (I_{PO}) was monitored with irradiation time and the presence and the absence of these additives. Results are shown in Table (3.5) and Figure (3.16).

Table (3.5) Polyene index ($I_{C=C}$) with irradiation time for PVC films in (40µm) thickness containing 0.5%w\w from the additives

Additive	Irradiation time (hours)					
	0	50	100	150	220	300
PVC (blank)	0.815	0.951	1.091	1.192	1.421	1.565
PVC+$[ZnL_2(H_2O)_2]$	0.754	0.872	0.979	1.087	1.236	1.291
PVC+$[CdL_2(H_2O)_2]$	0.696	0.778	0.891	0.989	1.173	1.184
PVC+CuL_2	0.669	0.732	0.821	0.882	1.094	1.119
PVC+$[SnL_2(H_2O)_2]$	0.592	0.677	0.779	0.814	0.992	1.014
PVC+$[NiL_2(H_2O)_2]$	0.551	0.632	0.729	0.774	0.898	0.921

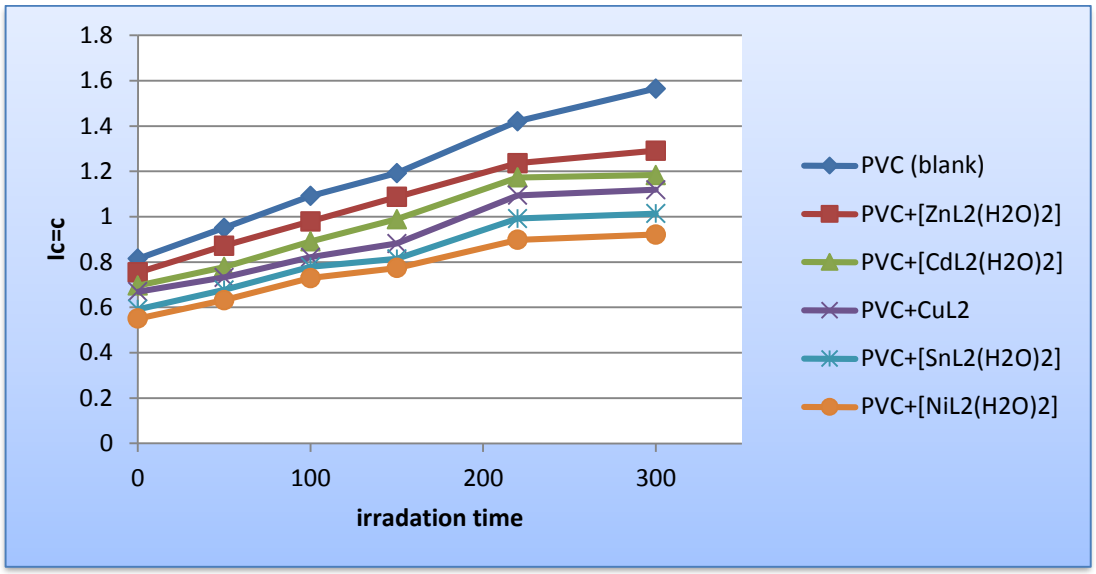

Figure (3.16) The relationship between the ($I_{C=C}$) and irradiation time for PVC films (40µm) thickness containing 0.5%w\w from the additives

It was mentioned before that several types of carbonyl compounds are produced during photodegradation of PVC. Therefore, carbonyl index (I_{CO}) was monitored with irradiation time and the presence and the absence of these additives. Results are shown in Table (3.6) and Figure (3.17).

Table (3.6) Carbonyl index (I_{CO}) with irradiation time for PVC films in (40µm) thickness containing 0.5%w\w from the additives

Additive	Irradiation time (hours)					
	0	50	100	150	220	300
PVC (blank)	0.815	0.951	1.091	1.192	1.421	1.565
PVC+[$ZnL_2(H_2O)_2$]	0.754	0.872	0.979	1.087	1.236	1.291
PVC+[$CdL_2(H_2O)_2$]	0.696	0.778	0.891	0.989	1.173	1.184
PVC+CuL_2	0.669	0.732	0.821	0.882	1.094	1.119
PVC+[$SnL_2(H_2O)_2$]	0.592	0.677	0.779	0.814	0.992	1.014
PVC+[$NiL_2(H_2O)_2$]	0.551	0.632	0.729	0.774	0.898	0.921

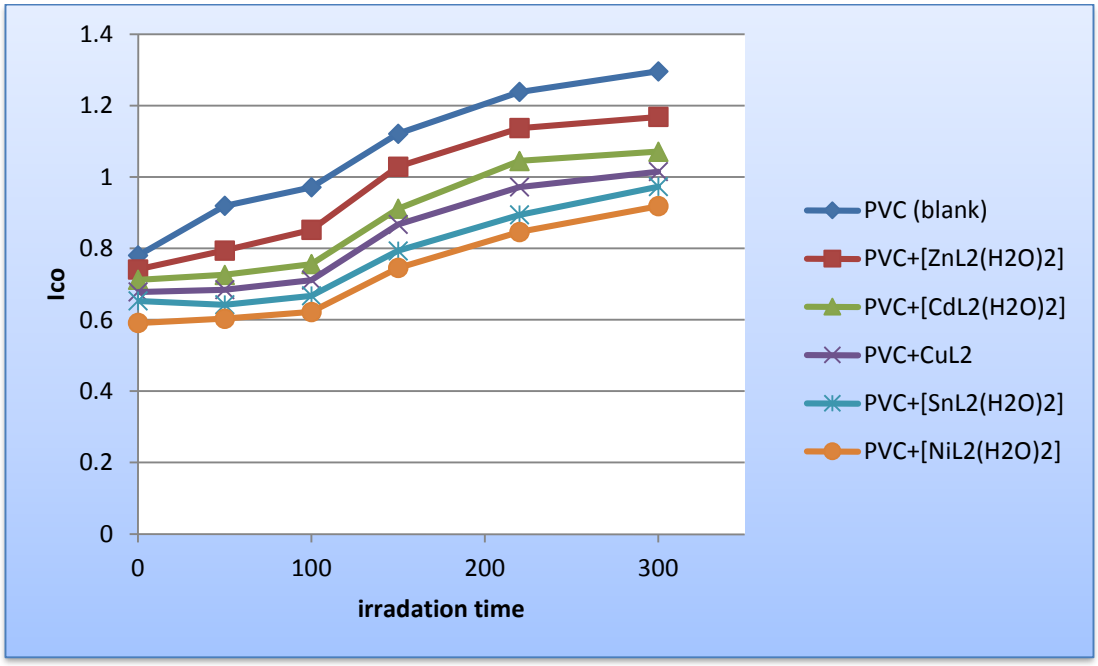

Figure (3.17) The relationship between the (I_{CO}) and irradiation time for PVC films (40µm) thickness containing 0.5%w\w from the additives.

Again the results confirmed that all these additives are photostabilizer for PVC films. However, from the rate of carbonyl index (I_{CO}) growth, and from the Figure (3.17), the $[NiL_2(H_2O)_2]$ is the most active photostabilizer, followed by $[SnL_2(H_2O)_2]$, CuL_2, $[CdL_2(H_2O)_2]$ and $[ZnL_2(H_2O)_2]$, are less active.

In unstabilized PVC films the carbonyl absorbance increased slowly during the first 50 hours and after this period the rate of formation of carbonyl groups increase quickly.

3.2.2. *Ultra-violet spectral studies of photodegradation rate of PVC films*

The poor light stability of PVC must be caused by structural abnormalities that are present to vary the extents in different types of commercially available polymer samples, such as unsaturated end groups, and oxidized structures such as hydroperoxide groups and carbonyl groups [87,88]. The PVC contains only C-C, C-H and C-Cl bonds, is not expected to absorb light of wavelength longer than (190-220nm). The fact that free radicals are formed after irradiation at longer wavelengths (220-370 nm) indicates that some kinds of chromophores must be present in a polymer [89].

It is generally accepted that carbonyl formed during UV irradiation of polymers, is most probable and are responsible for the yellow coloration of the polymer [90].

The carbonyl groups generated during the photooxidation process of polymer, extend the polymer film absorption to longer wavelengths [93]. These

groups absorb light when they irradiated with light of wavelength between (200-700 nm) and activated to the singlet and triplet excited states which enhances various successive photooxidation reactions [91].

The physical properties of additives and polymers play a very important role in determining the additives efficiency in photostabilization or photodegradation of polymers. For example, the compatibility that any type of additive (photostabilizer, antioxidant, thermal stabilizer…. etc.) must be evenly distributed which requires that it be compatible with the polymer matrix [92]. The additives used in this study were chosen to be completely soluble in polymer solvent (THF).

It has been notice that the additives used in the present work are photodecomposed during the photolysis. Thus the photo decomposition rate constant (K_d) was calculated, (See Chapter 2). The K_d values were computed using the UV. spectra changes of PVC films thickness 40μm containing 0.5% w/w from additives.

The additives were completely soluble in polymer solvent THF. It was noticed that the additives used in the present work are photo decomposed during the photolysis. The photodecomposition rate constant values of the additive were computed using the UV spectra changes of PVC films thickness (40μm) containing 0.5% of additives and that is clear in Figure 3.18 and 3.19. It is concluded from this figure that during the aging process, concentration of the double bonds are increased correspondingly. The plot of irradiation time versus ln (A_t-A_∞), gives straight line which indicate primarily the first order reaction. The slope equal to the decomposition rate constant K_d. Figures (3.20) to (3.25) shows the variation of ln (A_t - A_∞) with irradiation time for all additives in PVC

films at λ=320nm. The values of the first order rate constant of all the modified polymers films (k_d) calculated by the same way and shown in Table (3.7).

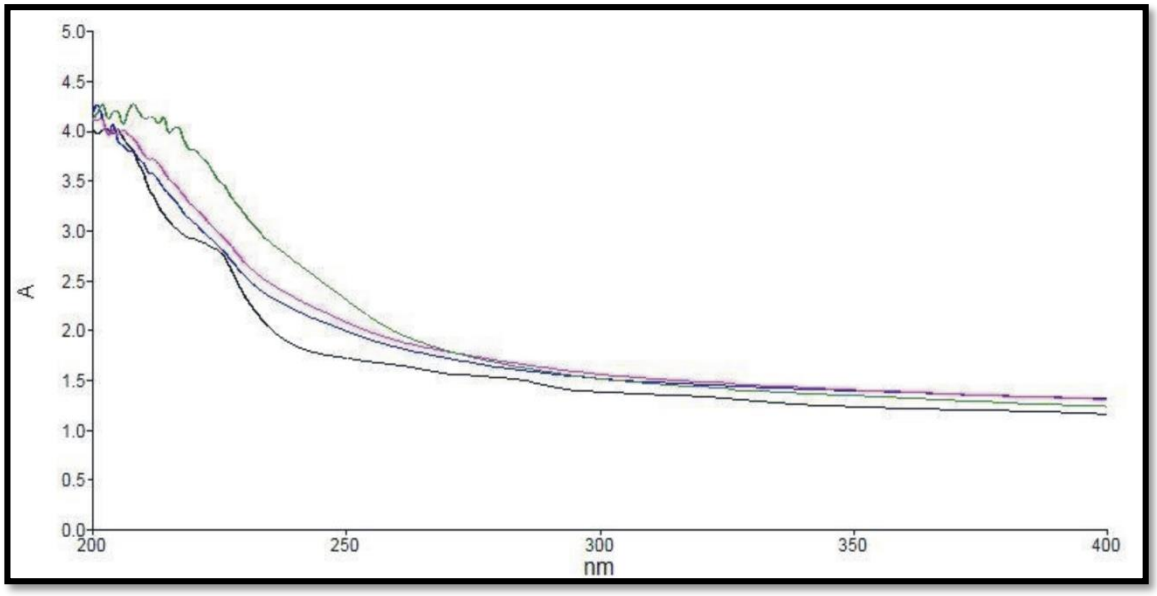

Figure (3.18) UV–Vis spectra of PVC + $[CdL_2(H_2O)_2]$ time:1-50, 2-100, 3-150 and 4-220

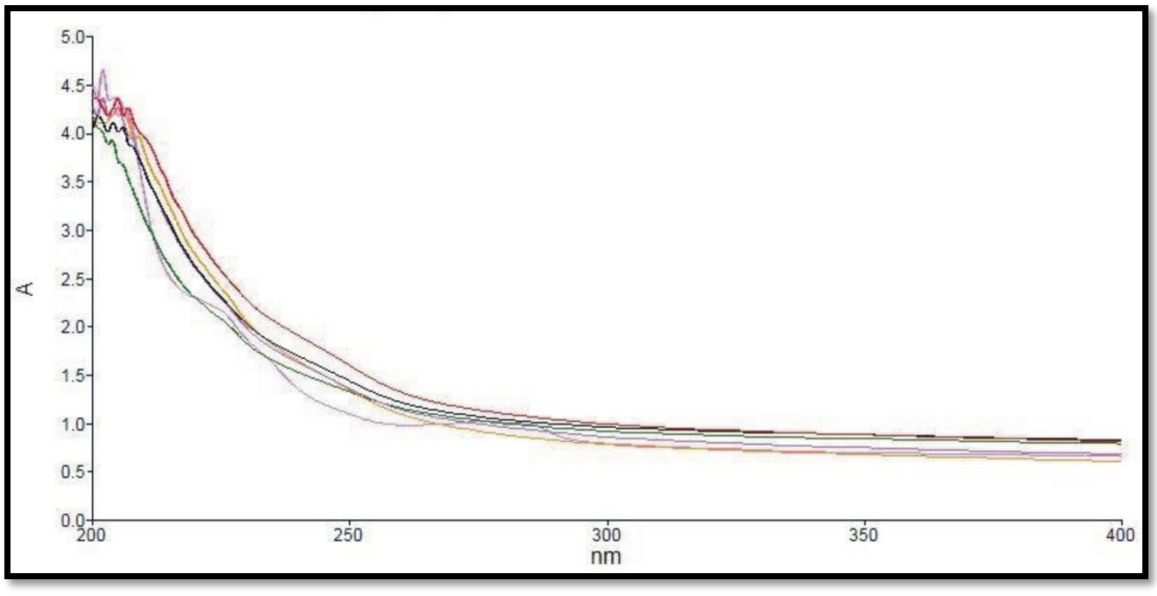

Figure (3.19): UV–Vis spectra of PVC+ $[NiL_2(H_2O)_2]$ time:1-50, 2-100, 3-150, 4-220 and 4-300.

Table (3.7) Photodecomposition rate constant (K_d) of PVC films thickness (40μm) containing 0.5%w\w of additives

Polymers	K_d (S^{-1})
PVC (control)	1.972×10^{-3}
PVC + CuL_2	1.323×10^{-3}
PVC + $[NiL_2(H_2O)_2]$	1.061×10^{-3}
PVC + $[ZnL_2(H_2O)_2]$	4.463×10^{-4}
PVC + $[CdL_2(H_2O)_2]$	3.067×10^{-4}
PVC + $[SnL_2(H_2O)_2]$	2.789×10^{-4}

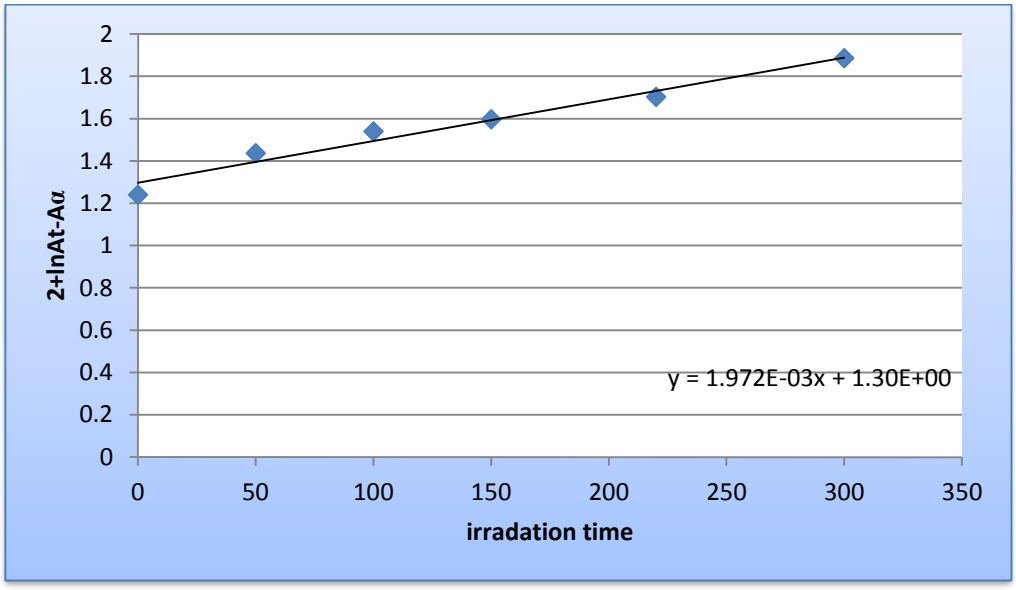

Figure (3.20) Variation of natural logarithm of ln ($A_t - A_\infty$) with irradiation time of PVC (blank) film.

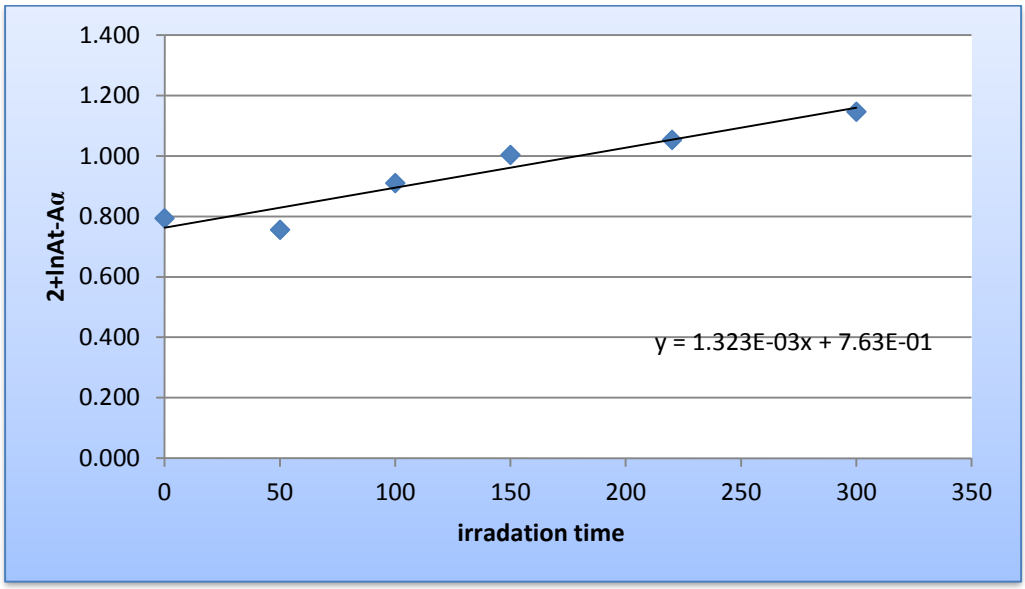

Figure (3.21) Variation of natural logarithm of ln ($A_t - A_\infty$) with irradiation time of CuL_2 in PVC film.

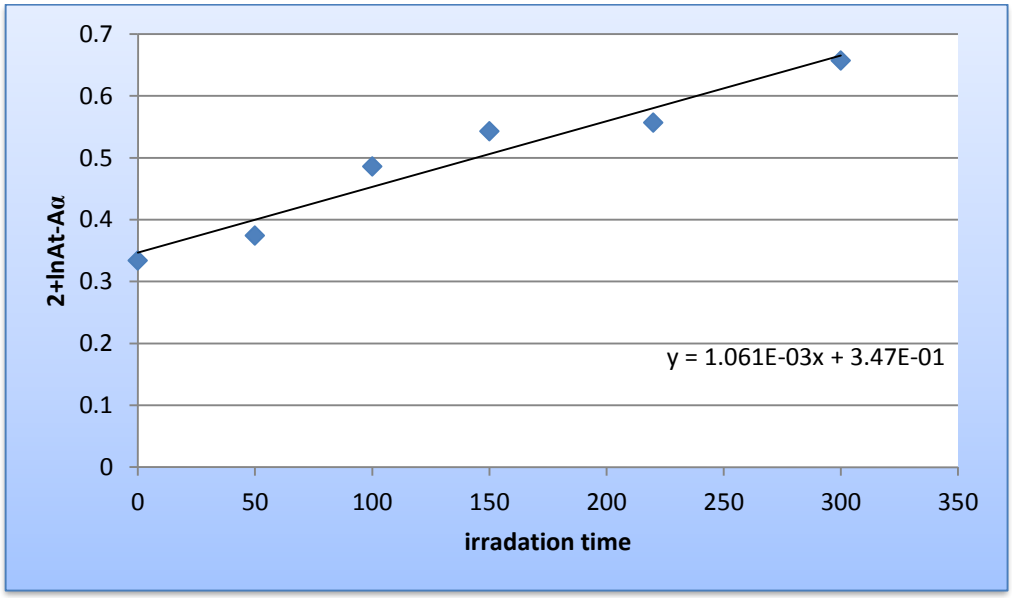

Figure (3.22) Variation of natural logarithm of ln ($A_t - A_\infty$) with irradiation time of $[NiL_2(H_2O)_2]$ in PVC film.

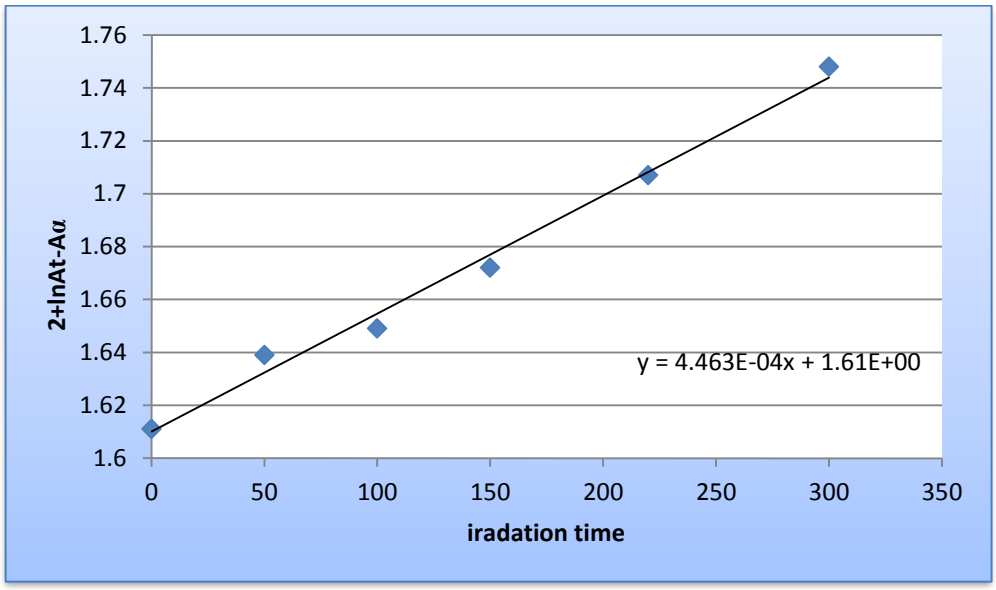

Figure (3.23) Variation of natural logarithm of ln ($A_t - A_\infty$) with irradiation time of $[ZnL_2(H_2O)_2]$ in PVC film.

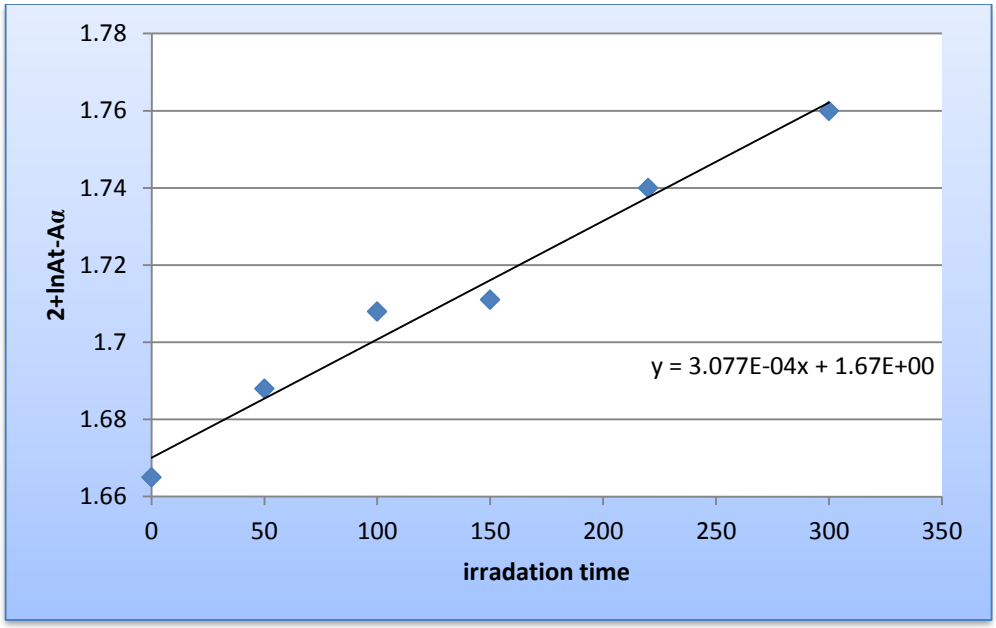

Figure (3.24) Variation of natural logarithm of ln ($A_t - A_\infty$) with irradiation time of $[CdL_2(H_2O)_2]$ in PVC film.

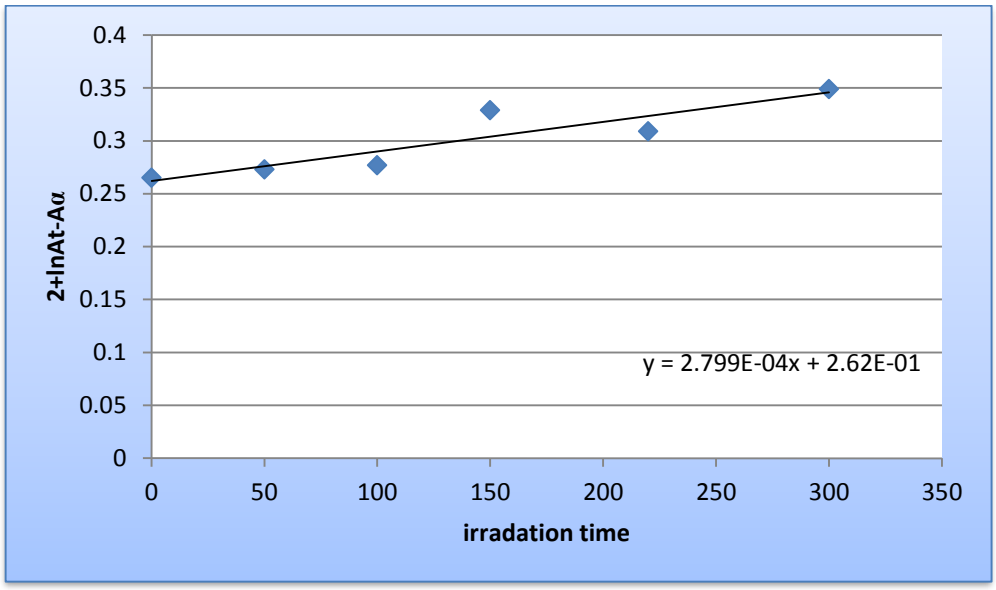

Figure (3.25) Variation of natural logarithm of ln ($A_t - A_\infty$) with irradiation time of $[SnL_2(H_2O)_2]$ in PVC film.

The photostabilizers always posses low K_d values, which mean that these modified polymers are stable towards UV light.

One could notice that K_d values are sensitive to the type of additives in PVC films, which decrease in the following order:

PVC (blank) > CuL_2> $[NiL_2(H_2O)_2]$ > $[ZnL_2(H_2O)_2]$ > $[CdL_2(H_2O)_2]$ > $[SnL_2(H_2O)_2]$

and this might point out to increase the photostability of this additives in this term.

3.2.3. *Determination of the Stabilizing Efficiency by Weight Loss Method*

The stabilizing efficiency was determined by measuring the % weight loss of photodegraded PVC films in absence and in presence of additives by applying the following equation, See Paragraph (2.5.3):

Weight loss % = [(W_1 -W_2) / W_1] 100 …… (3.4)

Volatile and low molecular weight product [93] formed on photodegradation of PVC led to a weight loss phenomenon.

The weight loss of poly(vinyl chloride) films increased gradually with the increasing degradation time [94], thus, the weight loss percentage as a function of the irradiation time can be a good measure of the degree of degradation and consequently can measure the stabilizing potency of the stabilizer and how long the stabilizer would protect the polymer.

The results of weight loss % as a function of irradiation time are represented in Figure (3.26) and Table (3.8), the increasing very small with PVC film modified by additives.

The results indicate that all of the five additives have stabilizing effect against photodegradation of PVC samples and leading to a considerable decrease in % weight loss compared with blank PVC. The stabilizing efficiency of the investigated photostabilizers was found to follow this order:

$[NiL_2(H_2O)_2]$ > $[SnL_2(H_2O)_2]$ > CuL_2 > $[CdL_2(H_2O)_2]$ > $[ZnL_2(H_2O)_2]$ > PVC

Table (3.8):Measurement of weight loss for PVC films (40µm) thickness containing 0.5% from the additives

Additives	Irradiation time (hours)					
	0	50	100	150	220	300
PVC (blank)	0	0.568	0.688	0.831	0.997	1.098
PVC+[$ZnL_2(H_2O)_2$]	0	0.454	0.59	0.729	0.887	0.998
PVC+[$CdL_2(H_2O)_2$]	0	0.381	0.528	0.672	0.842	0.953
PVC+CuL_2	0	0.278	0.461	0.627	0.772	0.889
PVC+[$SnL_2(H_2O)_2$]	0	0.222	0.387	0.553	0.714	0.823
PVC+[$NiL_2(H_2O)_2$]	0	0.149	0.322	0.489	0.646	0.768

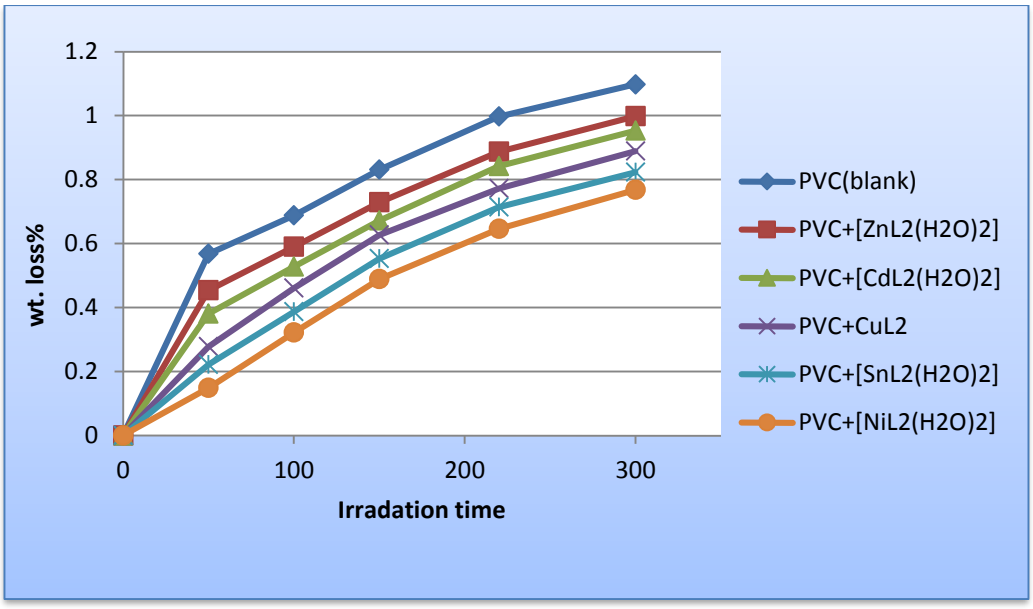

Figure (3.26) loss in weight vs. irradiation time for PVC films (40µm) thickness containing 0.5% w\w from the additives

3.2.4 Variation of PVC molecular weight during photolysis

An analysis of the relative change in viscosity average molecular weight (Mv) described by Scott [95] has been shown to provide a test for random chain scission. Figure (3.27) shows the plot of (Mv) versus irradiation time for PVC films with and without 0.5% (w/w) of five selected additives with absorbed light intensity of 7.75 X 10^{-5} Ein Dm^{-3} S^{-1}. By measuring the solution viscosity we should be able to get an idea about molecular weight. Viscosity techniques are very popular because they are experimentally simple [96]. (Mv) is measured using equation in chapter two and THF as a solvent at 25 ^{o}C, as shown in Table (3.9).

Table (3.9): Variation of $\overline{M}v$ with irradiation time of PVC films thickness (30µm) containing 0.5 % of additives

Additive	Irradiation time (hours)					
	0	50	100	150	220	300
PVC (blank)	150745	100452	73613	40263	20058	15947
PVC+[$ZnL_2(H_2O)_2$]	160102	110567	89845	58367	29936	25156
PVC+[$CdL_2(H_2O)_2$]	170370	131687	100675	68921	40876	39236
PVC+CuL_2	173252	144000	110763	79319	51801	48982
PVC+[$SnL_2(H_2O)_2$]	180100	150938	128439	99531	70397	65864
PVC+[$NiL_2(H_2O)_2$]	191300	170081	139006	125754	103463	95724

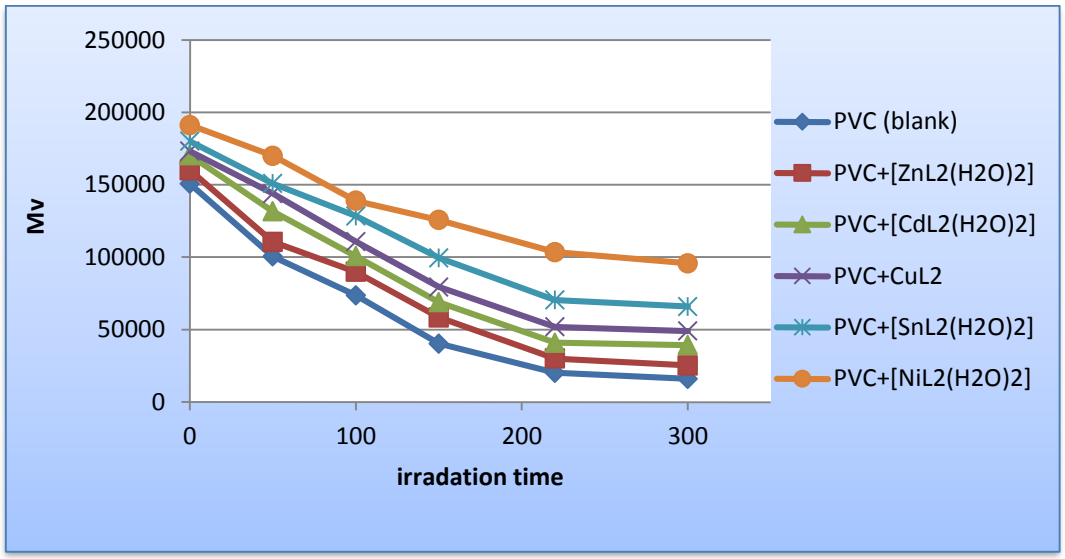

Figure (3.27) Changes in the average molecular weight during irradiation for PVC films (40 µm) control and with 0.5 wt % of additives

It is worth mentioning that traces of the PVC films with additives are not soluble in THF indicating that cross-linking or branching in the PVC chain does occur during the course of photolysis [97].

The plots indicate a rapid decrease in $(\overline{M}v)$ initially then it slows down, suggesting that the initial rapid drop in $(\overline{M}v)$ is due to the main chain scission at various locations that distributed along the polymer chain. The photodegradation becomes slower and bond scission may be random. For better support of this view, the number of average chain scission (average number cut per single chain) (S) [98] was calculated using the relation below:

$$\overline{S} = [\overline{M}v,o / Mv,t]-1 \quad \text{..... (3.6)}$$

Where $M_{v,o}$ and $M_{v,t}$ are viscosity average molecular weight at initial (0) and t irradiation time respectively.

Table (3.10):Variation of (S) values with irradiation time of PVC films thickness (40µm) containing 0.5 % of additives

compounds	Irradiation time (hrs)				
	50	100	150	220	300
PVC (blank)	0.501	1.048	2.744	6.515	8.453
PVC+[$ZnL_2(H_2O)_2$]	0.448	0.782	1.743	4.348	5.364
PVC+[$CdL_2(H_2O)_2$]	0.294	0.692	1.472	3.168	3.342
PVC+CuL_2	0.203	0.564	1.184	2.345	2.537
PVC+[$SnL_2(H_2O)_2$]	0.193	0.402	0.809	1.558	1.734
PVC+[$NiL_2(H_2O)_2$]	0.125	0.376	0.521	0.849	0.998

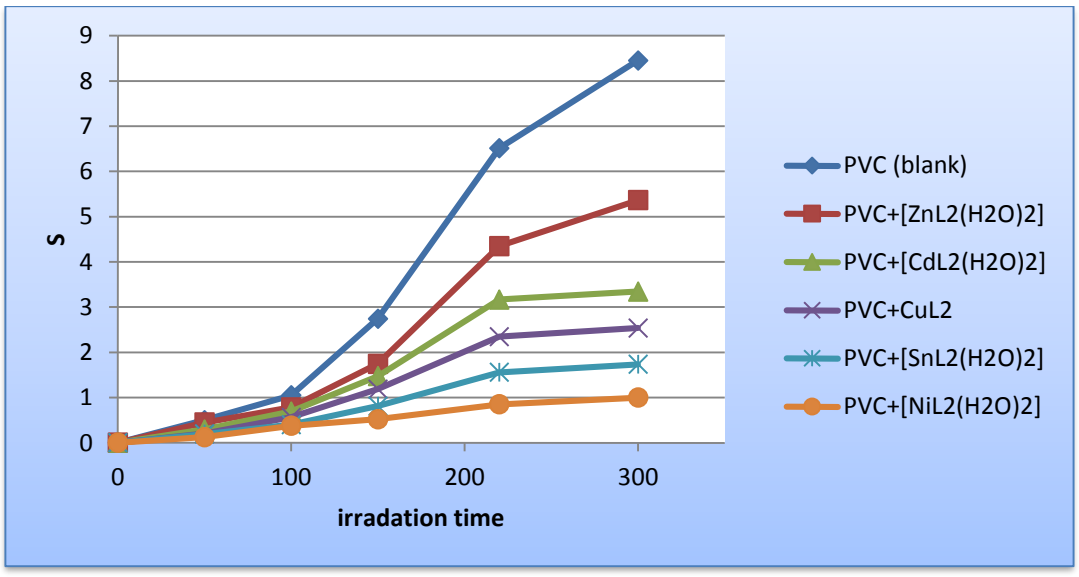

Figure (3.28):Changes in the main chain scission (S) during irradiation of PVC films (40 µm) control and with 0.5 wt% of additives

For randomly distributed weak bond links, which rapidly break in the initial stages of photodegradation, the degree of deterioration (α) is given as follows:

$$\alpha = m * S / Mv \quad \ldots\ldots\ldots (3.7)$$

Where **m** is the initial molecular weight. The plot of α as a function of irradiation time is shown in Figure (3.28).

The values of α of the irradiated samples are higher when additives are absent (PVC blank) and lower in the presence of additives when compared with the corresponding values of the additive-free PVC. In the initial stages of photodegradation of PVC, the value of α increase rapidly with time; these indicators indicate a random breaking of bonds in the polymer [99].

Table (3.11):Variation of (α) values with irradiation time of PVC films thickness (40µm) containing 0.5 % of additives

compounds	Irradiation time (hrs)				
	50	100	150	220	300
PVC (blank)	0.752	2.146	10.274	30.175	79.905
PVC+[$ZnL_2(H_2O)_2$]	0.649	1.394	4.781	23.254	34.138
PVC+[$CdL_2(H_2O)_2$]	0.38	1.171	3.639	13.204	14.512
PVC+CuL_2	0.244	0.882	2.586	7.843	8.974
PVC+[$SnL_2(H_2O)_2$]	0.23	0.564	1.464	3.986	4.714
PVC+[$NiL_2(H_2O)_2$]	0.146	0.517	0.793	1.571	1.994

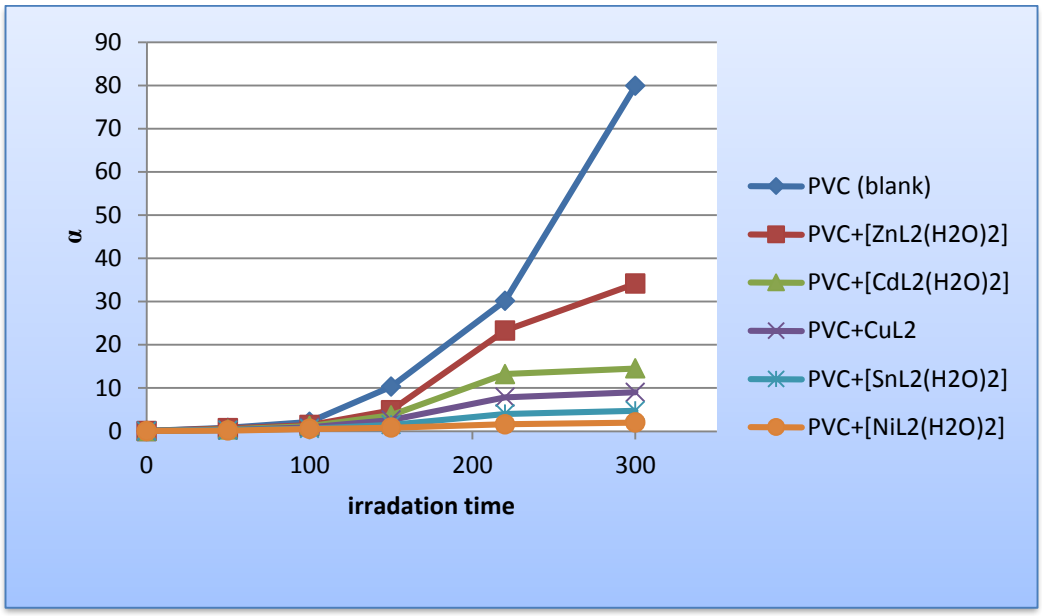

Figure (3.28):Changes in the degree of deterioration (α) during irradiation of PVC films (40 µm) control and with 0.5 wt% of additives

The degree of polymerization (DP) is usually defined as the number of monomeric units in a macromolecule or polymer. For a homopolymer, there is only one type of monomeric units and the number average degree of polymerization is given by:

$$DP_n = X_n = M_n / M_o \ldots\ldots\ldots (3.8)$$

Where M_n is the number-average molecular weight and M_o is the molecular weight of the monomer unit [72]. The plot of $1/DP_n$ versus irradiation time is adopted to characterize degradation reaction of polymer as shown in Figure (3.29). The curve indicates an increase in the inverse of number average degree of polymerization with irradiation time [100].

Table (3.12) The variation of DP_n with irradiation time for PVC films with 0.5% of additives, film thickness is (40 µm)

compounds	Irradiation time (hrs)					
	0	50	100	150	220	300
PVC (blank)	2411.9	1607.2	1277.8	644.2	320.9	255.6
PVC+$[ZnL_2(H_2O)_2]$	2561.6	1769.1	1437.5	933.9	478.9	402.5
PVC+$[CdL_2(H_2O)_2]$	2725.9	2106.9	1610.8	1102.7	654.0	627.8
PVC+CuL_2	2772.0	2304.0	1772.2	1269.1	828.8	783.7
PVC+$[SnL_2(H_2O)_2]$	2881.6	2415.0	2055.0	1592.5	1126.4	1053.8
PVC+$[NiL_2(H_2O)_2]$	3030.3	2702.7	2222.2	2000.0	1666.7	1538.5

Table (3.13) The variation of $1/DP_n$ with irradiation time for PVC films with 0.5% of additives, film thickness is (40 µm)

compounds	Irradiation time (hrs)					
	0	50	100	150	220	300
PVC (blank)	0.00042	0.00062	0.00085	0.0016	0.0031	0.0039
PVC+$[ZnL_2(H_2O)_2]$	0.00039	0.00057	0.00069	0.0011	0.0021	0.0025
PVC+$[CdL_2(H_2O)_2]$	0.00036	0.00047	0.00062	0.00091	0.0015	0.0016
PVC+CuL_2	0.00036	0.00043	0.00056	0.00079	0.0012	0.0013
PVC+$[SnL_2(H_2O)_2]$	0.00035	0.00041	0.00049	0.00063	0.00089	0.00095
PVC+$[NiL_2(H_2O)_2]$	0.00033	0.00037	0.00045	0.0005	0.0006	0.00065

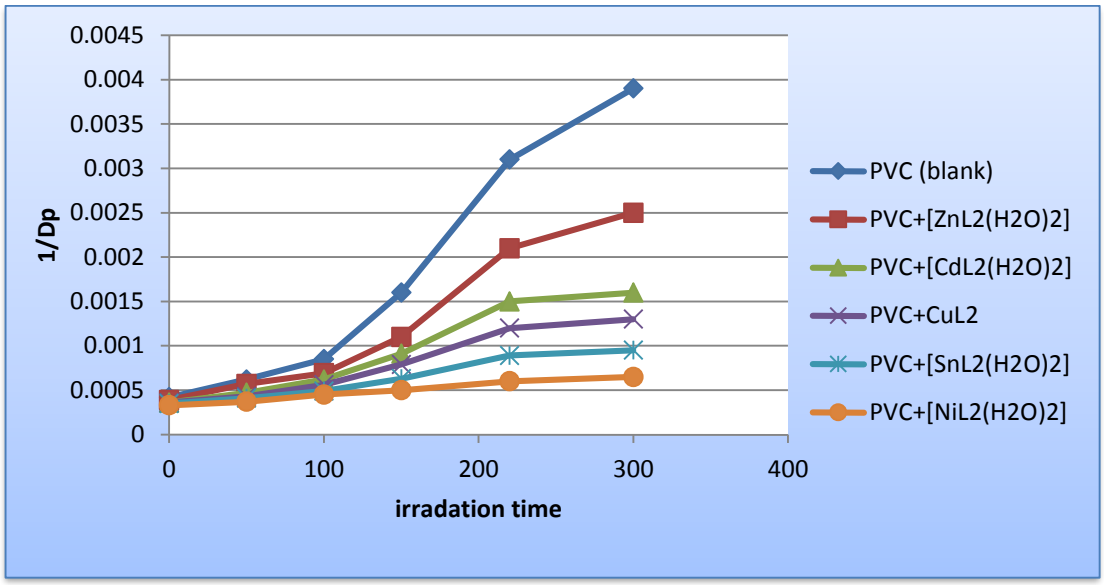

Figure 3.29 Changes in the reciprocal of number average of polymerization ($1/DP_n$) during irradiation of PVC films (40µm) (control) and modified PVC films

Another way of degradation reaction characterization is the measurements of the quantum yield of the chain scission (Φcs). The quantum yield for chain scission was calculated for PVC films with and without 0.5% (wt/wt) of additive. The Φcs values for these polymers are tabulated in Table 3.14.

Table(3.14) Quantum yield (Φcs) for the chain scission for PVC films (40µm) thickness with and without additives after 300 hrs irradiation time

compounds	Quantum yield of main chain scission (Φcs)
PVC (control)	5.106E-06
PVC + $[ZnL_2(H_2O)_2]$	2.054E-06
PVC + $[CdL_2(H_2O)_2]$	8.205E-07
PVC + CuL_2	4.989E-07
PVC + $[SnL_2(H_2O)_2]$	2.537E-07
PVC + $[NiL_2(H_2O)_2]$	1.005E-07

The Φcs values for PVC films in the presence of additives are less than that of additive free PVC (control), which increase in the order:

$$PVC > [ZnL_2(H_2O)_2]_2 > [CdL_2(H_2O)_2] > CuL_2 > [SnL_2(H_2O)_2] > [NiL_2(H_2O)_2]$$

The low values of Φcs is due to the large molecule PVC the energy is absorbed at one site, then the electronic excitation is distributed over many bonds so that the probability of a single bond breaking, or the absorbed energy is dissipated by nonreactive processes [101].

Through the overall results obtained, the efficiency of metal complexes as photostabilizers for PVC films can take the following order in photostabilization activity according to their decrease in hydroxyl, polyene, and carbonyl indices for PVC films as shown in Figures 3.15, 3.16 and 3.17:

$$PVC < [ZnL_2(H_2O)_2]_2 < [CdL_2(H_2O)_2] < CuL_2 < [SnL_2(H_2O)_2] < [NiL_2(H_2O)_2]$$

3.3 Surface analysis

Polymer macrochains can be completely disordered (amorphous) or partially ordered. Physical and mechanical properties of plastics depend not only on the chemical structure of polymers, but also on their morphology [102].

Microscopic technique such as atomic force microscopy (AFM), allows examination of polymer samples from the scale of micrometres down to angstroms. The arrangement of individual polymer chains is visualized, and in some cases the observation of single atoms is possible [103]. Although microscopic methods are so popular and frequently used in the investigation of polymers, very little is known about their applications to the study of the degradation processes in polymer [104].

The influence of UV irradiation on the surface morphology of films were investigated using lab. microscope and Atomic Force Microscopy (AFM). The photodegraded samples exhibited a degree of surface damage. The formation of cracks and holes resulting from the degradation and evolution of volatile products was observed. Figure 3.30b shows the microscopic image of PVC film irradiated for 300 hrs in air. Active free radicals are able to abstract hydrogen atoms from macromolecules and initiate efficient polymer decomposition. In PVC films without additives, the growth of cracks with irradiation time was observed. The extent of photodegradation in the presence of UV light leads to an increase of film embrittlement. In PVC samples photodegraded in the presence of metal ion complexes as additives, the cracks are lighter, Figures (3.31b) to (3.35b). The formation of micro-cracks on the polymer surface is mainly due to the chain scission reaction occurring in degraded samples. Breaking of polymer bonds produces fragments which occupy more volume than the original macromolecules. This causes strains and stresses responsible for the formation of micro-cracks and damaging the irradiated polymer [105].

It should be noted that the undegraded PVC film (Figure 3.30a) to (3.35a) does not exhibit any special microstructure; films are smooth and without any visible structural defects.

Very often during U.V. irradiation of polymers the volatile, gaseous degradation products coming out of the sample leave behind micropores with different shapes and sizes. This is exemplified by the photodegraded PVC film (Figure 3.35b, 3.36b, 3.37b),in which holes are observed. PVC has a simple chemical structure, consisting of alternating ethylene and chloride groups, and can undergo efficient degradation due to hydrogen abstraction and main chain scission reaction [106]. The radiation stability of a polymer is dependent upon

the chemical structure of the material because radiation induced excitation is not coupled to entire chemical system, but is localized at a specific bond. The addition of energy absorbing aromatic rings to the chemical structure significantly increases the radiation stability of some polymers by aiding in the redistribution of the excitation energy throughout the material [107], The volatile, low molecular product mainly HCl, owing to the voids and holes formed [108], the number of sorption sites and diffusion channels increases. Thus, oxygen diffuses rapidly into the bulk of the polymer and causes further, fast oxidation of PVC polymer film.

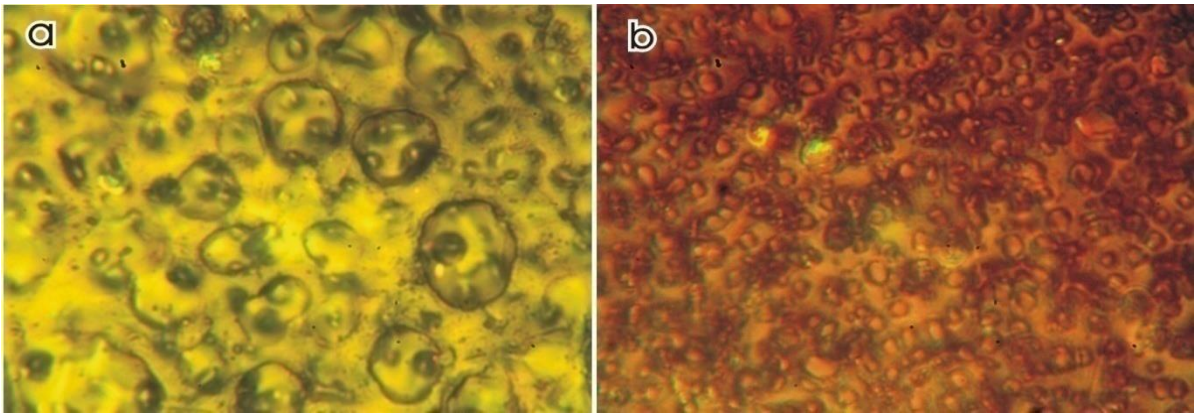

Figure (3.30) Microscopic images of PVC film (control) (a) before irradiation, (b) after 300hrs irradiation time

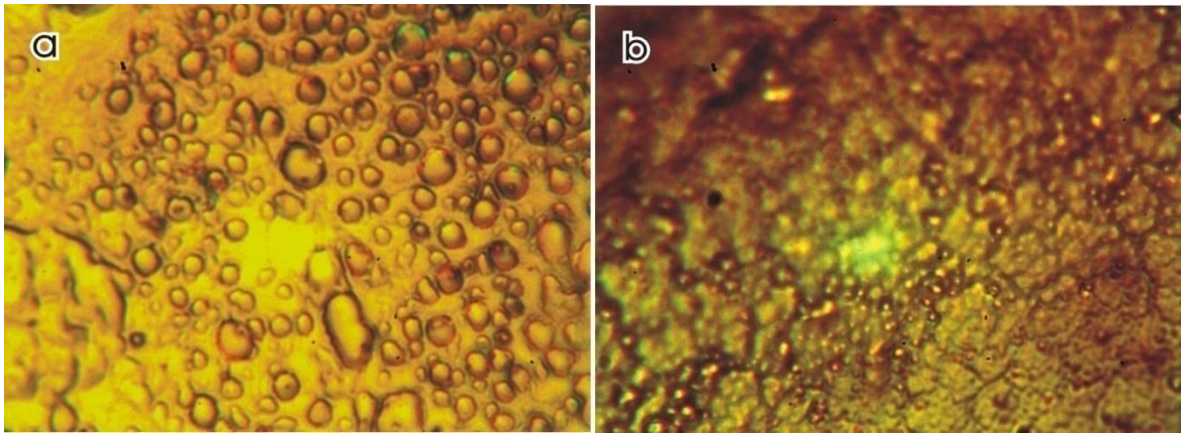

Figure (3.31) Microscopic images of PVC+[$NiL_2(H_2O)_2$] (a) before irradiation, (b) after 300hrs irradiation time

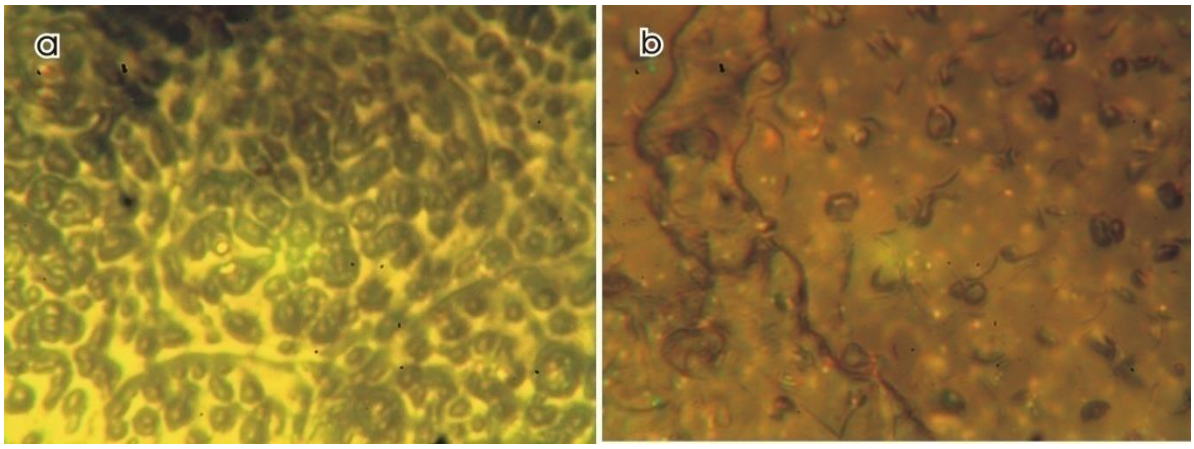

Figure (3.32) Microscopic images of PVC+[$ZnL_2(H_2O)_2$] (a) before irradiation, (b) after 300hrs irradiation time

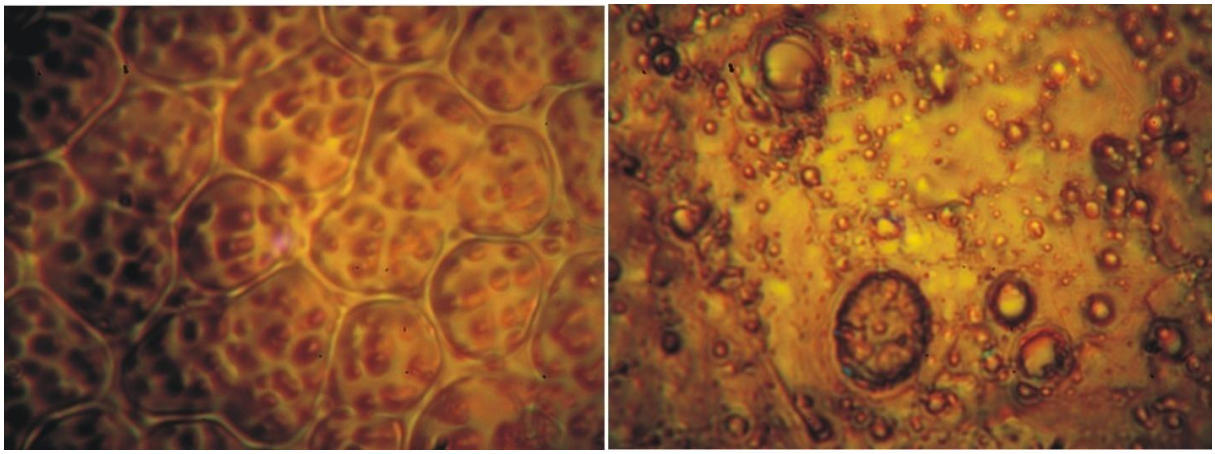

Figure (3.33) Microscopic images of PVC+CuL_2 (a) before irradiation, (b) after 300hrs irradiation time

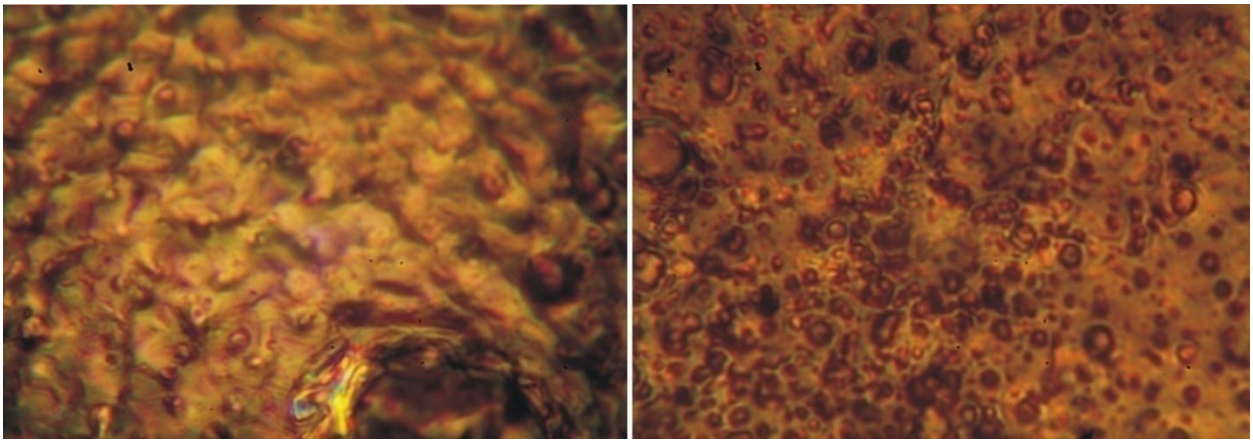

Figure (3.34) Microscopic images of PVC+[$CdL_2(H_2O)_2$] (a) before irradiation, (b) after 300hrs irradiation time

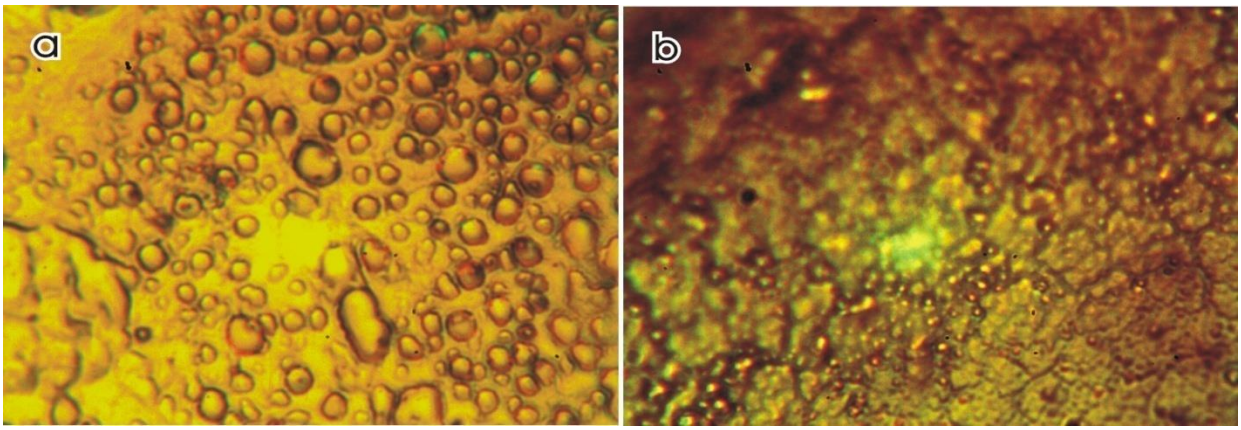

Figure (3.35) Microscopic images of PVC+[$SnL_2(H_2O)_2$] (a) before irradiation, (b) after 300hrs irradiation time

AFM is used to study the surface morphology and bulk microstructure of polymers before and after exposure to UV. Atomic force microscopy (AFM) is powerful technique that can provide direct spatial mapping of surface morphology with nanometer resolution. Further, the phase contrast in tapping mode AFM often reflects differences in the properties of individual components of materials. AFM studies of surface physical degradation were performed on specimens exposed to UV. The root mean square of roughness (Rq) is a function that takes the square of the measures. Values of root mean square roughness (Rq) are listed in Table 3.15. In the presence of additives, it can be observed that there is a decrease in roughness values when films exposer to 300h irradiation time. Films with additives present smaller values than control [109].

The two (2D) and three-dimensional (3D) AFM images of polymer surface after exposure to UV light are given in Figures3.36 to 3.41. The variations of the topography depend on the chemistry of the substrate material as well as the type of additives used.

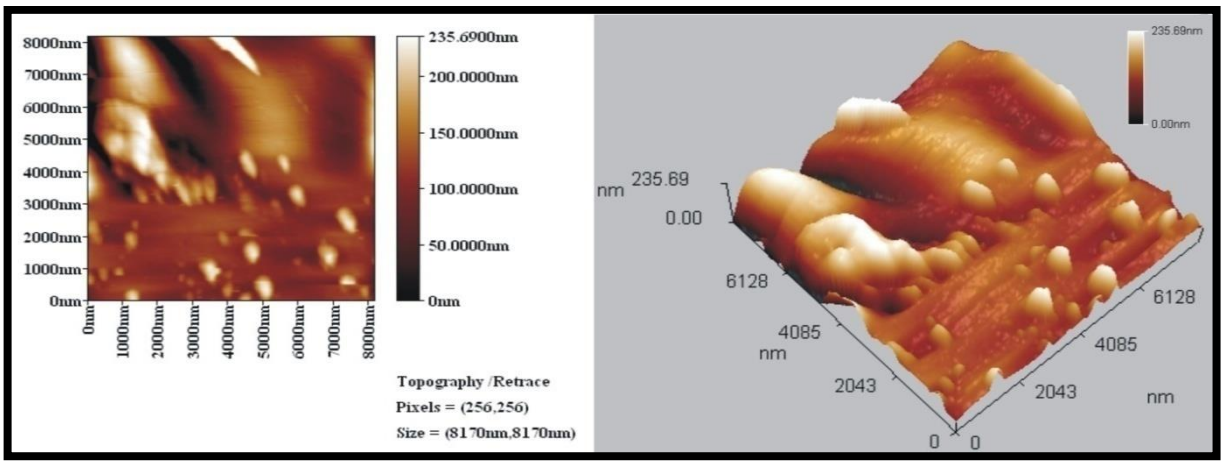

Figure (3.36): 2D and 3D of AFM images of PVC (control) film exposed to 300hrs UV light

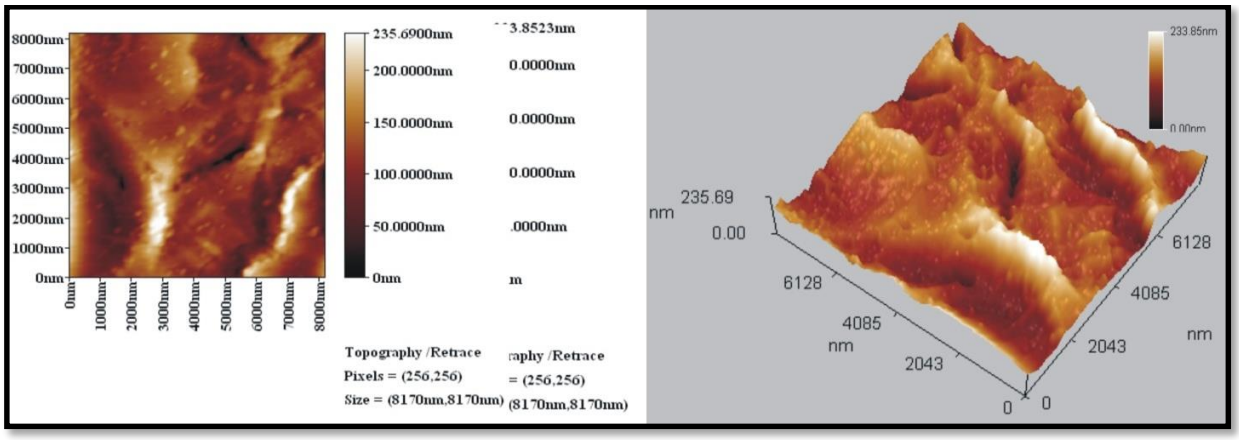

Figure (3.37): 2D and 3D of AFM images of PVC+[$ZnL_2(H_2O)_2$] film exposed to 300hrs UV light

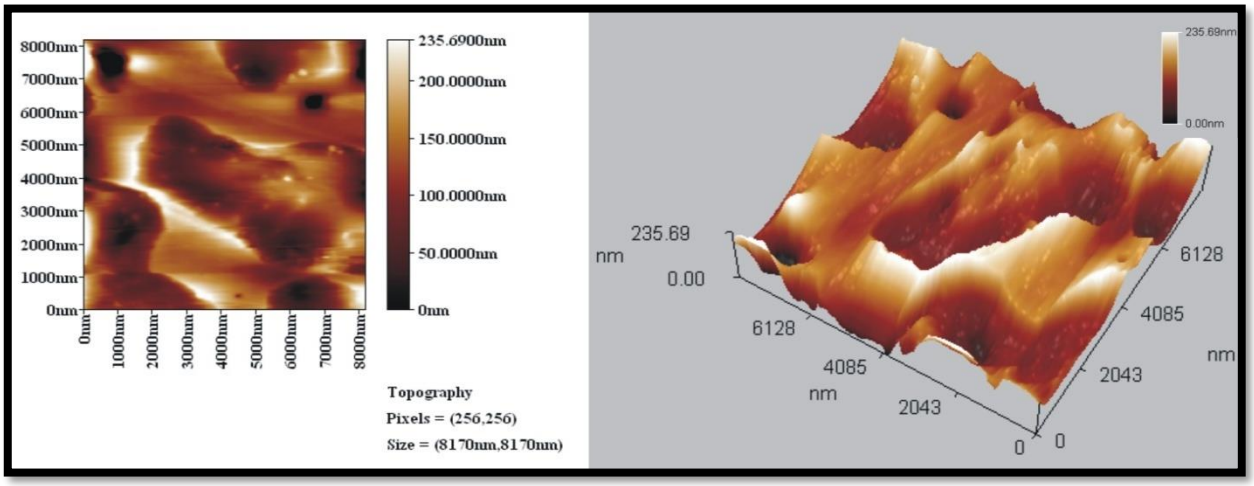

Figure (3.38): 2D and 3D of AFM images of PVC+[$CdL_2(H_2O)_2$] film exposed to 300hrs UV light

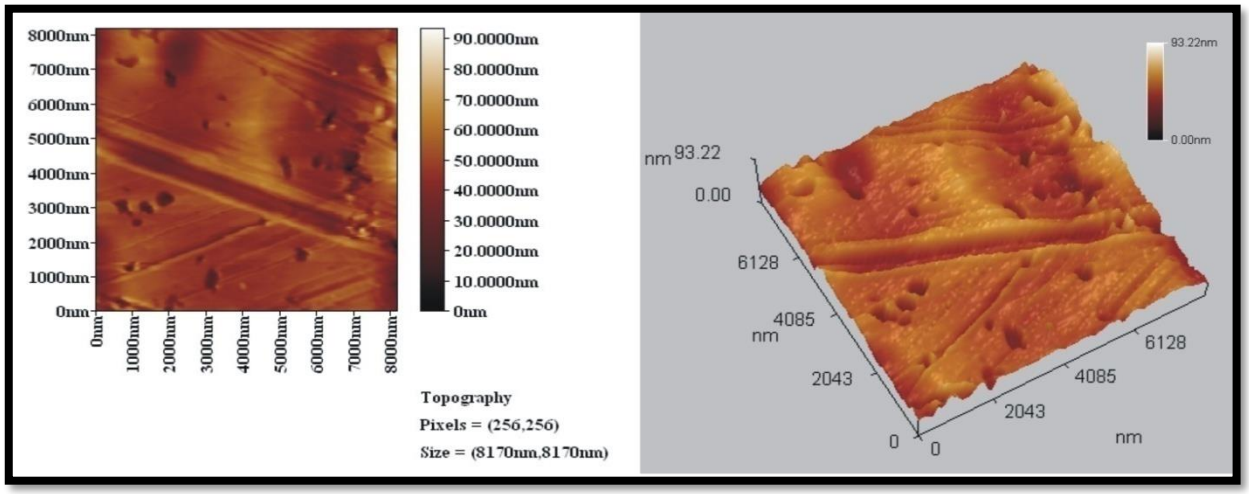

Figure (3.39): 2D and 3D of AFM images of PVC+CuL_2 film exposed to 300hrs UV light

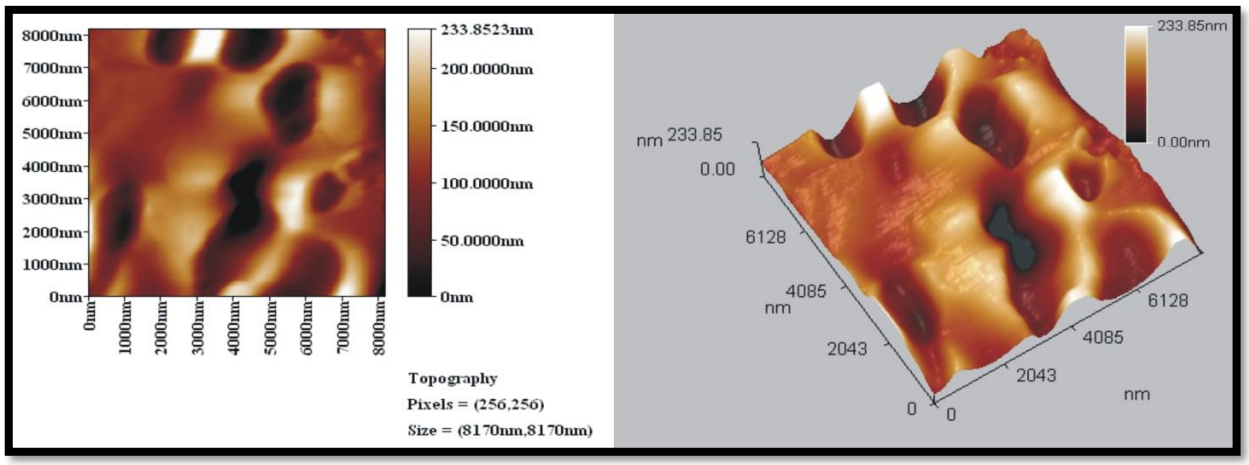

Figure (3.40): 2D and 3D of AFM images of PVC+[$SnL_2(H_2O)_2$] film exposed to 300hrs UV light

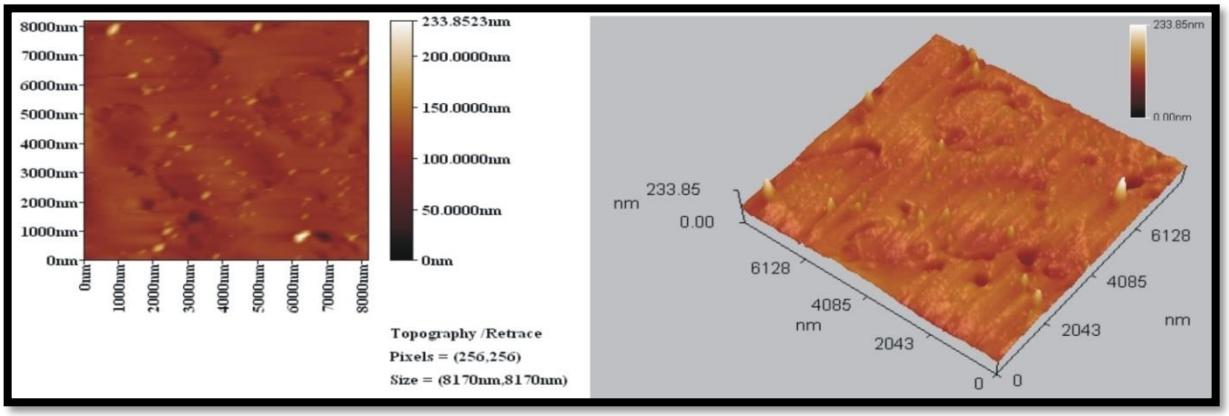

Figure (3.41): 2D and 3D of AFM images of PVC+[$NiL_2(H_2O)_2$] film exposed to 300hrs UV light

Surface of irradiated PVC film with Ni(II) complex was very smooth compared to other samples (Rq = 7.72 nm). PVC (control) and with Zn(II) complex films were highly rough (Rq = 48 nm). This can be explained by breaking of some bonds after exposer to UV light, removal of leachables from the surface and creating roughness. Complexes addition protect the polymer against degradation leading to less Rq value [110].

Table (3.15) Rq values of surface modified PVC films

Sample	Rq
PVC (control)	48.3
PVC+[$ZnL_2(H_2O)_2$]	48
PVC+[$CdL_2(H_2O)_2$]	38.5
PVC+[$SnL_2(H_2O)_2$]	27.5
PVC+CuL_2	9.46
PVC+[$NiL_2(H_2O)_2$]	7.72

3.4 *proposed mechanisms of photostabilization of PVC by the 2-(4-(2-methylpropyl) phenyl) propanoate complexes*

Through the overall results obtained, the efficiency of 2-(4-(2-methylpropyl) phenyl) propanoate complexes as stabilizers for PVC films can be arranged according to the change in the carbonyl, polyene and hydroxyl concentration as a reference for comparison as shown in Figure (3.14), (3.15) and (3.16).

$[NiL_2(H_2O)_2] > [SnL_2(H_2O)_2] > CuL_2 > [CdL_2(H_2O)_2] > [ZnL_2(H_2O)_2] >$ PVC

Metal carboxylates stabilize PVC by mechanisms, depending on the metals such as Cd, Zn, Sn, Ni and Cu which are stronger lewis acids and form covalent carboxylates, not only scavenge HCl, but also substitute carboxylate for the allylic chlorine atoms [111].

These stabilizers provide very good long-term stability and are usually referred to as secondary stabilizers, Scheme (3.2).

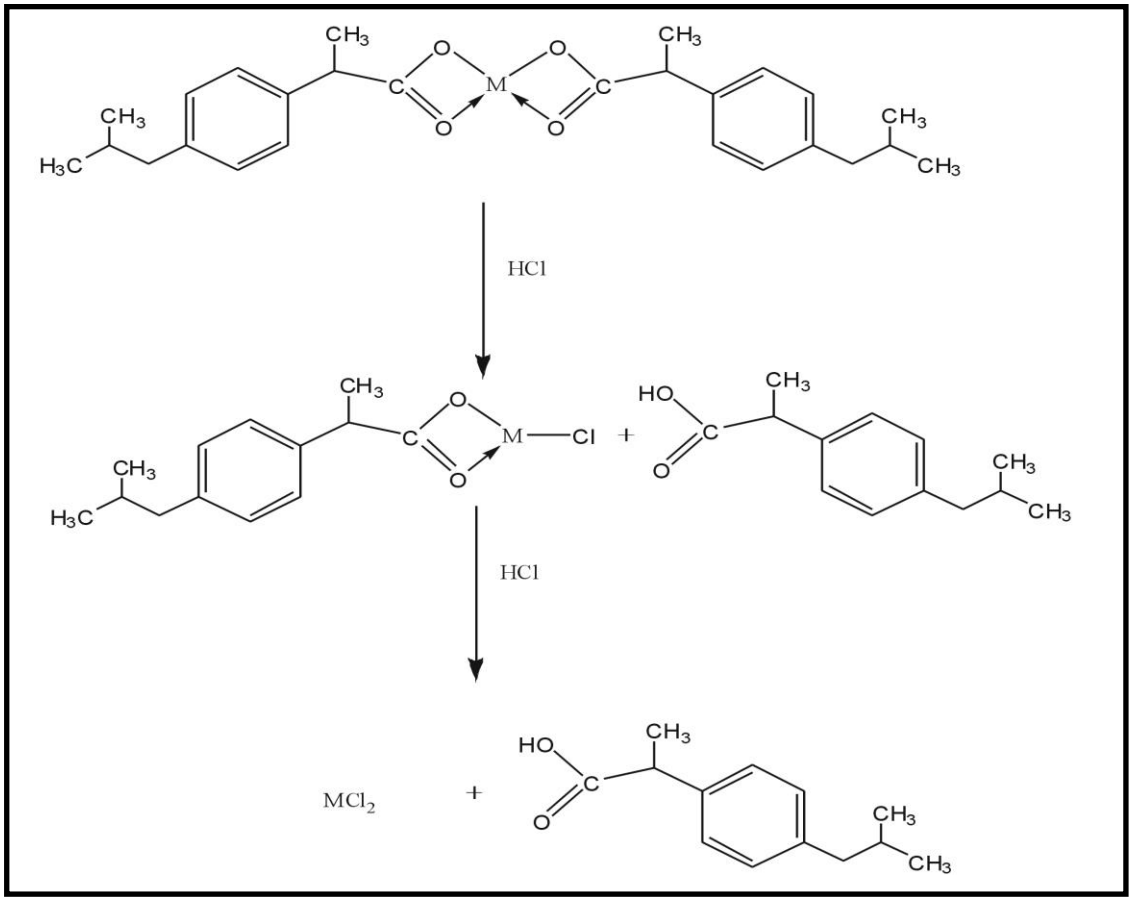

Scheme (3.2): proposed mechanism of photostabilization of ML_2 complexes as HCl scavengers.

IR spectroscopy has shown that metals carboxylates associate with PVC molecules at the surface of primary particles[112] and are consequently, very effective in the substitution of allylic chlorine. In this mechanism the stabilizer classified as primary stabilizers.

It has been postulated that metals stabilizers associate with chlorine atoms at the surface of PVC primary particles which explains their high efficiency in PVC stabilization[113], Scheme (3.3).

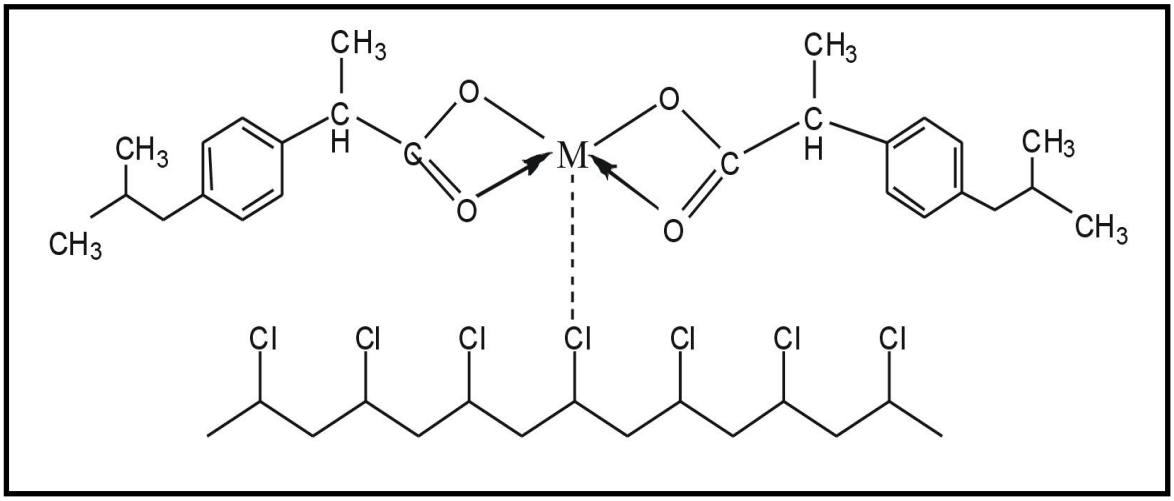

Scheme (3.3): proposed mechanism of photostabilization of ML_2 complexes as primary stabilizers .

Metal chelate complexes generally known as photostabilizers for poly olefins[114] through both peroxide decomposer and excited state quencher. Therefore, it is expected that these complexes act as peroxide decomposer through the following proposed mechanism, Scheme (3.4).

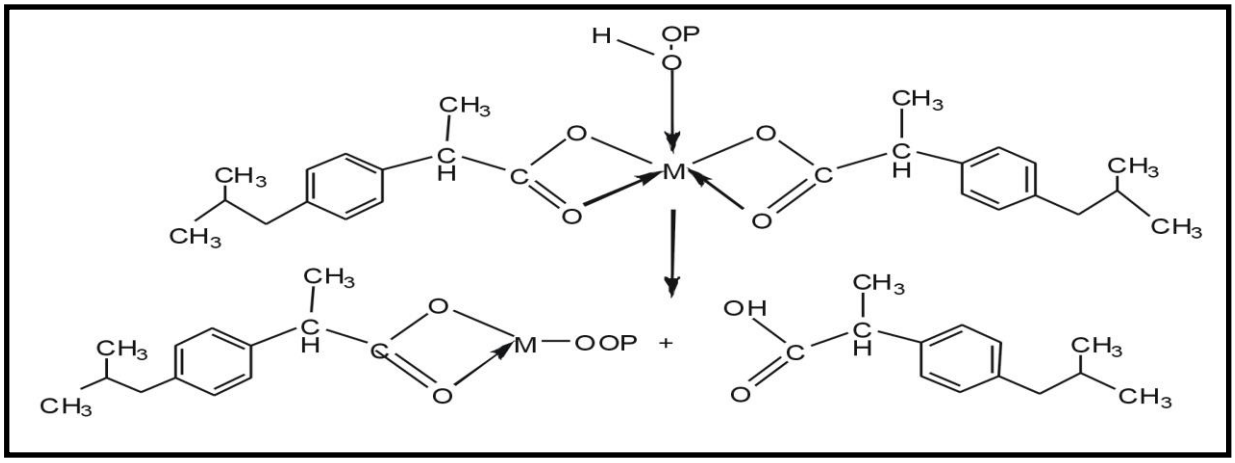

Scheme (3.4): proposed mechanism of photostabilization of ML_2 complexes as peroxide decomposer.

These metal chelate complexes also function as radical scavengers through energy transfer and by forming unreactive charge transfer complexes between the metal chelate and excited state of the chromophore ($POO^{\cdot}$) and stabilize through resonating structures as shown in Scheme (3.5).

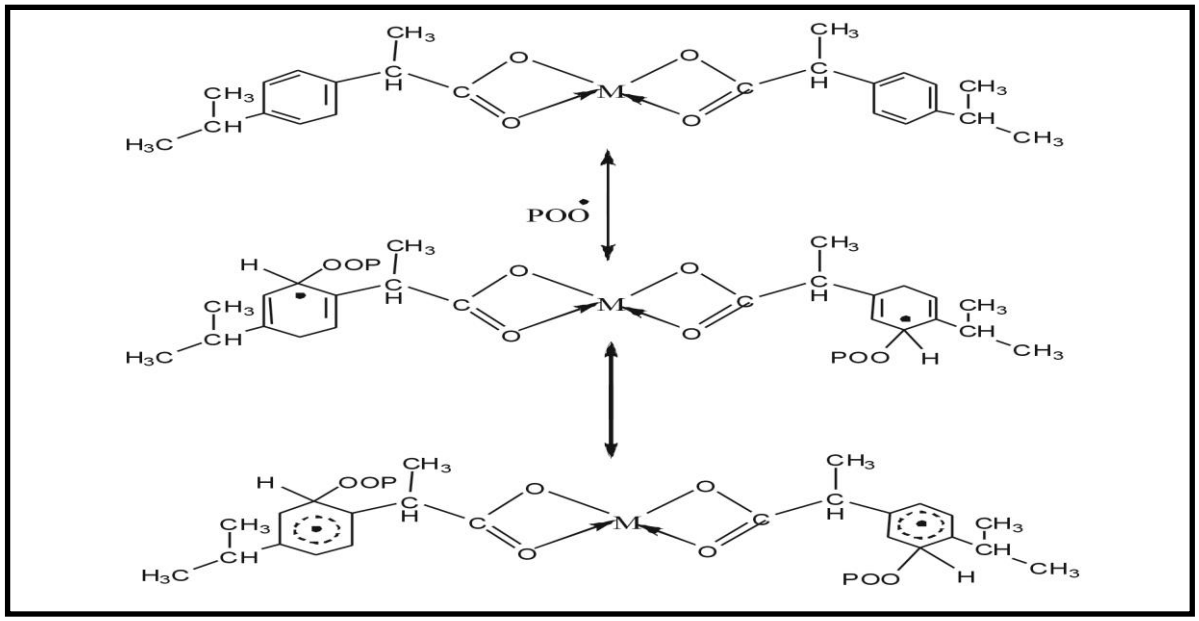

Scheme (3.5): proposed mechanism of photostabilization of carboxylates complexes as radical scavengers through energy transfer and forming unreactive charge transfer and stabilize through resonating structure.

3.4 *Conclusion*

1. The additives used in this study behave successfully as photostabilizers for PVC films.
2. Their activity in photostabilization is following the order

PVC < $[ZnL_2(H_2O)_2]$ < $[CdL_2(H_2O)_2]$ < CuL_2 < $[SnL_2(H_2O)_2]$ < $[NiL_2(H_2O)_2]$

according to their decrease in carbonyl, hydroxyl and polyene (I_{CO}, I_{OH}, Ipo) and the weight loss for PVC films.

3. These additives stabilize the PVC films through HCl scavenging, UV. absorption or screening, peroxide decomposer and radical scavenger mechanisms.
4. The Nickel complex was found to be the more efficient in photostabilization process according to the photostability, this supports to use Nickel complex as a commercial stabilizer for PVC.

3.1. *Suggestions for future work*

1. Studying the photoactivity of the additives with other polymers such as PS, PVA, LDPE, HDPE comparing the activity of these additives in photostabilization of PVC.

2. Comparing the efficiency of the additives with some commercial stabilizers.

3. Study the effect of additives in the outdoor weathering.

4. Study the effect of additives in polymer solution.

5. Study the effect of substitution of the some groups on the aromatic rings in the structure of the complexes and study their effect on polymers.
6. Since fixed thickness was used in this presented the study can be extended by using different films thickness and studying their effect on the photostabilization process.
7. Study the effect of temperature on the efficiency of the additives.
8. Extend the study by using different concentration from additives and studying their effect on the photostabilization process.

REFERENCES

Reference

(1) M. A. Fox, J. K. Whitesell, Organic Chemistry Massachusetts: Jones and Bartlett Publishers, Sudbury, (2^{d} ed.), 1040-1047, (1997).

(2) E. Hans-Georg, Plastics General Survey, in Ullmann's Encyclopedia of Industrial Chemistry, Wiley-VCH, 7th ed., (2000).

(3) A. L. Andrady, A. Torikai, Consequences of stratospheric ozone depletion and climate change on the use of materials, Photochem. Photobiol. Sci., 14, 171-172, (2015).

(4) E. Moretti, M. Zinzi and E. Belloni, Polycarbonate panels for buildings: Experimental investigation of thermal and optical performance, Energy Build., 70, 23–35, (2014).

(5) C. Buratti and E. Moretti, Glazing systems with silica aerogel for energy savings in buildings, Appl. Energy, 98, 396-403, (2012).

(6) S. Kubba, Green Building Materials and Products, in Handbook of Green Building Design and Construction, Butterworth-Heinemann, Boston, 227–311, (2012).

(7) G. Akovali, S. Jalali and A. Fucic, Plastic materials: poly(vinyl chloride) (PVC), in Wood head Publishing Series in Civil and Structural Engineering, eds. F. Pacheco-Torgal, Wood head Publishing, 23–53, (2012).

(8) L. Sobczak, R. W. Lang and A. Haider, Polypropylene composites with natural fibers and wood - General mechanical property profiles, Compos. Sci. Technol., 72, 550–557, (2012).

(9) B. Singh, N. Sharma, Mechanistic implications of plastic degradation, Polymer Degradation and Stability, 93, 561-584, (2008).

(10) C. Homkhiew, T. Ratanawilai and W. Thongruang, Effects of natural weathering on the properties of recycled polypropylene composites reinforced with rubber wood flour, Ind. Crops Prod., 56, 52-59, (2014).

(11) C. Wang, J. Torng, Experimental study of the absorption characteristics of some porous fibrous materials, Applied Acoustics, 62, 447-459, (2001).

(12) T. Ojeda, Degradability of linear polyolefins under natural weathering, Polym. Degrad. Stab., 96, 703-707, (2011).

(13) V. Sharratt, C. A. Hill and D. P. Kint, A study of early colour change due to simulated accelerated sunlight exposure in Scots pine, Polym. Degrad. Stab., 94, 1589-1594, (2009).

(14) A. F. Bais and R. L. Mckenzie, Ozone depletion and climate change: Impacts on UV radiation, Photochem. Photobiol. Sci., 14, 9-52, (2015).

(15) IPCC, Intergovernmental Panel on Climate Change Working Group I Contribution to the IPCC Fifth Assessment Report Climate Change 2013: The Physical Science Basis, Cambridge University Press, United Kingdom and New York, NY, USA, (2010).

(16) C. C. Mathias, Review of polymer oxidation and its relationship with materials performance and lifetime prediction, Polym. Degrad. Stab., 98, 2419–2429, (2013).

(17) J. L. Pablos and C. Abrusci, Photodegradation of polyethylenes: Comparative effect of Fe and Ca-stearates as pro-oxidant additives, Polym. Degrad. Stab., 95, 2057–2064, (2010).

(18) H. H. G. Jellinek and A. K. Chaudhuri, "Inhibited degradation of nylon 66 in presence of nitrogen dioxide, ozone, air, and near-ultraviolet radiation", J. polym. Sci., 10, 1773- 1788, (2003).

(19) S. Madronich and C. Fischer, A Climatology of UV Radiation, 1979-2000, 65S-65N, in UV Radiation in Global Climate Change: Measurements, Modeling and Effects on Ecosystems, Springer-Verlag and Tsinghua University Press, 1-20, (2010).

(20) Y. Lian and Y. Zhang, Properties and Morphologies of PVC/Nylon Terpolymer blends, Journal of Applied Polymer Science, 80(14), 2823–2832, (2001).

(21) B. E. Tahira and M. I. Khan, Thermal Degradation and Stabilization of Poly (Vinyl Chloride), International Journal of Research (IJR), 1(6), 732-750, (2014).

(22) E. Yousif, J. Salimon and N. Salih, Mechanism of photostabilization of poly(methy methacrylate) films by 2-thioacetic acid benzothiazol complexes, Arab. J. Chem., 7, 206–311, (2014).

(23) A. P. Pereira and J. L. Grandette, Artificial accelerated weathering of poly(vinyl chloride) for outdoor application, Polym Degrad. Stab., 82, 235-243, (2003).

(24) E. Yousif and Z. Hussain, Study the Rate Constant of Photostabilization of PVC in Presence of Schiff's Bases of Sulphamethoxazole, Journal of Al-Nahrain University, 17, 3-5, (2014).

(25) A. Lindström and M. Hakkarainen, "Environmentally friendly plasticizers for poly(vinyl chloride)- Improved mechanical properties and compatibility by using branched poly(butylene adipate) as a polymeric plasticizer", Journal of Applied Polymer Science, 100, 2180-2188, (2006).

(26) J. Robert and J. Pierotti,; "Additives for plastics", academic press, New York, 2,103-112, (1978).

(27) J. K. Sears and J. R. Darby, “The Technology of Plasticizers”, Wiley, New York, (1982).

(28) V. Koleste and L. H. Warimam, “Poly(Vinyl chloride)” London, (1969).

(29) D. Feldman and A. Barbalata, Synthetic Polymer, Chapman & Hall, London, (1996).

(30) I. Jakubowicz, N. Yarahmadi and T. Gevert, Effects of accelerated and natural ageing on plasticized poly(vinyl chloride)(PVC), Polym. Degrad. Stab., 66: 415-421, (1999).

(31) H. A. Essawy, N. A. Abd El-Wahab and M. Abd El- Ghaffar, PVC–laponite nanocomposites: Enhanced resistance to UV radiation, Polymer Degradation and Stability, 93, 1472-1478, (2008).

(32) J. L. Gardette, J. Lemaire, Photo-oxidation of poly(vinyl chloride): Part 3-Influence of photo-catalytic pigments, Polym. Degrad. Stab., 33, 77-92, (1991).

(33) P. A. Christensen and T. A. Egerton, “Rapid measurement of Polymer Photo-Degradation by FTIR Spectrometry of evolved Carbon Dioxide”, Polymer Deg. & Stab., (2006), 91, 1755 - 1760.

(34) J. Botkin, “Light Stabilization of Polypropylene: An Independent Perspective”, SPE International Polyolefins Conference, 1, 1-26, 2007.

(35) D. M. Wiles and J. F. Rabek, "New Trend in the Photochemistry of Polymers", Elsevier Appli. Sci., London, 1-147 (1985).

(36) J. Kresta, "Polymer Additives", Plenum Press, New York, 400-408, (1984).

(37) A. L. Andrady, K. Fueki & A. Torikai, Photodegradation of rigid PVC formulations. I. Wavelength sensitivity of light induced

yellowing by monochromatic light, Journal of Applied Polymer Science, 37, 935–946, (1989).

(38) B. Dindar, S. Icli , Unusual photo reactivity of zinc oxide irradiated by concentrated sunlight, J. Photochem. Photobio Chem., 140, 10-16, (2001).

(39) J. Pospisil, S. Nespurek, Degradation and Stabilization of Polymers Conference, Prog. Polymer Science, 25, 1261-1335, (2000).

(40) A. Frank, H. Leonard and L. Robert, UV Stabilizer, Encyclopaedia of Polymer Science and Technology, 8, 269-309, (2002).

(41) S. R. Dunhua, Plastic additive, Chitec technology, 20, 20-49, (2015).

(42) J. Štěpek, H. Daoust, Additives for Plastics Polymers, Springer New York 5, 144-166, (1983).

(43) M. Salem, Mechanical Properties of UV-Irradiated Low-Density Polyethylene Films Formulated With Carbon Black and Titanium Dioxide, Egyp. J. Sol., 24(2): 141-150, (2001).

(44) R. Williams, W. Jordan and M. Dannerberg, Reinforcement of elastomers by fillers: Review, J. Appl. Polym. Sci., 9, 861-871, (1969).

(45) G. Wypych, PVC degradation & stabilization, , 2nd ed., chem. tech. puplishing, 400-442, (2008).

(46) A. Bottino, R. Cinquegrani and Giovanna D., , Study on chemical modification, mechanical properties and surface photooxidation of films of polystyrene stabilized by hinderd amines (HAS), Polymer Testing, 23, 779-789, (2004).

(47) T. Kurumoda, H. Ohsawa and O. Oda, Entropy and enthalpy effects of 4-(phenylthio)-substituted phenols, J. Polym. Sci. Polym. Chem. Ed., 23, 1477-1482, (1985).

(48) B. B. Troitskii, L. S. Troitskaya and A. S. Yakhnov, Institute of Organometallic Chemistry, Russian Academy of Sciences, Russia, (1996).

(49) E. Yousif, N. Salih and J. Salimon, Improvement of the Photostabilization of PVC Films in the Presence of 2-N-Salicylidene-5-(Substituted)-1,3,4-Thiadiazole., Journal of Applied Polymer Science, 120, 2207–2214, (2011).

(50) D. Feldman, Polymer weathering: photooxidation, Journal of polymer and the environmental, 10, 163-173, (2002).

(51) E. Yousif and A. Hasan, Photostabilization of poly(vinyl chloride) - Still on the run, Journal of Taibah University for Science, 9, 421-448, (2015).

(52) A. Keller, Morphology of polymers, Pure & Appl. Chem., 64, 2, 193-204, (1992).

(53) P. H. Geil and S. Carr, The Morphology of Crystalline Polymers, J. Chem. Educ., 58, 879-885, (1981).

(54) R. H. Burgess, Manufacture And Processing of PVC, Applied Science Publisher, London, 48,127-134, (2005).

(55) C. Singleton, J. Isner, and D. M. Gezovich, Processing-morphology-property studies of poly(vinyl chloride), Polym. Eng. Sci., 14(5), 1-371, (1974).

(56) D. N. Bort, V. G. Marinin and A. I. Kalinin, Certain kinetic parameters of the bulk polymerization of vinyl chloride and their effect on the structural-morphological features of vinyl chloride, 10(11), 2574–83, (1968).

(57) A. W. Michael, The development and importance of suspension PVC morphology, Pure & Appi. Chem., 53,449-465,(1981).

(58) C. Núñez and A. F. Lodeiro, Synthesis spectroscopic studies and in vitro antibacterial activity of Ibuprofen and its derived metal complexes, Inorganic Chemistry Communications, 45, 61-65, (2014).

(59) M. Shneshil and M. Redayan, Photostabilization of PVC films by using some novel tetra Schiff's bases derived from 1,2,4,5-tetra-[5-amino-1,3,4-thiadiazole-2-yl]-benzene, Diyala j. for pure science, 7(1), 34-77, (2010).

(60) E. Yousif, J. Shneine and A. Ahmed, Synthesis and Characterization of some Metal Ions of 2-(6-Methoxynaphthalen-2-Yl) Propanoate Complexes, Journal of Al-Nahrain University, 16(2), 46-50, (2013).

(61) E. Yousif, A. Ahmed and R. Abood, Poly(vinyl chloride) derivatives as stabilizers against photodegradation, Journal of Taibah University for Science, 9, 203–212,(2015).

(62) S. M. Aliwil, E. Yousif and A. Otaiwi, Synthesis and photochemical study of some metal complexes of poly(vinyl chloride)-2-mercapto-5-phenyl 1,3,4-oxadiazole, Journal of Al-Nahrain University, 8(2), 49-54, (2005).

(63) E. Yousif, R. Haddad and R. M. Yusop, Ultra Violet Spectra Studies of Polystyrene Films in Presence of Some Transition Metal Complexes with 4-amino-5-pyridyl)-4h-1,2,4-triazole-3-thiol., 31(1), 591-596, (2015).

(64) E. Yousif, A. Ahmed and N. Shalan, Photochemical and Physical Study of PVC- Amines Polymers, Australian Journal of Basic and Applied Sciences, 8(17), 394-401, (2014).

(65) E. Yousif and A. Hasan, Ultra-violet spectra studies of photo stabilization rate in PVC films by using some transition metal complexes, , Arab . Phys. Chem, 1(2), 34-35., (2014).

(66) E. Yousif , R. M. Yusop and A. Ahmed, Photostabilizing effecincy of PVC based on epoxidized Oleic acid, Malaysian Journal of Analytical Sciences, 19(1), 213 - 221, (2015).

(67) J. Mark, Physical Properties of Polymers Handbook, Springer Verlag, New York, 1-1067, (2007).

(68) N. Nakajima, M. Sadeghi and T. Kyu, Photodegradation of poly(methyl methacrylate) by monochromatic light:Quantum yield, effect of wavelengths and light intensity, Journal of Applied Polymer Science, 41, 889 – 1363, (1990).

(69) B. Kordoghli, R. Khiari and H. Dhaouadi, UV irradiation-assisted grafting of poly(ethylene terephthalate)fabrics, Colloids and Surfaces, A: Physicochem. Eng. Aspects, 441, 606-613, (2014).

(70) A. A. Mohammed, Synthesis and Investigations on Coordination Compounds Having Oxygen and Nitrogen Donors, National Journal of Chemistry, 38, 325-332, (2010)

(71) K. Nakamoto, Infrared and Raman spectra of inorganic and coordination compounds, Wiley, New York, 5th edition, 57-104, (1997).

(72) E. Yousif, Y. Farina and S. Khadum, Triorganotin(IV) of benzamidoglycin: Synthesis and fungicidal activity, Int. J. Chem. Tech. Res., 1(3), 789-792, (2009).

(73) M. G. Abd El-Wahed, M. S. Refat and S. M. El-Megharbel, Spectroscopic studies on the complexation of some transition metals with Chloramphenicol drug, J. Mol. Struct., 892, 402-413, (2008).

(74) A. Saxena, Synthesis and characterization of schiff base salicylaldehyde and thiohydrazones and its metal complexes, Advances in Applied Science Research, 4(4), 152-154, (2013).

(75) E. Yousif, Synthesis spectroscopic studies and fungicidal activity of some diorganotin(IV) with 2-[(phenylcarbonyl)amino] propanoato, J. King Saud. Univ. Sci., 24, 167-170, (2012).

(76) E. Yousif and E. Rentschler, Synthesis and characterization of some metal ions with {[5-(4-chlorophenyl)-1,3,4-oxadiazo l-2-yl]thio}acetic acid, J. Al-Nahrain Unv., 13(2), 86-92, (2010).

(77) D. M. Boghaei and M. Gharagozlou, Spectral characterization of novel ternary zinc(II) complexes containing 1,10-phenanthroline and Schiff bases derived from amino acids and salicylaldehyde-5-sulfonates, Spect. Chem. Acta A., 67, 944-949, (2007).

(78) N. N. Greenwood and A. Earnshaw, Chemistry of the Elements, Elsevier Science Ltd., New York, 2nd ed., (2002).

(79) Y. Win, E. Yousif and A. Majeed, Synthesis, characterization and *in vitro* antimicrobial activity of Co(II), Cu(II), Zn(II), Cd(II) and Sn(II) ions with {[5-(4-bromophenyl)-1,3,4-oxadiazol-2-yl]thio}acetic acid, Asian J. Chem., 23(11), 5009-5012, (2011).

(80) Z. Chohan, Antibacterial dimeric copper(II) complexes with chromone-derived compounds, Trans. Met. Chem., 34, 153-161, (2009).

(81) A. Majeed, E. Yousif and Y. Farina, Synthesis and characterization of transition metal complexes of −2-thioacetic acid benzothiazole ligand, J. Al-Nahrain Uni.,13,36-42, (2010).

(82) S. V. Chavan, S. S. Sawant and R. S. Yamgar, Synthesis and Characterization of Novel Transition Metal Complexes of Benzo-Pyranone Derivatives and Their Biological Activities, Asian J. Research Chem., 4(5), 835-836, (2011).

(83) A. Majeed, Synthesis structure and antibacterial activity of some 2-amino-5-(2-acetyloxyphenyl)-1,3,4-thiadiazole complexes, Al Mustansiriya J. Sci., 21(5), 195-204, (2010).

(84) E. Yousif, J. Salimon and N. Salih, New photostabilizers for PVC based on some diorganotin(IV) complexes, Journal of Saudi Chemical Society, 19, 133-141, (2015).

(85) E. Yousif, N. Salih and J. Salimon, Improvement of the photostabilization of PVC films in the presence of 2N-salicylidene-5-(substituted)-1,3,4-thiadiazole, J. Applied Polymer Science, 120, 2207-2214, (2011).

(86) A. Andrady and N. Searle, Photodegradation of rigid PVC formulations. II. Spectral sensitivity to light-induced yellowing by polychromatic light, J. Appl. Polym. Sci., 37, 2789–2802, (1989).

(87) O. Naif and H. Salih, Synthesis of New Modified PVC and their Photostability Study, Tikrit Journal of Pure Science, 16(4), 1813-1662, (2011).

(88) B. Cooray and G. Scott, The effect of thermal processing on PVC-Part VIII: The role of thermally formed peroxides on photo-degradation, Poly. Degrad. Stabil., 3, 127-135, (1981).

(89) B. Cooray and G. Scott, The effect of thermal processing on PVC-VI. The role of hydrogen chloride, Eur. Polym. J., 16(2), 169-177, (1980).

(90) E. Yousif and R. Haddad, Photodegradation and photostabilization of polymers, especially polystyrene: review, SpringerPlus, 398(2), 1-32, 2013.

(91) F. Mori, M. Koyama and Y. Oki, Physical Properties of Polymers Handbook, Angew. Makromol. Chem., (75), 113-122, (1979).

(92) B. Cooray and G. Scott, Polymer Photodegradation: Mechanisms and Experimental Methods, J. Eur. Polym., 169(16), 177-189, (1980).

(93) F. Gugumus, Development in Polymer Stabilization-1, Applied Science Publishers Ltd., London, 261-272, (1979).

(94) I. S. Kuzina, A. I. Mikhailov and I. Alfa, The photooxidation of polymers, The main reaction of chain propagation in polystyrene photoxidation, Eur. Polym. J., 34(8), 1157-1162, (1998).

(95) L. Zan, S. Wang and K. Deng, Solid-Phase Photocatalytic Degradation of Polystyrene with Modified Nano-TiO_2 Catalyst, J. of Polymer, 47(24), 8155-8162, (2006).

(96) G. Scott, "Polymers and Ecological Problems", J. E. Guillet ed., Plenum press, New York, 1-27, (1973).

(97) W. Gooch, Encyclopedia dictionary of polymers, springer science, USA, 772-783, (2007).

(98) W. Gibb and J. MacCallum, The photodegration of poly(vinyl chloride). V. The effect of wavelength of irradiation on the dehydrochlorination reaction, J. Eur. Polym., 10, 1-529, (1974).

(99) S. Rabie , A. Ahmed, M. Sabaa, Abd M. El-Ghaffar, Maleic diamides as photostabilizers for polystyrene, J. of Industrial and Engineering Chemistry (2013), 19, 1869-1878.

(100) Y. Foo, E. Yousif, S. Tiong and A. Majeed, Synthesis Characterization and Preliminary in vitro Antibacterial Screening Activity of Metal Complexes Derivatives of 2-[5-(4-Nitrophenyl)-1,3,4-thiadiazolylimino]methyl phenol, Asian J. Chem., 25(8), 4203-4206, (2013).

(101) R. Allcock, W. Lampe and P. Mark, Contemporary Polymer Chemistry, Pearson Prentice-Hall, 3^{d} ed., (2003).

(102) E. Yousif and A. Hameed, , Synthesis and Photostability Study of Some Modified Poly(vinyl chloride) Containing Pendant Benzothiazole and Benzimidozole Ring, International J. Chemistry, 2(1), 65-80, (2010).

(103) H. Kaczmarek, Changes to polymer morphology caused by U.V. irradiation: I. Surface damage, Polymer Degradation and Stability, 37(2), 189-194, (1996).

(104) R. Bretas and De B. Carvalho, Crystallization kinetics of a Peek/LCP blend, J. Appl. Polym. Sci., 55, 233-246, (1995).

(105) S. Magonov, G. Bar and I. Müller, Atomic force microscopy on polymers and polymer related compounds, 26, 223-230, (1991).

(106) E. Kramer, Developments in Polymer Fracture-1, Applied Science Publishers, London, (1979).

(107) J. Rabek, Mechanism of Photophysical Processes and Photochemical Reactions in Polymers, Wiley, London, (1987).

(108) J. Kaminski, F. Rozploch and H. Kaczmarek, Effect of copolymers modifying PVC on its physical and mechanical properties and its UV-radiation resistance, IX. Photodeformation of surface of pure PVC films and films containing MMA/MA and traces of cyclohexanone, Anger. Makromol. Chem., 169, 185-192, (1989).

(109) G. Junior, A. Silva and L. Guinesi, Synthesis, characterization and electropolymerization of a new polypyrrole iron(II) Schiff-base complex, Polyhedron, 23, 1953-1960, (2004).

(110) F. Kara, E. Aksoy and S. Aksoy, Synthesis and surface modification of polyurethanes with chitosan forantibacterial properties, Carbohydrate Polymers, 112, 39-47, (2014).

(111) Z. Chohan, Antibacterial dimeric copper (II) complexes with chromone-derived compounds, Trans. Met. Chem., 34, 153-161, (2009).

(112) P. Simon, and L. Valko, Spectroscopic study of the effect of a new metal chelate on the stability of PVC, Polym. Degrad. Stab., 35, 249-253, (1992).

(113) M. Fisch and R. Bacaloglu, Study of additive compatibility with poly(vinyl chloride) (PVC). 2: Dynamic mechanical analysis of PVC lubrication by stearic acid and its derivatives, J. Vinyl Addit. Technol., 4, 1-4, (1998).

(114) J. C. Alfonso, Mechanistic aspects of polymer photostabilization Journal of Photochemistry and Photobiology A: Chemistry, 49, 1-39, (1989).

الخلاصـــــــة

حضرت خمس معقدات لايونات النحاس (II), الكادميوم (II), الخارصين (II), القصدير (II) و النيكل(II) مع ليكاند 2-(4-ايزوبيوتيل فينيل) بروبانوات البوتاسيوم في وسط كحولي. شخصت جميع هذه المركبات من خلال مطيافية الأشعة تحت الحمراء (FTIR) والأشعة فوق البنفسجية والمرئية (.UV-Vis) وقياسات التوصيلية الكهربائية المولارية والحساسية المغناطيسية للمعقدات. واتضحت بأن هذا الليكند هو ثنائي السن، لأنه يرتبط مع ايون الفلز عن طريق ذرتي الاوكسجين لمجموعة الكاربوكسيل. ومن خلال القياسات وجد ان جميع اشكال هذه المعقدات هي ثمانية السطوح عدا معقد النحاس حيث يأخذ شكل مربع مستو.

تم متابعة سرعة التجزئة والتثبيت الضوئي للرقائق البوليمرية بسمك (40) مايكروميتر لمتعدد كلوريد الفينيل يحتوي على تركيز 0.5% من المعقدات التي حضرت. تم دراسة عملية التثبيت الضوئي لرقائق بوليمر كلوريد الفينيل عند درجة حرارة الغرفة استخدم ضوء بطول موجي (313nm) وبشدة 7.75×10^{-7} $einstein\ dm^{-3}\ sec^{-1}$.

وجد ان قياس سرعة التجزئة والتثبيت الضوئي للرقائق البوليمرية مع زمن التشعيع بقياس قيم معامل الهيدروكسيل I_{OH} والبولين $Ic_{=c}$ والكاربونيل I_{CO} و حسابات نقصان الوزن تزداد مع زيادة زمن التشعيع وان هذه الزيادة تعتمد على نوع المضاف المستخدم.

كما تم خلال البحث دراسة السطح مع زمن التشعيع وكذلك قطع السلسلة البوليمرية وقيم منتوج الكم وذلك بقياس مقدار التغير في متوسط اللزوجة للوزن الجزيئي مع زمن التشعيع، فوجد ان مقدار التغير في متوسط اللزوجة للوزن الجزيئي يقل بزيادة زمن التشعيع.

وجد أن المضافات المحضرة تسلك كمثبتات للتجزئة الضوئية، والتي أخذت الترتيب التالي :

$$PVC<ZnL_2<CdL_2<CuL_2<SnL_2<NiL_2$$

زيادة الاستقرارية

من خلال النتائج العملية المستحصلة اقترحت بعض الميكانيكيات اعتماداً على الصيغة التركيبية للمادة المضافة لذلك هي قانصات HCl, ممتصات اشعة فوق البنفسجية مجزئات ,البيروكسيد وقانصات الجذور الحر.

جمـــــــــــــــــهورية العراق
وزارة التعليم العالي والبحث العلمي
جامعـــــــــــــــة النهريـــــــن
كليـــــــــــــــة العـــــــلوم
قـــــــــــــــسم الكيميـــــــاء

التثبيت الضوئي لمتعدد كلوريد الفينيل باستخدام معقدات لاعضوية

رسالة

مقدمة الى كلية العلوم- جامعة النهرين

وهي جزء من متطلبات نيل درجة الماجستير في علوم الكيمياء

من قبل

رفاه فاهم محمد

بكالوريوس علوم كيمياء/كلية العلوم/جامعة بغداد

(2013)

المشرف
الاستاذ المساعد
الدكتور عماد عبد الحسين يوسف السراج

ربيع الثاني 1437 **كانون الاول 2016**